Sleep stage-specific regulation of hippocampal activity – linked to signatures of memory processing

Dissertation

der Mathematisch-Naturwissenschaftlichen Fakultät

der Eberhard Karls Universität Tübingen

zur Erlangung des Grades eines

Doktors der Naturwissenschaften

(Dr. rer. nat.)

vorgelegt von

Diego Marco Pagano

aus Palermo (Italien)

Tübingen

2024

Gedruckt mit Genehmigung der Mathematisch-Naturwissenschaftlichen Fakultät der Eberhard Karls Universität Tübingen.

Tag der mündlichen Qualifikation:	08.03.2024
Dekan:	Prof. Dr. Thilo Stehle
1. Berichterstatter/-in:	Prof. Dr. Olga Garaschuk
2. Berichterstatter/-in:	Prof. Dr. Andrea Burgalossi

Erklärung / Declaration

Ich erkläre, dass ich die zur Promotion eingereichte Arbeit mit dem Titel:

„ Sleep stage-specific regulation of hippocampal activity – linked to signatures of memory processing “

selbständig verfasst, nur die angegebenen Quellen und Hilfsmittel benutzt und wörtlich oder inhaltlich übernommene Stellen als solche gekennzeichnet habe. Ich versichere an Eides statt, dass diese Angaben wahr sind und dass ich nichts verschwiegen habe. Mir ist bekannt, dass die falsche Abgabe einer Versicherung an Eides statt mit Freiheitsstrafe bis zu drei Jahren oder mit Geldstrafe bestraft wird.

I hereby declare that I have produced the work entitled “Sleep stage-specific regulation of hippocampal activity – linked to signatures of memory processing”, submitted for the award of a doctorate, on my own (without external help), have used only the sources and aids indicated and have marked passages included from other works, whether verbatim or in content, as such. I swear upon oath that these statements are true and that I have not concealed anything. I am aware that making a false declaration under oath is punishable by a term of imprisonment of up to three years or by a fine.

Leverkusen, den ....

Datum / Date Unterschrift /Signature

Abstract

Sleep is a universal behavior that has been described in a wide range of animal taxa, from flies to lizards or cetaceans. The evolution of sleep mechanisms in different animals suggests the vital importance of this state of mind, despite the risks associated with a long dissociation from the surrounding environment.
In recent years, sleep has been proposed to play a central role in synaptic plasticity and in the homeostatic regulation of the neocortical and subcortical networks. Sleep seems to play two opposite and complementary roles: it promotes the downscaling of not relevant information, and it protects newly encoded and relevant information from being downscaled. In this way, the networks can still acquire new information and do not reach a saturation point. The hippocampus represents a transient station in which information coming from different associative areas is combined in one representation that, through repetitive reactivations during sleep, is sent to the neocortical areas to be integrated into long-term memory storage. For these reasons, the present work aims to describe sleep-specific changes in the neuronal dynamics of pyramidal cells in CA1, using two-photon microscopy with mice expressing a genetically encoded Ca^{2+} indicator (GCaMP7b). Also, considering the role of SOs and sleep spindles in consolidating hippocampus-dependent memories, the neuronal population was dissected in subgroups of cells active during slow oscillations (SOs) or sleep spindles. Our findings indicate that the global activity during SWS and REM sleep increases, in contrast to results obtained in the neocortex. On the other hand, considering sequences of SWS epochs interleaved by REM sleep, we found that the pyramidal cells, specifically active during spindles nesting in the upstate of a SO, dramatically reduced their activity. This decrease was not observed for the entire population, suggesting that REM sleep does not downregulate the activity globally, but specifically targets the networks previously involved in encoding memory information.

Zusammenfassung

Schlaf ist ein universelles Verhalten, das bei einer Vielzahl von Tierarten beschrieben wurde, von Fliegen über Eidechsen bis hin zu Walen. Die Entwicklung von Schlafmechanismen bei verschiedenen Tieren deutet darauf hin, dass dieser Zustand trotz der Risiken, die mit einer langen Abkopplung von der Umgebung verbunden sind, von entscheidender Bedeutung ist.
In den letzten Jahren wurde vorgeschlagen, dass der Schlaf eine zentrale Rolle bei der synaptischen Plastizität und bei der homöostatischen Regulierung der neokortikalen und subkortikalen Netzwerke spielt. Der Schlaf scheint zwei entgegengesetzte und sich ergänzende Rollen zu spielen: Er fördert die Herabstufung nicht relevanter Informationen und schützt neu kodierte und relevante Informationen vor einer Herabstufung. Auf diese Weise können die Netzwerke weiterhin neue Informationen aufnehmen und erreichen keinen Sättigungspunkt. Der Hippocampus stellt eine Übergangsstation dar, in der Informationen aus verschiedenen assoziativen Bereichen in einer Repräsentation zusammengefasst werden, die durch wiederholte Reaktivierungen während des Schlafs an die neokortikalen Bereiche weitergeleitet wird, um in das Langzeitgedächtnis integriert zu werden. Aus diesen Gründen zielt die vorliegende Arbeit darauf ab, schlafspezifische Veränderungen in der neuronalen Dynamik von Pyramidenzellen in CA1 zu beschreiben, wobei Zwei-Photonen-Mikroskopie mit Mäusen verwendet wird, die einen genetisch kodierten Ca^{2+}-Indikator (GCaMP7b) exprimieren. In Anbetracht der Rolle von SOs und Schlafspindeln bei der Konsolidierung von Hippocampus-abhängigen Erinnerungen wurde die neuronale Population außerdem in Untergruppen von Zellen unterteilt, die während langsamer Oszillationen (SOs) oder Schlafspindeln aktiv sind. Unsere Ergebnisse deuten darauf hin, dass die globale Aktivität während SWS und REM-Schlaf ansteigt, im Gegensatz zu den Ergebnissen, die im Neokortex erzielt wurden. Andererseits haben wir bei der Betrachtung von Sequenzen von SWS-Epochen, die durch REM-Schlaf unterbrochen werden, festgestellt, dass die Pyramidenzellen, die während Spindeln, die sich in die Aufwärtsphase eines SO einnisten, aktiv sind, ihre

Aktivität drastisch reduzieren. Dieser Rückgang wurde nicht für die gesamte Population beobachtet, was darauf hindeutet, dass der REM-Schlaf die Aktivität nicht global herunterreguliert, sondern speziell auf die Netzwerke abzielt, die zuvor an der Codierung von Gedächtnisinformationen beteiligt waren.

Ackowledgements

First of all, I would like to express my sincere gratitude to my first supervisor Prof. Dr. Olga Garaschuk for all her support and help during my PhD. Besides, I would like to thank also Prof. Dr. Andrea Burgalossi.

I must also thank Dr. Yury Kovalchuk for his technical and experimental support. I acknowledge Dr. Nima Mojtahedi for his encouragement during these years and his help during my PhD. I would like to thank also the other members of my doctoral committee, Professor Arrenberg and Professor Veit. In addition, I appreciated the help of all the colleagues I had the pleasure of working with over the years in the neurophysiology group.

Finally, I would like to thank my parents and Martina for their unconditional love and support and for helping me become the person I am today. Most importantly, thank you Roberta for your help and for being part of my life.

Table of contents

List of abbreviations

AAV	Adeno-associated virus
abGC	Adult-born granule cell
AMPAR	α-amino-3-hydroxy-5-methyl-4-isoxazolepropionic acid receptor
ANOVA	Analysis of variance
b.w.	Body weight
BMI	Brain-machine interface
CA	Cornu ammonis
Ca^{2+}	Calcium
CCK+	Cholecystokinin
DG	Dentate gyrus
DV	Dorso-ventral
ΔF/F	Relative changes in fluorescence
EC	Entorhinal cortex
ECDF	Empirical cumulative distribution function
EEG	Electroencephalogram
EMG	Electromyogram
FOV	Field of view
GABA	γ-aminobutyric acid
GECI	Genetically encoded Ca^{2+} indicator
i.p.	Intraperitoneal
IQR	Interquartile range
LEC	Lateral entorhinal cortex

LFP	Local field potential
MEL	Medial entorhinal cortex
NA	Numeric aperture
NOR	Novel-object recognition task
NREM	Non-REM sleep
PV+	Parvalbumin-positive
REM	Rapid Eye Movement
ROI	Region of interest
s.c.	Subcutaneous
SC	Schaffer collateral
SD	Standard deviation
SHY	Synaptic homeostasis theory of sleep
SO	Slow Oscillation
SOM+	Somatostatin-positive
SWR	Sharp wave ripple
SWS	Slow Wave Sleep
TRN	Thalamic Reticular Nucleus
WT mice	Wild-type control mice

1. Introduction

1.1 Sleep

Sleep is a recurrent and reversible state of mind, often referred to as a temporary detachment of the mind from the body, characterized by reduced responsiveness, immobility, and disconnection of the brain from the surrounding environment (Cirelli and Tononi 2008). Alongside feeding, reproduction and exploration, sleep is considered an essential survival function, especially in view of risks related to the disconnection from the surroundings and the decreased vigilance (Tononi and Cirelli 2014). Sleep is a universal behavior, present in a wide range of animal taxa (Anafi et al. 2019). Despite the initial reluctance to attribute sleep to low orders of vertebrates or invertebrates due to the lack of conventional electrophysiological patterns resembling those found in mammals and birds, recent evidence reported that the neuronal mechanisms are substantially conserved among vertebrates and also in animals with a very primitive nervous organization such as *Hydra vulgaris* (Kanaya et al. 2020), *Caenorhabditis elegans* (Raizen *et al.*, 2008) or more complex nervous system as the fruit fly *Drosophila melanogaster* (Hendricks et al. 2000; Paul et al. 2000). It is interesting to consider how the necessity for sleep for survival had also acted as a driving force in the evolution of uncanonical mechanisms of sleep, such as the case of unihemispheric sleep reported in cetaceans. Dolphins and whales swim continuously in order not to drown, but during sleep, only one hemisphere is disconnected while the other one remains online (Mukhametov 1987; Rattenborg et al. 2000).

Electrophysiological recordings, based on the electroencephalogram (EEG) and electromyogram (EMG), are used to dissect the sleep process. In mammals, sleep is characterized by the alternation of two stereotyped patterns of activity: Non-REM (NREM) sleep and rapid eye movement (REM) sleep (Vorster and Born 2015). In humans, episodes of REM sleep were first described by Aserinsky and Kleitman 1953, which eventually led to the most widely accepted manual for describing the human sleep process (Rechtschaffen and Kales 1968). Sleep

consists of the cyclic occurrence of NREM sleep stages 1, 2, 3 with interleaved REM episodes. The deep stages 3 and 4 of NREM sleep are characterized by high amplitude and slow rhythmic EEG activity and are also known as slow wave sleep (SWS) (Figure 1 A). However, in rodents, the subdivision of NREM sleep is not applied (Genzel et al. 2014); therefore, in the present work, the terms NREM and SWS are equivalent.

The sleep architecture across a night is influenced by multiple behavioral and biological factors (Yetton et al. 2018), but usually normal human adults undergo 4/5 consecutive NREM-REM cycles lasting on average for 70-100 minutes (Rasch and Born 2013). Rodents are nocturnal animals, therefore, sleep occurs during the light phase of the day (Penicaud et al. 2013). The reoccurring alternations of NREM-REM cycles are also observed, although the duration is reduced and frequently interrupted by episodes of wakefulness (Figure 1 B) (Miyawaki and Diba 2016). Also, circadian and homeostatic processes influence the distribution of sleep stages across the night (Achermann et al. 1993). NREM sleep is prevalent in the early stages of sleep, while REM sleep increases as the night progresses (Rasch and Born 2013).

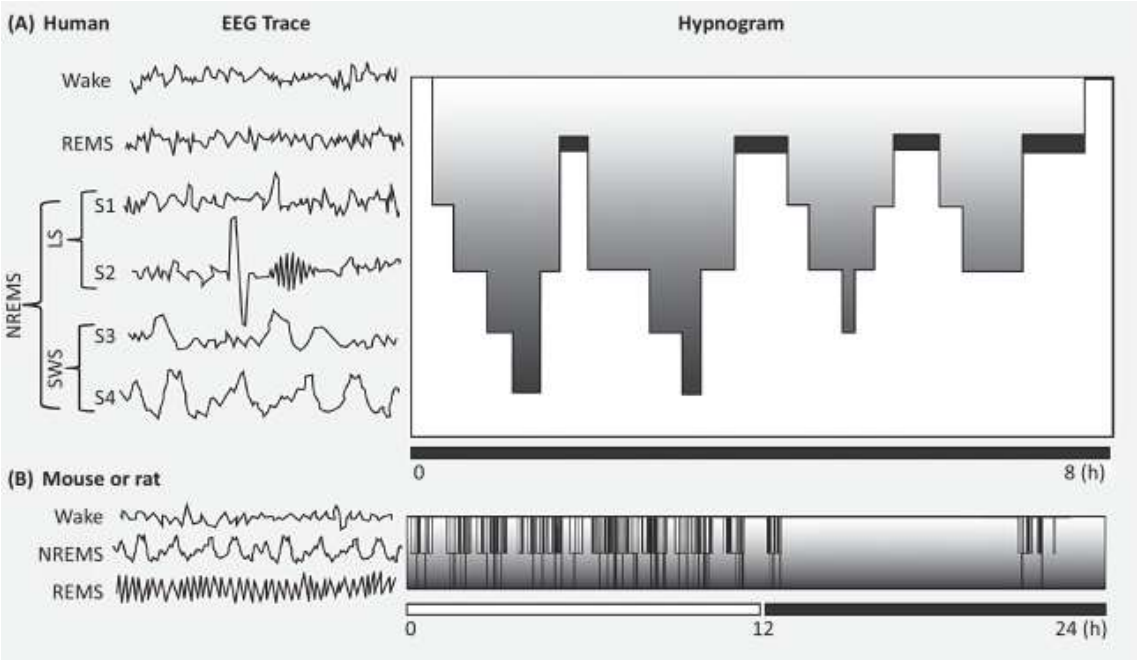

Figure 1. Schematic sleep hypnogram for humans and rodents. In all species, NREM and REM alternate in a cyclic fashion. (A) In humans, NREM dominates the first half of sleep and is generally subdivided into 4 stages (S1-S4), with S1-S2 being considered as “light sleep” and S3-

S4 as slow wave sleep (SWS). (B) In rodents, which are nocturnal animals, the SWS-REM cycles are very short and interrupted by wake episodes. Adapted from Genzel et al. 2014.

In the last decade, the technological advancements in the electrophysiological recordings in humans and rodents revealed a complex and multifaced organization of sleep-related activity in space and time (Adamantidis et al. 2019).

1.1.1 Oscillations during SWS

SWS is characterized by a complex and orchestrated pattern of multiple brain oscillations, including the < 1Hz slow oscillations (SOs) and sleep spindles (~12-15 Hz).

1.1.2 Slow oscillations

SOs are high-amplitude and slow field potential rhythms, which reflect the synchronized fluctuations of the neuronal membrane potentials between depolarized 'UP' states and hyperpolarized 'DOWN' states in cell across thalamocortical and corticothalamic projections (Steriade et al. 1993; Vyazovskiy et al. 2009, 2011). These oscillations can be recorded across multiple areas such as the primary sensory and motor cortex (Einstein et al. 2017; Funk et al. 2017), and the thalamic reticular nucleus (TRN) (Steriade et al. 1993). SOs originate in cortical networks, likely from a group of pacemaker cells in the layers 2/3 and 5 (Sanchez-Vives, 2000; Chauvette et al. 2010), and propagate from the anterior to the posterior regions (Massimini et al. 2004; Mohajerani et al. 2010; Nir et al. 2011), also reaching subcortical areas, such as the hippocampus (Wolansky et al. 2006; Varela et al. 2013; Staresina et al. 2015) and thalamus (Stroh et al. 2013). Interestingly, non-invasive brain stimulation in humans, such as transcranial current stimulation (Marshall et al. 2004, 2006; Binder et al. 2014) or acoustic stimulation (Tononi et al., 2010; Ngo et al., 2013; Ong et al., 2016), led to an increase of the density and amplitude of SOs as well as to an enhancement of the effect of sleep on memory processing, such as consolidation of

hippocampus-dependent declarative memory. Optogenetic disturbance of firing activity in rats during the upstate of SOs impaired the task performance at the post-sleep test, suggesting a role for SOs for preserving and consolidating newly encoded memories (Kim et al. 2019). Interestingly, the depolarizing UP state of the SOs drives a synchronized reactivation of the activity in the circuits associated with memory consolidation, such as the thalamus and the hippocampus (Sirota and Buzsáki 2005).

1.1.3 Sleep spindles

Sleep spindles are waxing and waning oscillations of 12-15 Hz of 0.5-2 s duration (Lüthi 2014), originating from the interaction of GABAergic neurons in the nucleus reticularis thalami and the glutamatergic thalamocortical projections (Destexhe et al. 1998; Steriade and Timofeev 2003), through which spindles spread in the cortex (Steriade 2006) and the hippocampus (Steriade et al. 1993; Varela et al. 2013; Staresina et al. 2015). In human subjects, sleep spindles have been extensively related to cognitive functions (Clawson et al. 2016), such as learning and memory (Rasch and Born 2013). Indeed, learning is a strong predictor of the increase of density and magnitude of the sleep spindles in post-encoding sleep (Gais et al. 2002). In numerous studies, sleep spindles have been associated with improvements in sensorimotor tasks (Fogel and Smith 2006; Tamaki et al. 2008; Rasch et al. 2009) or declarative memory performance (Gais et al. 2002; Schabus et al. 2004). Furthermore, the density of spindles seems to be topologically specific to the cortical regions previously engaged in the task encoding (Bergmann et al. 2012; Johnson et al. 2012). Interestingly, long-term memory consolidation improved by boosting sleep spindles via transcranial alternating current stimulation (Lustenberger et al. 2016). However, recent studies have suggested that the beneficial effects generally associated with sleep spindles on memory consolidation, synaptic plasticity, or brain communication might not derive only from the spindle event per se (Helfrich et al. 2019), but also from the specific timing of the spindle event relative to the SO (Diekelmann and Born 2010; Rasch and Born 2013; Klinzing et al. 2016). The depolarizing phase

of the SO can also recruit sleep spindles, generating sequences in which the depolarizing state of the SO (UP state) is coupled to a sleep spindle (Steriade, 2006). In humans, the coupling of sleep spindles to the UP-states of the SOs is enhanced after learning (Mölle et al. 2011). The SO-spindle coupling seems to facilitate synaptic plasticity in cortical circuits (Rosanova and Ulrich 2005a; Seibt et al. 2017). A two-photon Ca^{2+} imaging study showed that the activity of excitatory cortical pyramidal neurons is amplified when the spindle coincides with the SO peak, along with parvalbumin-positive interneurons that exert a somatic inhibition (Freund and Katona 2007). On the other hand, somatostatin-positive interneurons, which exert a dendritic inhibition (Gentet et al. 2012), showed low activity (Niethard et al. 2018). The increased perisomatic inhibition, in presence of a weak dendritic inhibition might suggest that when a spindle is nested in the up-state of a SO, the pyramidal neurons are more sensitive to receive excitatory inputs originating from reactivated memory representations coming from subcortical regions, such as the hippocampus. Also, this coupling is thought to drive the reactivation of newly encoded information, preventing the downscaling effects of sleep and therefore promoting synaptic plasticity and memory consolidation (Latchoumane et al. 2017).

1.1.4 REM sleep

Initially, Aserinsky et al. noticed that during sleep, periods of quiet sleep were interleaved with periods of sleep characterized by bursting the activity of eye muscles. These periods were defined as sleep with Rapid Eye Movements. REM sleep is also known as ‘paradoxical sleep’ or as ‘active sleep’ because of the features of the EEG signal, which resemble the ones observed during wakefulness (Jouvet 1965; Xi et al. 2001; Jones 2004). REM sleep is characterized by low-voltage and high-frequency activity in the theta range (6-9 Hz in rodents, 4-6 Hz in humans), which is evident predominantly in the parietal regions above the hippocampus (Cantero et al. 2003). REM sleep is also accompanied by the absence of muscular tone in the EMG, interrupted by sparse

muscle twitching (De Gennaro et al. 2000; Burgess et al. 2008). According to the 'sequential hypothesis', REM sleep is always preceded by a period of SWS and might serve to complement the functions of SWS (Giuditta et al. 1995).

1.1.5 Role of sleep

Although, as mentioned above, the neurophysiological characteristics of sleep as well as the enormous benefits deriving from sleep have been well characterized, an important remaining question regards the role of sleep.

1.1.6 Synaptic homeostasis hypothesis

The two-process model (Borbély 1982) acknowledged a homeostatic role to sleep. According to this model, sleep is regulated by a precise balance between a circadian process (C) and a homeostatic process (S). Process C represents the propensity to sleep at specific times of the day, while process S represents the 'sleep debt' after long wake periods or sleep deprivation (Borbély and Achermann 1999). This model has been recently updated in a theory known as "synaptic homeostasis theory of sleep" (SHY) (Tononi and Cirelli 2003, 2006). The SHY theory was the first to link the homeostatic role of sleep to synaptic networks.
According to this theory, computationally demanding waking experiences, such as learning (Roman et al. 1987) or exploration (Moser et al. 1993), lead to a net synaptic potentiation throughout the brain. If not homeostatically regulated, this potentiation over time can cause a stress-related damage caused by an increase in energy demand (Salim, 2017) or saturation of the network and inability to acquire more information (Tononi and Cirelli 2014).
Thus, a global renormalization of the synaptic strength by a net downscaling has to occur during sleep, improving the signal-to-noise ratio within the network and maintaining the network's plasticity within an optimal range (Figure 2) (Balduzzi and Tononi 2013; Hashmi et al. 2013). Since the first time SHY was formulated, a plethora of studies have been designed to test it, ranging from biochemical

(Vyazovskiy et al. 2008) to electrophysiological (Vyazovskiy et al. 2009) and structural (de Vivo et al. 2017) studies.

In an elegant study, the levels of α-amino-3-hydroxy-5-methyl-4-isoxazolepropionic acid receptors (AMPARs) and the electrically evoked potentials within the cortex were measured as an indicator of synaptic strength. Both measures increased after wake but decreased after sleep (Vyazovskiy et al. 2008). At the cellular level, neurons in the somatosensory cortex increased the firing rate across wakefulness and decreased across sleep (Vyazovskiy et al. 2009). According to this evidence, slow wave-dependent synaptic downscaling keeps cellular excitability within a biologically viable range while minimizing the amount of energy spent to sustain potentiated synapses. In this way, SWS downscales by the same factor all synapses, leaving only those that have been strongly potentiated during awake above the baseline (Giuditta et al. 1995). On the other hand, during subsequent REM sleep, the synapses which have been spared from downscaling are further potentiated (Diekelmann and Born 2010) through local increases in plasticity-related immediate-early gene activity (von der Kammer et al. 1998).

In recent updates of the theory, the concept of general downscaling is substituted by selective downscaling, to consider also the other functions of sleep (Tononi and Cirelli 2014). In particular, SWS seems to be responsible for a ‘competitive down-selection mechanism’ in which synapses intensively activated during wake are spared from depression, while synapses that have been less activated during the previous wake are depressed (Hashmi et al. 2013). Reconstructions of the axon-spine interface in the motor and sensory cortices with serial scanning electron microscopy revealed a net decrease in the interface area across the wake-sleep cycle, especially in the so-called ‘weak synapses’, suggesting a causal role of sleep for synaptic downscaling (de Vivo et al. 2017). However, recent evidence suggests that sleep-induced synaptic downscaling might not exert the same effects in different cortical areas or within subgroups of cells. In the visual cortex of rats, the firing rate distribution across wake-sleep cycles did not change, suggesting stable global connectivity (Hengen et al. 2016). At the cellular level, either in the frontal or visual cortex, cells with high firing rates during

wake tended to decrease their activity during sleep, whereas cells with low firing rate during awake tended to increase their activity during sleep (Watson et al. 2016).

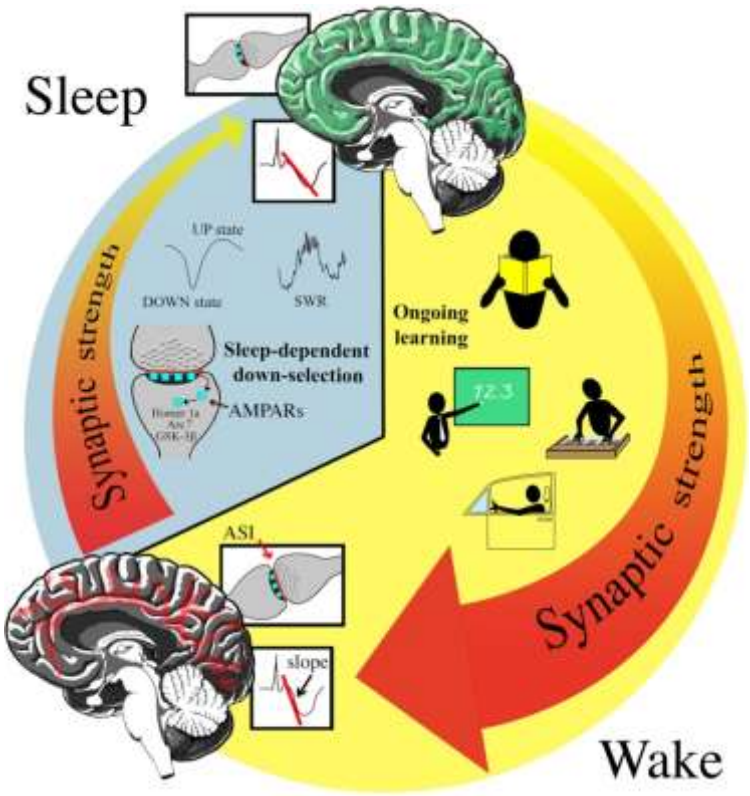

Figure 2. Schematic depiction of the synaptic homeostasis hypothesis (SHY). Synaptic strength increases in many brain circuits during wake as a result of ongoing learning. When the brain is disconnected from the environment during sleep, most, if not all, circuits undergo synaptic downscaling (green lines). Sleep-dependent renormalization is dependent on specific activity patterns during NREM sleep, specifically the UP states of cortical slow waves and hippocampal sharp waves/ripples (SWR). Adapted from Tononi et al. 2020.

Also, recent evidence suggests that during sleep, other forms of plasticity, apart from synaptic weakening, may be promoted, such as synaptic potentiation (Chauvette et al. 2012). Although a global decrease in firing rate has been reported during sleep (Vyazovskiy et al. 2009), the cells which constitute an engram (Tonegawa et al. 2015) may be differently regulated during sleep (Puentes-Mestril and Aton 2017). Prior learning experiences influence the activity of specific subsets of neurons in post-encoding sleep, showing an increase in the firing rates of neurons encoding novel spatial information (Grosmark and Buzsáki

2016). Long recording of activity in the CA1 area of the hippocampus showed that sleep exerts a decline in firing rates across the pyramidal cell population, regardless of the prior state of activity; however, across sleep, the neurons with low firing rates declined in activity, while neurons with moderate or high firing rates showed an increase in the firing properties (Miyawaki and Diba 2016).
To summarize, sleep seems to be involved in global downscaling and target potentiation at the synaptic and cellular levels. Therefore, these findings may stimulate the research to describe the plastic mechanisms occurring during sleep in subcortical regions, such as the hippocampus, which have not been sufficiently studied.

1.1.7 Active system consolidation theory

To maintain a high level of plasticity and capacity to detect and store new information, besides storing newly encoded information, our brain needs to discard all irrelevant information to prevent the saturation of neural networks. However, a crucial question, known as the "stability plasticity dilemma" (Abraham and Robins 2005), is how the brain acquires new information without overwriting or deleting older memories. The standard two-stage model of memory offers a solution to this dilemma and assumes that there are two different stores collecting different types of memories: one that learns at a fast rate but forgets fast, and the other that learns at a slow rate but shows a slow rate of forgetting (Marr, 1971; Buzsáki, 1989). The information is initially encoded in both stores. In this system, the hippocampus is conceptualized as the 'fast learner' (O'Reilly and Rudy 2000), characterized by high demands of plasticity and encoding for the episodic features of an event. The episodic event is decomposed as an abstract painting in specific features, such as visual or auditory stimuli, stored in different brain areas. The hippocampus receives the features of an event and melts them back together in one single episodic memory (Teyler and DiScenna 1986). These representations have limited stability. Sleep, especially SWS, plays an active and major role in the consolidation of the memory, contributing through repeated reactivations (see above) to the dialogue between the hippocampus and the

cortex (Figure 3) (Buzsáki 1996). The cortex is conceptualized as a ‘slow learner’ (Lisman and Morris 2001) and requires multiple reactivations for building up long-term and stable memories. The intense crosstalk between the hippocampus and cortex is also suggested by the high level of correlation in the EEG events (A G Siapas and Wilson 1998; Sirota et al. 2003). The process of ‘corticalization’ gradually makes the memory trace more stable and independent from the hippocampus (McClelland, et al. 1995; Eichenbaum 2000; Frankland and Bontempi 2005).

Interestingly, a recent study in rats has shown that even for the encoding of non-hippocampus-dependent memories, such as the ones acquired during a novel-object recognition task (NOR), the hippocampus plays a fundamental role in the consolidation of the memory, but not in the encoding or retrieval of the memory itself (Sawangjit et al. 2018). The off-line reactivations, which range from minutes to weeks, allow the integration of newly encoded information to the stable store in the cortex, reorganizing the memory and integrating many and overlapping experiences (Buzsáki 1998). Recently it has been hypothesized that breathing could play a central role as a pacemaker by coordinating the reactivation of previous wake experiences across multiple brain regions and therefore mediating the coordinated offline flow of information across the hippocampal-cortical circuit (Karalis and Sirota 2022).

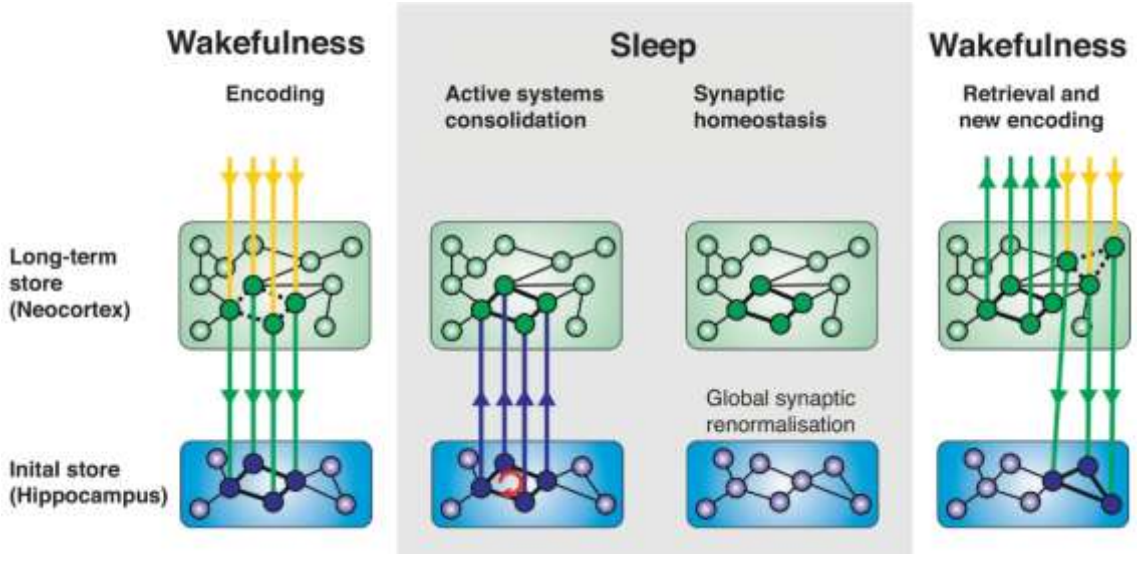

Figure 3. Schematic depiction of the active consolidation theory. During wakefulness in the hippocampus-dependent declarative memory domain, information (yellow arrows) flows through the sensory cortices to the hippocampus (green arrows), which quickly binds the information into a transient representation. During sleep the memory trace is repeatedly replayed (red arrows). In parallel, sleep also renormalize synapses, by erasing irrelevant information. During subsequent wakefulness, the consolidated information trace is already saved in the neocortex (green upward arrows) and new information can be encoded into the hippocampal store (downward yellow and green arrows). Adapted from Feld and Born, 2017.

1.1.8 Neuronal ensemble reactivation

Given the central role of the hippocampus in the formation and consolidation of memory, the first studies focused on the description of reactivation in this region. In the rodent and human hippocampus, cell assemblies that were entrained to fire together during wakefulness tended to reactivate together during the subsequent sleep (O'Keefe and Nadel 1978; Pavlides and Winson 1989; Wilson and McNaughton 1994;Gelbard-Sagiv et al. 2008). Multielectrode recordings also showed that pyramidal cells with overlapping place fields during maze-running were also preferentially co-reactivated during subsequent sleep (Dupret et al. 2010; M. A. Wilson and McNaughton 1994). Co-reactivation means that a pair (or larger groups) of neurons can have the same rate of firing observed during wakefulness (Peyrache et al. 2009), or neurons can fire in the sequence in which they fired during wakefulness (Dragoi and Tonegawa 2011). However, neuronal reactivations do not occur exclusively in the hippocampus. There is also evidence reported within the motor cortex (Hoffman and McNaughton 2002), the prefrontal cortex (Euston et al. 2007), the visual cortex (Ji and Wilson 2007), and other subcortical regions such as the ventral striatum (Pennartz et al. 2004). Usually, the neuronal reactivations represent time-compressed sequences of activity and occur in temporal association to hippocampal sharp-wave ripples (SWRs) either during SWS (Mölle et al. 2006; Ramadan et al. 2009) or quiet wakefulness (Dupret et al. 2010; Carr et al. 2011), but rarely during REM (Louie and Wilson 2001).

The causal relationship between hippocampal SWRs and memory consolidation was demonstrated both in humans with hippocampus-dependent visuo-spatial learning tasks (Rasch et al. 2007) and in rats, by suppressing SWR-activity during

post-learning sleep, leading to an impairment of spatial memory (Girardeau et al. 2009).

1.1.9 Interplay between oscillations during SWS

Hippocampal reactivations are thought to be orchestrated by neocortical SOs (Diekelmann and Born, 2010). Recent evidence suggest a loop scenario, where the depolarizing UP-state of the migrating SOs drives thalamic sleep spindles, which subsequently synchronize hippocampal ripples to the excitable troughs of the spindles (Latchoumane et al. 2017; Maingret et al. 2016; Klinzing et al. 2019). The nesting of the SWRs is believed to optimize the dialogue between the hippocampus and cortex (Figure 4) (Buzsáki 1998; Mölle et al. 2009). Also, spindle activity, which coincides with the depolarizing SO up-state, prepares the network for additional synaptic plastic changes (Bergmann et al. 2012; Mölle et al. 2011). Spindle activity during SWS essentially primes the expression of the plasticity-related immediate early genes – the markers of synaptic potentiation – by increasing Ca^{2+} concentration in selected cortical neurons, preparing these memory traces for synaptic strengthening during REM sleep (Sejnowski and Destexhe, 2000; Rosanova and Ulrich, 2005).

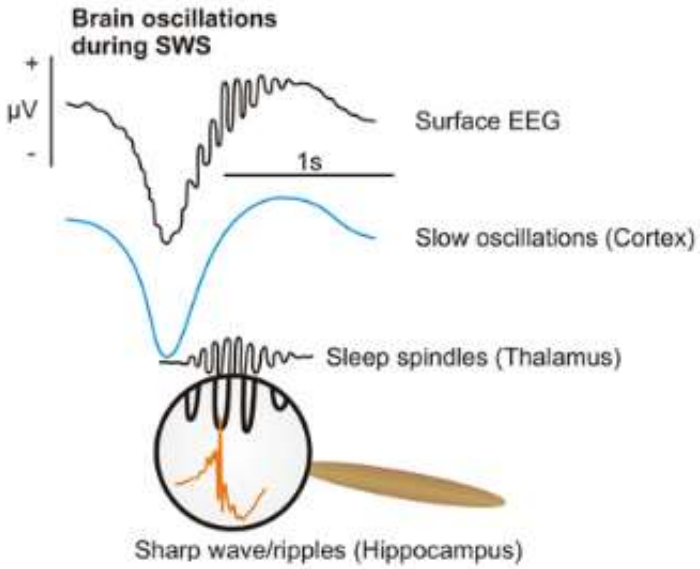

Figure 4. Schematic illustration of interaction between different oscillations during slow-wave sleep. Memories are replayed in the hippocampus in the form of SWRs primarily during the up-state of slow oscillations. Spindle-ripple events occur as a result of fast spindle coupling to the up-state. This enables reactivated memories to reach the cortex. Feld and Diekelmann (2015) adapted.

1.1.10 Effects of SWS and REM sleep

Both SWS and REM sleep play complementary roles in the homeostatic regulation of experience-dependent plasticity at the synaptic and cellular levels. Generally, because of the reduced cortical excitability during sleep, SWS has been linked to global synaptic downscaling. However, SWS is also involved in synaptic potentiation (Chauvette et al. 2012) or synapse formation. Structural imaging in the motor cortex of mice showed that SWS had not only a protective role for newly formed dendritic spines but also promoted the formation of new spines after a motor learning task. These effects were exerted through the cortical reactivation of the motor-task-related circuit during SWS (Yang et al. 2014).

As for REM sleep, many effects have been reported. Different from SWS, REM sleep is not responsible for the formation of new dendritic spines but selectively strengthens the ones which are critical during development (Li et al. 2017) or are experience-dependent (Y. Zhou et al. 2020). This selective process seems to rely on the generation of dendritic Ca^{2+} spikes.

In the hippocampus, the firing rates of neurons and interneurons strongly decrease across epochs of SWS interleaved by REM (Figure 5) (Grosmark et al. 2012). In addition, the firing rate distributions in the hippocampus and neocortex are not uniform but follow a log-normal distribution (Watson et al. 2016). The transition from REM to SWS produces a substantial decrease in the neurons with high firing rate but an increase in activity of neurons with low firing rate. This finding is extremely interesting because the neurons with low firing rate are, in their majority, place cells, encoding for new information. (Grosmark and Buzsáki 2016). In the framework presented, REM sleep represents the timeframe during which plastic changes are integrated, as suggested by the strong correlation between theta activity during REM and the incidence of sleep spindles and SWRs (Miyawaki and Diba 2016). Also, a recent optogenetic study reported that sleep

spindle incidence in SWS significantly increased before the onset of REM sleep (Bandarabadi et al. 2020). To summarize, REM sleep exerts a long-lasting modulation of the activity of the network in the hippocampus and neocortex across sleep.

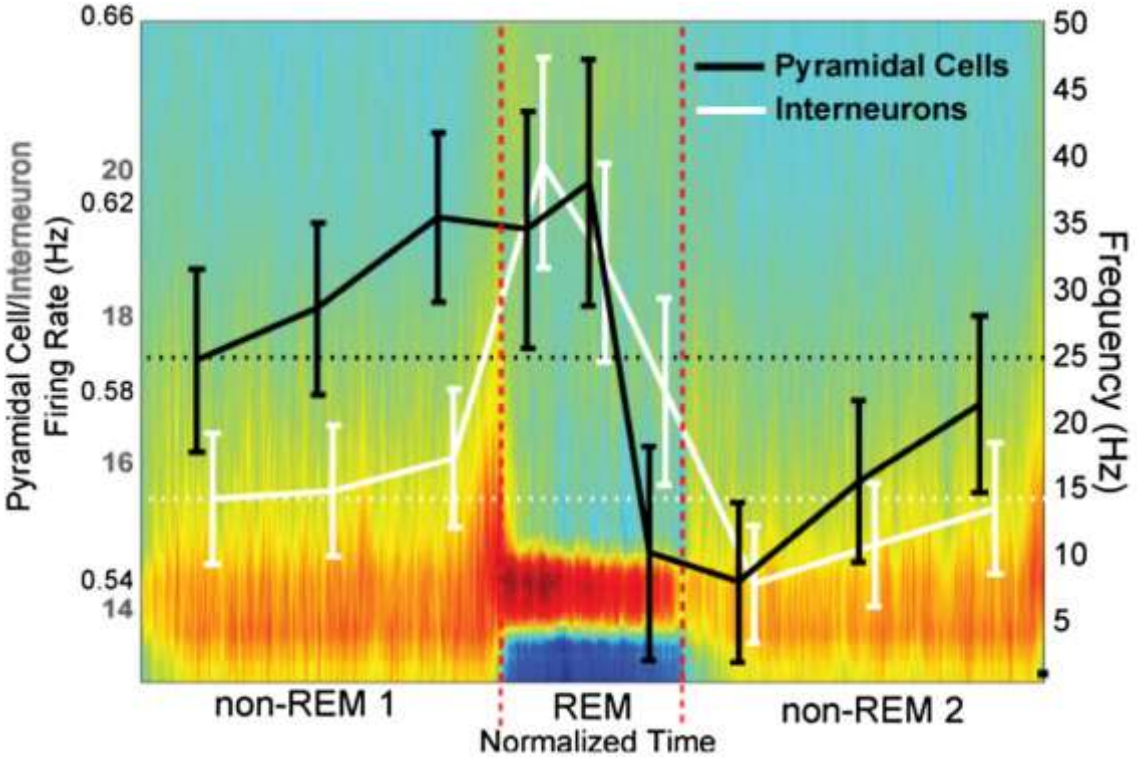

Figure 5. REM sleep exerts long-lasting effects on the activity of pyramidal cells and interneurons across SWS. 45 Epochs of SWS, interleaved by REM epochs, were considered. Each epoch was divided into thirds. The figure shows the increase of firing during SWS epochs of neurons (black line) and interneurons (white lines). However, REM sleep causes a strong downregulation of the activity during the subsequent SWS epoch. Adapted from Grosmark et al. 2012.

1.2 Hippocampus

The hippocampus is an essential structure for space navigation, episodic memory or memory retrieval. By separating the elements from past and present experiences, the hippocampus creates representations in a relational framework independent of the current time and location. With our minds, we can travel in space and time and relive past experiences or be able to exactly remember the route to go from the Colosseum to the Pantheon in Rome while being in the other part of the world. This process is defined as “recollection” and is associated with strong self-knowledge of space and time (Tulving, 2002). In this way, the

hippocampus creates a form of representation that can be used in prospective or retrospective cognition.

Since the description of the H.M. case the strong link between the hippocampus and memory became clear. In 1953 Henry Molaison (patient H.M.), underwent a radical surgery to treat severe epileptic seizures: the bilateral removal of large portions of the hippocampus. The outcome was unexpected (Penfield and Milner 1958; Corkin, 1984). Despite the ethical implications, such as many other famous studies in the past (e.g., Henrietta Lacks), the study of H.M. gave extremely interesting insights into the formation of memories and the role of the hippocampus. The patient's perceptual and cognitive abilities, as well as working memory and motor skill learning, were intact. However, he developed a severe case of amnesia in declarative memory. He was able to remember past experiences, suggesting that the long-term episodic memory was not impaired, but he was unable to recall events that occurred recently after the onset of the amnesia. These findings suggested that the hippocampus's role in memory processing begins during learning and contributes to memory consolidation for a prolonged period of time (Eichenbaum, 2004). Many studies were carried out, confirming the distinction between hippocampus-dependent and non-hippocampus-dependent memory (Squire, 1992; Moscovitch et al. 2016).

1.2.1 Anatomical features of the hippocampal circuit

The hippocampus is a structure located within the medial temporal lobe and characterized by several subregions, which include the dentate gyrus (DG), CA3, CA2, and CA1 (Lorente De Nó 1934). There are approximately 1.000.000 DG granule neurons, 300.000 CA3 pyramidal neurons, 30.000 CA2 pyramidal neurons, and 300.000 CA1 pyramidal neurons in the rat brain (Amaral and Witter 1989). In addition, based on their morphology, molecular markers, and electrophysiological properties only in the CA1 at least 21 classes of GABAergic interneurons have been identified (Klausberger and Somogyi 2008; Geiller et al. 2020). Before entering the hippocampus, polymodal sensory inputs activate

primary and associated sensory cortices and then flow into superficial layers of the entorhinal cortex (EC) (Andersen et al. 2006). EC is a polymodal association area representing the major source of glutamatergic inputs to the hippocampus (Figure 6). The sensory information which is introduced into the circuit is processed in the hippocampus and leaves the circuit through CA1 (Van Strienet al. 2009). The information from superficial layers of EC (layer II) reaches CA1 through a route called the “indirect pathway” or trisynaptic circuit: granule cells in the DG are excited through the performant path, and the mossy fiber projections excite CA3 pyramidal neurons. At this point, the excitation propagates through the Schaffer collateral (SC) pathway, reaching the pyramidal neurons in CA1. Principal neurons in the trisynaptic circuitry fire modulated spikes whenever the animals reach a specific portion of the environment, a so-called “place field” (O’Keefe and Dostrovsky 1971). In this way, the output of the circuit is a spatial representation, supporting either spatial navigation or episodic memory (Buzsáki and Moser 2013).

Also, from layer III of the EC, glutamatergic projections directly reach the pyramidal neurons in CA1 (“direct pathway”) (Van Strien et al. 2009; Witter 2010). Recent evidence suggests that CA1 also receives strong excitatory inputs from CA2. This region provides a strong and direct connection from the cortical to the hippocampal output (disynaptic path) (Basu and Siegelbaum 2015). CA1 pyramidal neurons send projections to various brain regions, including the subiculum, prefrontal cortex, and amygdala (van Groen and Wyss 1990). Another important output closes the loop with the EC, exciting the deep layers (Naber, et al. 2001).

The complex architecture of the hippocampus has been studied with conventional lesions or genetic approaches, identifying specific roles in the cortico-hippocampal circuit (Basu and Siegelbaum 2015).

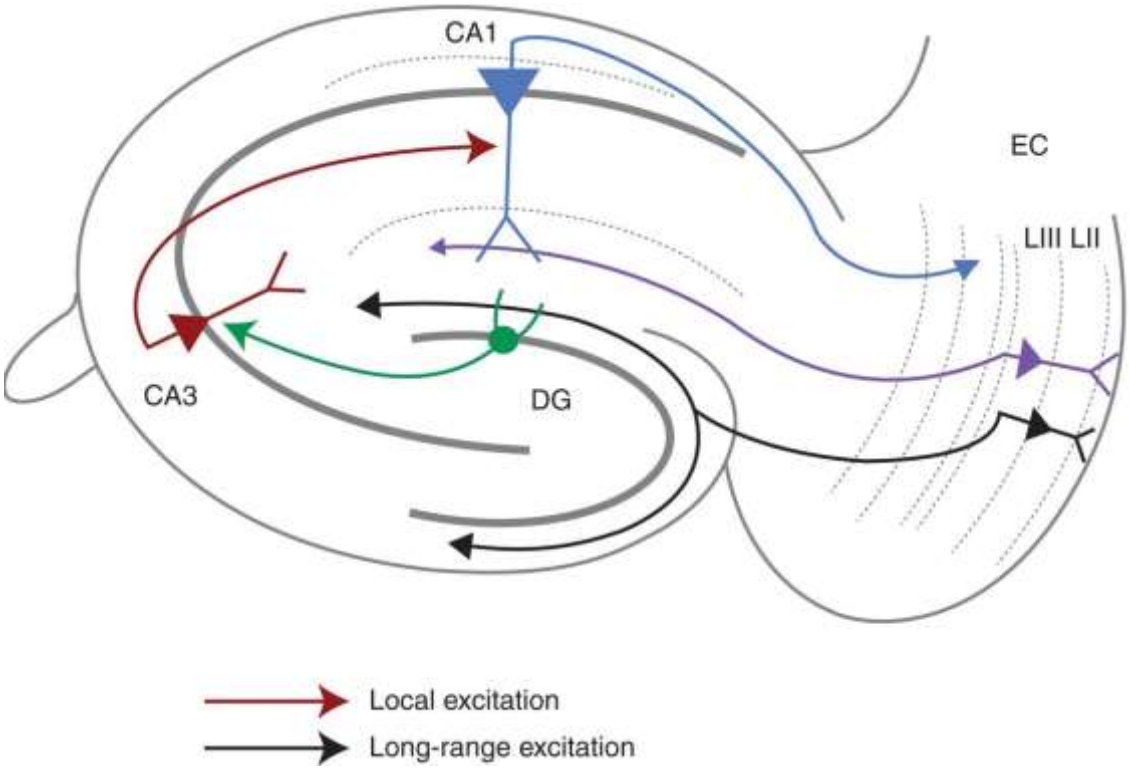

Figure 6. Classic schematics of the glutamatergic cortico-hippocampal circuits. Glutamatergic inputs from the superficial entorhinal cortex (EC) layers (L II and L III) reach CA1 through the trisynaptic and monosynaptic paths. Sensory inputs from EC LIII reach the dendrites of CA1 via the performant path (light blue). Inputs from EC LII activate dentate gyrus (DG) (black line), which sends mossy fiber axons (green line) to CA3 and then CA1. Adapted from Basu and Siegelbaum, 2015

In this way, it has been proposed that parallel processing (Lee et al. 2020) of information in different neural systems can support the variegate memory processes and allow at the same time the acquisition of new learning-related information without overwriting or deleting the old ones. Indeed, there is growing evidence that the hippocampus has dual (non-spatial and spatial sensory) input streams. Spatial information, such as location (O'Keefe and Dostrovsky 1971), head direction (Sargolini et al. 2006), or speed (Solstad et al. 2014), reach the hippocampus from the medial entorhinal cortex (MEL). On the other hand, the primary source of non-spatial sensory information, including sounds (Sakurai 2002), faces (Fried et al. 1997), or odors (Eichenbaum et al. 1987), is the lateral entorhinal cortex (LEC) (Aronov et al. 2017). These two streams remain relatively segregated (Neunuebel et al. 2013; Knierim and Solomon 2014). In addition,

recently, parallel processing at the cellular or microcircuit level has also been proposed (Soltesz and Losonczy 2018). Considering each subfield of the hippocampus as an independent station for processing, CA1 might act as a novelty detector by comparing the input with the memories stored in the DG and the sensory and spatial information coming from EC (Lisman and Grace 2005). Two main types of parallel processing have been hypothesized: uniform modules and heterogeneous modules. In the first case, the modules, or circuits, process different inputs similarly and then send the processed information to different downstream structures.

On the other hand, the heterogeneous modules are not identical and therefore exert different transformations on inputs of varying nature. Recent evidence suggests that radially defined subpopulations of CA1 pyramidal cells (Jarsky, et al. 2008; Kim and Spruston 2012) modulate the functional separation of streams of information into parallel and not uniform channels, meaning that the input-output transformation differs for different behaviors (Soltesz and Losonczy 2018). This is suggested as the overall organizing principle of the hippocampus supporting a large variety of behaviors (Soltesz and Losonczy 2018).

1.2.3 CA1 heterogeneity

The pyramidal neurons reside in the *stratum pyramidale*. The other layers of CA1 are the *stratum oriens*, *stratum radiatum*, and *stratum lacunosum-moleculare*. CA1 represents the hippocampus's primary output and plays an essential role in novelty detection, input comparison, and enrichment of hippocampal output (Soltesz and Losonczy 2018). As mentioned in the previous paragraph, a potential explanation for this set of variegate abilities might be the heterogenous composition of CA1 at a cellular level. Early anatomical studies showed a high degree of heterogeneity in the laminar organization, in particular in the radial axis, deep (dorsal), and superficial (ventral) regions (Lorente De Nó 1934). An emerging set of studies show that along the radial axis of CA1, there are transcriptional gradients, which lead to the expression of different proteins and electrophysiological properties (Jarsky et al. 2008; Hartzell et al. 2013). Then, the radial organization also influences the output behavior. Deep pyramidal cells

in CA1 are more active and tend to form place fields (Mizuseki et al. 2011) and spatial maps (Danielson et al. 2016), which are more stable than superficial pyramidal cells. In addition, an electrophysiological study showed that slow oscillations more strongly modulated deep pyramidal cells during sleep (Mizuseki et al. 2011). Also, different pyramidal cells are contacted in the radial axis by afferents coming from LEC and MEC, conveying non-spatial and spatial information, respectively (Ito and Schuman 2012; Nakamura et al. 2013).

1.2.4 Two-photon in vivo Ca^{2+} imaging of hippocampal circuits

Studying how cellular networks encode complex mammalian functions, such as learning, spatial navigation, or memory consolidation, requires *in vivo* analyses of spatiotemporal network activity at the single-cell resolution. This is only possible using imaging techniques, as electrophysiological recordings despite having high temporal, largely lack the spatial resolution and are unable to identify inactive cells (Grinvald and Hildesheim 2004; Buzsáki 2004) or to follow the same neuronal population longitudinally (Wei et al. 2020). Combining the use of genetically encoded Ca^{2+} indicators (Chen et al. 2013; Dana et al. 2019) with high-resolution *in vivo* two-photon imaging (Stosiek et al. 2003), it became gradually possible to study large groups of neurons in deep cortical layers and the hippocampus.

The procedure for an acute cranial hippocampal window was established in 2004 (Mizrahi et al. 2004) and later improved in 2010 (Dombeck et al. 2010). Typically, the procedure requires the removal of the cortex overlying the dorsal portion of the hippocampus. For two-photon imaging, animals are either head fixed under the two-photon microscope (Mizrahi et al. 2004; Dombeck et al. 2010; Pilz et al. 2016; Danielson et al. 2016; Hainmueller and Bartos 2018) or free-behaving, implanted with a miniaturized one-photon (Zhou et al. 2019; Kumar et al. 2020) or two-photon (Zong et al. 2022) miniscope. One-photon miniscopes allow imaging in freely moving mice of the neuronal activity at a nearly cellular resolution in sparsely active brain regions (Rubin et al. 2019). However, this technique might be severely affected by background fluorescence in densely

labeled areas (Aharoni et al. 2018), such as CA1. So far, imaging analyses of the CA1 pyramidal neuron activity focused on specific behavioral tasks, such as virtual navigation (Dombeck et al. 2010; Sheffield and Dombeck 2015; Hainmueller and Bartos 2018), exploratory behavior (Zong et al. 2022), locomotion and sensory processing (Kaifosh et al. 2013), spatial reward learning (Grosmark et al. 2021) or fear conditioning (Lovett-Barron et al. 2014; Kumar et al. 2020) with very few studies (Zhou et al. 2019) analyzing the activity of CA1 pyramidal neurons across brain states, differently from other brain regions (Niethard et al. 2016, 2018, 2021; Xu et al. 2015; Cox et al. 2016). The role of SWRs in orchestrating the reactivation over time of specific neuronal circuits in CA1 has been deeply described in a recent set of studies (Malvache et al. 2016; Zhou et al. 2019; Grosmark et al. 2021). Interestingly, all studies mentioned above reported an increase in the somatic Ca^{2+} activity around the detected SWR event (although, see Zhou et al. 2019), which is fundamental for the consolidation of the memory trace.

Although multiple studies showed the role of SOs, solitary spindles and spindles occurring in the upstate of a SO event in the formation of memories during sleep in the neocortex (Rosanova and Ulrich 2005; Diekelmann and Born 2010; Rasch and Born 2013; Klinzing et al. 2016; Seibt et al. 2017), it is still not clear the function of these oscillations in orchestrating the activity of the CA1 pyramidal cells.

1.3 Aim of the project

Sleep and the hippocampus play a central role in memory consolidation. For this reason, the present study aimed to obtain a detailed picture of the neuronal circuits during sleep in the CA1 region of the hippocampus. The study's first aim was to describe the changes in the activity of pyramidal cells during natural sleep. We used two-photon Ca^{2+} imaging to detect cellular activity and simultaneous surface EEG recordings for sleep stage classification. Then, since SOs, solitary spindles and spindles typically nesting in the SO upstate have been very consistently found to be involved in the consolidation of hippocampus-dependent

memories during sleep (Gais et al. 2002; Mölle et al. 2006; Rasch and Born 2013), the second aim was to consider the modulating effect of these oscillations on the network activity at single-cell resolution. Therefore, after detecting SOs, sleep spindles, and SO+spindles co-occurring events, the neuronal population, was dissected in subgroups of cells. In this way, we aimed to evaluate for the first time the modulating effect of SWS-related oscillations on the activity of the CA1 network.

2. Materials and Methods

2.1 Animals and surgery

All experiments were conducted in accordance with institutional animal welfare regulations and were approved by the state government of Baden-Württemberg, Germany. Since the features of the sleep cycle change in young and old mice (Soltani et al. 2019), in order to exclude any difference in the sleep architecture influenced by aging, all the experimental procedures were carried out on adults 5-6-month old C57BL6/N male mice (Charles River). Mice were housed in pathogen-free conditions on a 12-h light/dark cycle (lights at 8 a.m.) in groups of 2 or 3 and, after the viral injection, were individually housed. Temperature and humidity were continuously monitored and maintained at 22/23 °C and at 40%, respectively. Mice were provided with food and water *ad libitum*. All the experimental procedures were in accordance with the Directive 2010/63/EU of the European Parliament and the Council of the European Union.

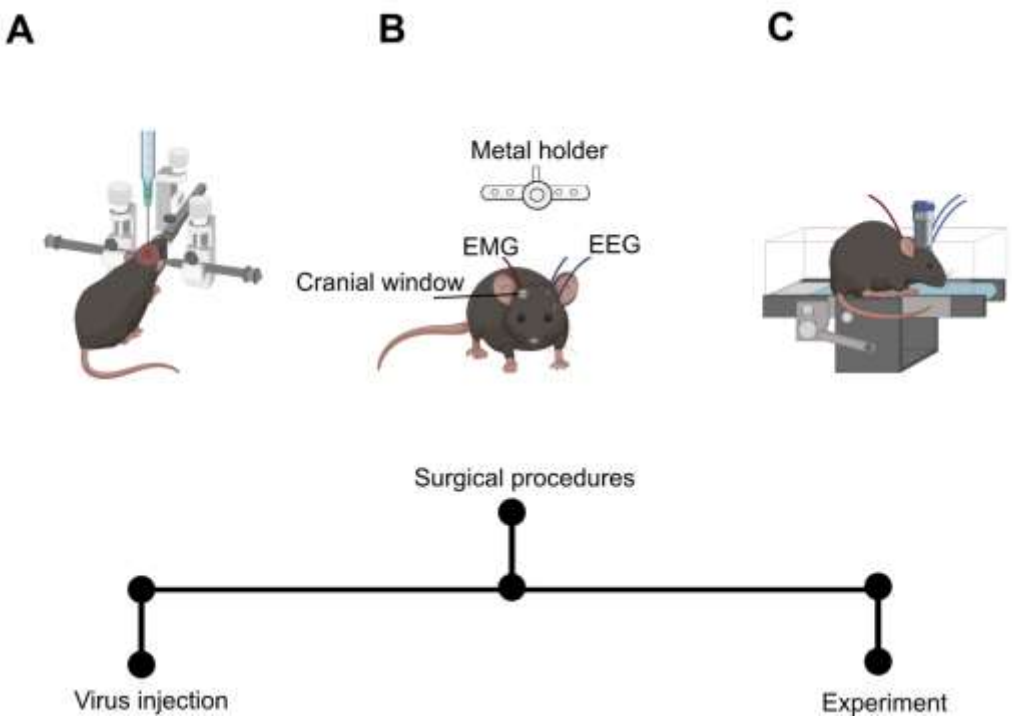

Figure 7. Schematics of the experimental procedure. (A) Stereotaxic viral injection. (B) Cranial window, EEG (blue) and EMG (red) electrodes implantation. On top the metal holder is shown. (C) Imaging apparatus for parallel acquisition of fluorescence, EEG and EMG signals.

2.2 Stereotaxic viral injection

Mice were anesthetized with an intraperitoneal (i.p.) injection of a mix (80/4 µg/g body weight (BW)) of ketamine (Fagron, Barsbuettel, Germany) and xylazine (Sigma-Aldrich, St. Louis, MO, USA). Prior to surgery, the depth of anesthesia was evaluated with a toe pinch. An additional dose of ketamine/xylazine was injected if needed. The fur was removed with a veterinarian fine trimmer without cutting whiskers. Subsequently, the mice were mounted in a stereotaxic apparatus and kept on a custom-made warming plate at 36-37 °C (Figure 7 A). The body temperature was measured using a rectal temperature probe. An ointment was applied to the eyes (Bepanthen^{TM}, Bayer, Germany) to avoid dehydration of the cornea. Subcutaneous (s.c.) injection of 2% lidocaine (AstraZeneca, Wedel, Germany) was used as topical anesthesia before the skin was cut in the midline with scissors and the skull was cleaned from connective tissue with tweezers while continuously irrigating it with ringer solution (containing in mM: 147 Na^+, 4 K^+, 2.2 Ca^{2+}, 156 Cl^-; B. Braun Melsungen AG, Germany).
For the viral injection, the dorsal hippocampus was targeted at 1.8 mm posterior to bregma and 1.5 mm lateral from the midline. A small (Ø 0.5-1 mm) craniotomy was performed with a high-speed dental driller (NSK, Eschborn, Germany) in the region of the hemisphere overlying the right hippocampus. Then, a borosilicated pipette containing 600 nL of viral solution (AAV-syn-jGCaMP7b-WPRE; titer ≥ 1×10^{13} vg/mL) was lowered to 1.5 mm below the dura (Dombeck et al. 2010). Before the injection procedure, the capillary was prepared with a Narishige PC-10 glass pipette puller. Also, in order to prevent damage to the cortical tissue during the insertion of the pipette, the glass tip was gently broken and then evaluated under an inverted microscope (Wilovert, Standard HF). For optimal outcomes of the procedures, capillaries with a tip diameter of 5-15 µm were chosen. After the injection, the pipette was left in place for 5 min before being slowly withdrawn, to allow the viral solution to diffuse in the brain tissue. The skin was closed with sutures. Postoperative care included an analgesic dose of carprofen (5 µg/g of BW) for 3 days (s.c.). Mice recovered for at least 2 weeks, to allow the expression of the Ca^{2+} indicator.

2.3 Cranial window implantation

The surgical procedure was performed 10 days after the viral injection according to the published protocol (Dombeck et al. 2010) (Figure 7 B). A trephine drill was used to perform a circular groove (Ø 3 mm), centered around the viral injection spot. Small pieces of bone and debris were removed with tweezers and with a gentle airflow, respectively. In order to avoid overheating of the tissue and consequent swelling, ringer solution was continuously added and absorbed with swabs (Kettenbach GmbH, Germany). After careful removal of the bone with fine tweezers, the dura overlying the cortex was gently peeled away with a needle. Then, a negative pressure (MZ 2 NT, vacuumbrand®) was applied to a 23-gauge needle for removing the cortical tissue above the hippocampus. Ringer solution was continuously applied to reduce the bleeding. The procedure continued until the external capsule was exposed, and bleeding was stopped. Then, the fibers were gently peeled away with a soaked swab until the surface of the hippocampus looked translucent. The imaging window, consisting of a glass coverslip (Ø 3 mm, Warner Instruments, Hamden, CT, USA) glued to the bottom of a stainless-steel cannula (3-mm diameter, 1.5 mm height), was inserted into the newly formed cortical cavity and placed on top of the hippocampus. The gaps between the bone and the stainless-steel cannula were filled with cyanoacrylate glue (UHU, Bühl, Germany). After the glue dried, the cranial window was further secured by blue light-cured dental cement (Ivoclar Vivadent AG, Liechtenstein).

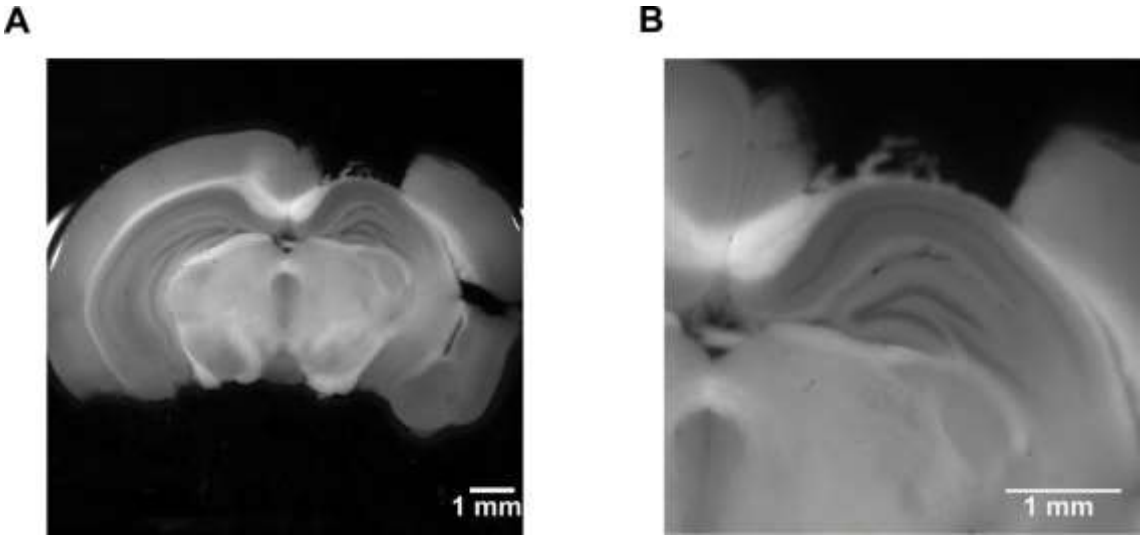

Figure 8. Coronal slices after the surgery: A 100 µm-thick slice with 2X magnification (A) and 5X magnification (B) showing the outcome of the surgical procedure. The layered structure of the hippocampus is visible. The cortex above the right hippocampus was aspirated in order to insert the cranial window. The fibers overlying CA1 were gently peeled away.

After the end of the experiments, the mice were sacrificed, and the brains were collected. Slices with a thickness of 100 µm were prepared with a vibratome (Microm HM 650 V, Microm International GmbH). Subsequently, the slices were observed under a stereomicroscope (MVX10, Olympus, Tokyo, Japan, magnification from 0.63 X to 6.3 X) with a 0.63 objective lens (NA 0.15; WD 87 mm) (Olympus, Japan) to evaluate the success of the surgical procedure (Figure 8 A-B).

2.4 EEG and EMG electrodes and holder implantation

During the same surgical procedure (Figure 7 B), three holes were drilled in the skull of the contralateral hemisphere to implant the EEG electrodes (Frontal: 1.5 mm posterior to bregma, 1.5 mm lateral from the midline; Parietal: 1.5 mm anterior to bregma and 2.5 mm lateral from the midline) (Niethard et al. 2018). The reference electrode was implanted 1 mm posterior to lambda. The EEG electrodes consisted of silver Teflon-coated wire (Ø without coating 480 µm) (Science Products) and were S-shaped. The tips of the electrodes were removed from the coating. The wires were inserted into the holes in direct contact with the

dura mater. The electrodes were secured with cyanoacrylate glue and strengthened with blue light-cured dental cement. Then, two stainless-steel wires (Ø 127 μm) (Science Products) were inserted in the nuchal muscles for EMG recordings.

A custom-made titanium holder was designed to be centered on the cranial window and not to interfere with the EEG and EMG electrodes. The holder was fixed to the skull with dental cement. The remaining exposed skull was also covered with dental cement.

Postoperative care included antibiotic enrofloxacin (Baytril, 1:100 v/v, Bayer, Leverkusen, Germany), dissolved in drinking water, for 10 consecutive days, and wet food, supplied in a petri dish within the cage. Mice were allowed to recover for at least 2-3 weeks and were subsequently examined for window clarity. Mice were singly housed after cranial window implantation on a 12 h light/dark cycle with food and water available *ad libitum*.

During the establishment of the surgical procedure for the implantation of EEG and EMG electrodes, I have tested different approaches and wires of different diameters. First, accordingly to published reports (Vogler et al. 2017; Wasilczuk et al. 2016). I implanted on the head of the mouse a 5-pin electric connector. After performing three small craniotomies on the skull (same coordinates as above), I inserted silver wires (Ø without coating 203 μm) (Science Products), which were soldered at the tip with a pin. After that, the pins from the EEG electrodes and the EMG wires were inserted in the connector, and all the apparatus was secured with glue and dental cement. Another approach (Oishi et al. 2016) was to implant jeweler screws with a silver wire soldered on top as EEG wires. I tried either to connect the soldered wires to a connector or to just leave the wires free. Although the quality of the electrophysiological signals was good in all cases and the impedance among the electrodes did not differ dramatically (~ 200 kΩ), the surgical procedure, including the cranial window implantation, was very challenging and required more than two hours. In addition, the procedure required a reduction of the head-mounted apparatus in order to decrease at the minimum the risks of the detachment of the electrodes or the cranial window. For these reasons, I simplified the surgical procedure by using the S-shaped electrodes,

managing also to reduce the time of the surgery by about one hour and the amount of injected anesthesia.

2.5 Training and head fixation procedure

Approximately 10 days after surgery, mice underwent to a training protocol consisting of several sequential steps: (i) gentle handling inside their home cages (~ one week), (ii) habituation to the experimental set-up, including head fixation (at least two weeks). Each habituation session consisted first in a gentle handling and at least 20 minutes of free exploration of the set-up. After that, mice were head-fixed under the microscope on a custom-made linear treadmill for an increasing time interval (1 min, 10 min, 30 min, 60 min). Each fixation was followed by a 5-min-long interval. After this initial habituation phase, in the next days the animals were head-fixed for longer periods (2-3 hours), mimicking the imaging sessions. The training sessions, as well as the imaging experiments (see below), started at 9-10 a.m. The stress level and the brain state of the animals were continuously monitored with a USB camera (IDS GmbH). In order to observe naturally occurring sleep, I mimicked with the head-fixation procedure the natural position of the body and the angle of the head observed during natural sleep, as reported in other works (Niethard et al. 2016; Bojarskaite et al. 2020; Yüzgeç et al. 2018) (Figure 7C). The treadmill was not blocked, and the animals were able to move or quietly rest. Generally, in well-habituated animals, the first episodes of SWS were visible within the first hour, and episodes of REM sleep within 2 hours. Across the training phase, sleep episodes tended to appear earlier and more frequently. The training was conducted until 24 h before the first imaging session during the early light phase.

2.6 EEG and EMG recordings

All the devices used in the experimental procedure, including the acquisition apparatus for EEG and the imaging system, were grounded to a common star point to avoid ground loop and electrical noise. An oscilloscope was also used to determine the presence of 50 Hz noise. EEG and EMG signals were first evaluated after the surgical procedure and then were recorded during the training and the imaging sessions. The electrophysiological signals were amplified, filtered (EEG. 0.01-300 Hz; EMG: 30-300 Hz), and sampled at 1 kHz by using a differential and low-noise amplifier (AD Instruments; Ltd, Oxford, United Kingdom). The differential amplifiers measured the difference in voltage between the reference electrode and the frontal or parietal electrode (Teplan, 2002). Electrodes were directly clamped with micro-hooks (MLA1212, AD Instruments). The electrophysiological signals were digitally acquired and post-processed with LabChart v9 (AD Instruments).

2.7 Long-term in vivo two-photon imaging of pyramidal cells

Mice were placed in a custom-made linear treadmill and head fixated under a two-photon microscope. Preliminary experiments were conducted with a customized two-photon microscope based on an Olympus FV100 system (Olympus, Tokyo, Japan), connected to a mode-locked laser (Spectra Physics, Mountain View, CA) (Kovalchuk et al. 2015; Liang et al. 2016). GCaMP7b was excited at 930 nm, and a 570-nm dichroic mirror was used to split the emission light. Time series were acquired at 8 Hz, therefore with low temporal resolution and small FOVs. In addition, the software used for the acquisition of the images was not programmed to continuously acquire and fast save new time series, causing the interruption of the recording until the saving was finished. These conditions, including low temporal resolution, small FOVs, and continuous interruption of the experiment, did not represent the optimal conditions for studying the evolution of cellular activity across sleep.

To overcome the problems listed above, the experiments were conducted with a two-photon resonant scanner microscope (FemtoSmart-Dual, Femtonics Ltd) with an imaging frame consisting of 256 x 256 µm and a frame rate of 30 Hz. Excitation of GCaMP7b was generated at 930 nm with a femtosecond-pulsed two-photon laser (Mai Tai DeepSee, Spectra-Physics). This Ca^{2+} indicator has a higher brightness at rest among the GCaMP sensors and allows robust imaging and better correction of motion artifacts (Dana et al. 2019). Images of the pyramidal layer of CA1 were collected with a Nikon 40x objective (Figure 9) (0.8 NA, Nikon, Tokyo, Japan) immersed in imaging oil (Carl Zeiss™, Immersol). Concurrently to the image acquisition, EEG and EMG signals were collected in order to classify the brain states. To facilitate the following analysis, the experiments consisted of files containing batches of 10-min-long time series. In general, FOVs contained 150-300 cells. Considering the heterogeneity along the radial axis in CA1 (Soltesz and Losonczy 2018), images were acquired from the *stratum pyramidale* at a depth of 100 µm from the hippocampal surface.

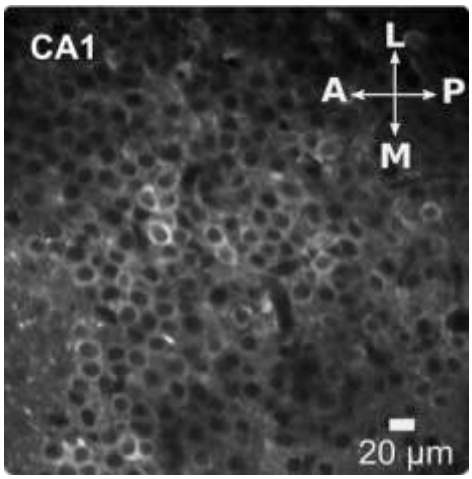

Figure 9. Representative FOV of the *stratum pyramidale*: Mean image (average of 200 frames, ~ 100 µm from the surface) showing around 300 pyramidal cells expressing GCaMP7b. Note also neurons with no activity showed a high fluorescence at the baseline level. Scale bar indicates 20 µm. In the top-right corner, the axis coordinates are shown.

Since the imaging sessions started at 9-10 a.m. and lasted until 3-6 p.m., one of the biggest challenges was to avoid the evaporation or the leakage of the immersion liquid over time with consequent decay of the fluorescent signal.

Initially, dH_2O was used, and despite the physical barrier created around the cranial window with the dental cement, the water solution tended to evaporate after ~ 60 minutes, causing the interruption of the experiment. A second approach was to use a carbomer gel (Vidisic; Bausch& Lomb/Dr. Mann Pharma, Berlin, Germany) or a thermostable ultrasound gel (Sonosid® Asid Bonz GmbH, Herrenberg, Germany) as immersion media. However, these approaches were characterized by a higher tendency to form bubbles within the cannula, which were difficult and dangerous to remove for the high risk of inadvertently detaching the glass coverslip. To overcome this problem, I finally opted to use an imaging oil, which allowed for long, stable, and uninterrupted experimental sessions.

2.8 Data analysis

High-speed recording of images in deep tissue, synchronized with the acquisition of EEG and EMG signals, generates data in the range of ~ 25 GB/h. The storage and processing of this data is a challenging task itself. In order to analyze the dataset, we generated a pipeline to analyze Ca^{2+} fluorescence data and electrophysiological recordings. The pipeline, schematized in Figure 10 contains two main branches, one for the processing of Ca^{2+} data and one for the processing of EEG/EMG data.

In vivo Ca^{2+} imaging data were analyzed offline with ImageJ (https://imagej.nih.gov/ij/) and with custom-made routines in Matlab (MATLAB v. R2018b, MathWorks) and Python (Van Rossum and Drake 2009). EEG and EMG signals were processed in the software Spike2 (CED Limited, Cambridge, UK). The analysis steps of the pipeline will be discussed in detail in the following paragraphs.

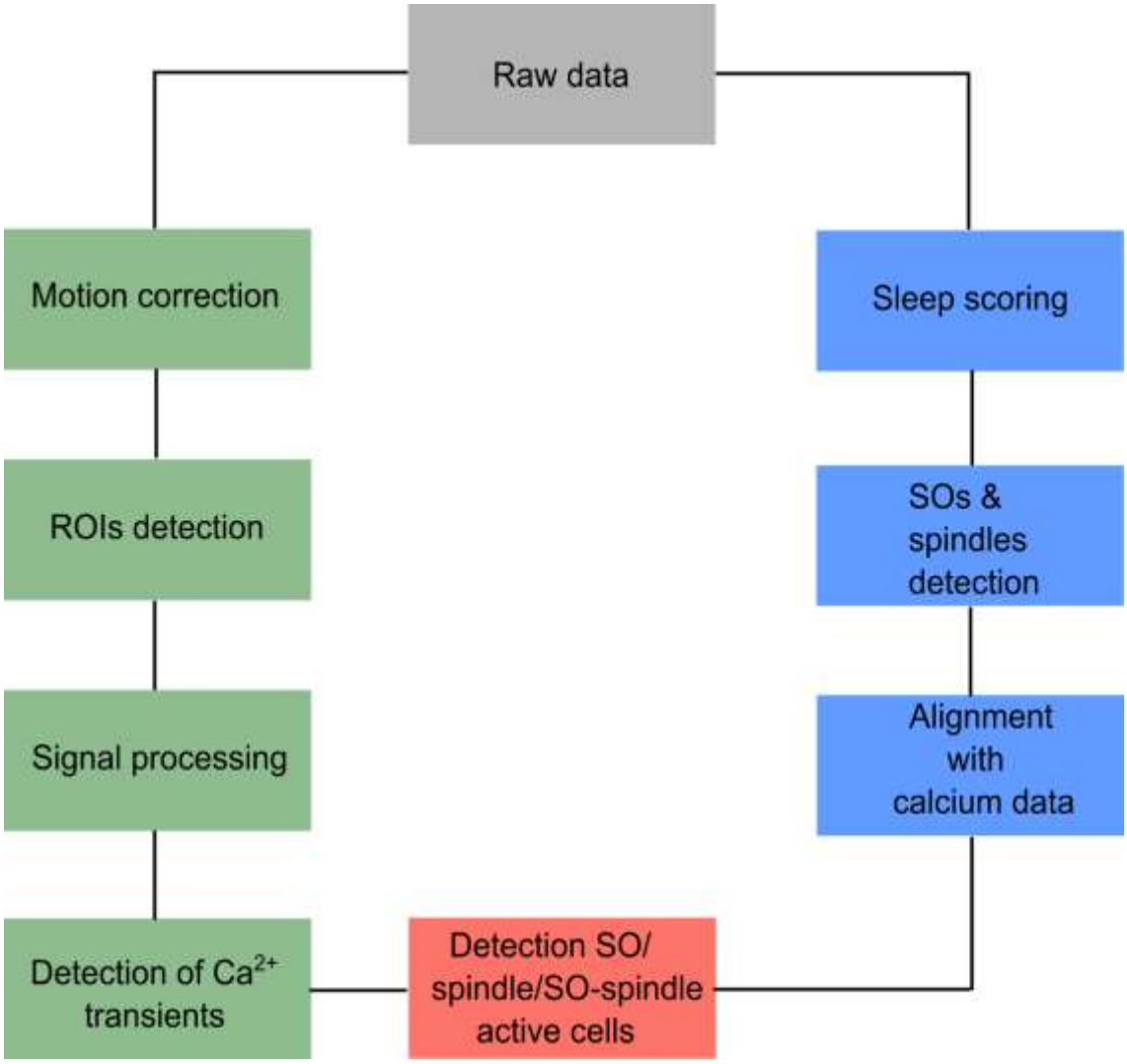

Figure 10. Analysis pipeline. The diagram illustrates the parallel pipeline analysis for imaging and electrophysiological data. The analysis starts with the motion correction of the data and the extraction of the fluorescence data. In parallel, sleep scoring and detection of SO, spindles, and spindle nesting in the upstate of SOs are performed. In the end, the two branches of analyses are merged to detect the SO-, spindle-, and SO+spindle-active cells

2.8.1 Motion correction

In order to reduce image distortions and remove motion artifacts, caused by the movement of the animals during the experiment, each 10-min-long time series was processed independently by using Suite2p (Pachitariu et al. 2016). First, in order to perform the registration, a reference image was generated. During an iterative alignment phase, a random set of frames are aligned in order to get a

sharp reference image. In order to do that, it was calculated the average of the top 20 frames with the highest correlation. Then, the reference image was refined by aligning iteratively the random frames to it and then generating again the reference image as the average of the best aligned frames. The images were aligned to the reference image in batches of 1000 frames. The rigid transformation was based on phase-correlation and evaluated the shift between images by normalizing the Fourier spectra. A default value for maximum x and y shift was chosen (0.1). Finally, in the case of residual motion artifacts, non-rigid registration was performed. The image was divided into blocks of 128 pixels, and phase correlation was applied for each block.
All recordings were visually inspected for residual motion, and all frames with uncorrected motion artifacts were identified and removed from any further analysis.

2.8.2 ROI detection

The motion-corrected time series were individually imported in Image J. A region of interest (ROI) was drawn over each cell based on the shape of the soma. Cell bodies were inspected for each run to ensure that the segmented cells were visible throughout the experimental sessions. Cells that were not visible in all runs, for example, because of the shifting of the FOV, were identified and lately removed from any further analysis. Visual inspections were also indispensable to avoid ROI overlaps and reduce the rate of detection of false positive Ca^{2+} transients lately. For each neuron, the fluorescence trace was calculated as the average pixel intensity.

2.8.3 Signal processing and transient detection

Then, the fluorescent traces were imported in Matlab and were preprocessed. Slow baseline fluctuations were removed from the fluorescent traces by analyzing the distribution of the fluorescence in a rolling window of 60 s and then subtracting

the 8th percentile (Dombeck et al. 2010). The baseline F_0 was calculated by measuring the 10th percentile of the corrected trace and was used to calculate relative changes in fluorescence (ΔF/F) for individual neurons. Finally, using the Matlab (MathWorks) peak detection function, the ΔF/F changes were counted as Ca^{2+} transients when the amplitude of the signal was higher than the tenfold standard deviation (SD) of the corresponding baseline noise. The baseline noise was estimated with a wavelet-based approach (Asavapanumas et al. 2019). A cell was considered as "active" if at least one Ca^{2+} transient was detected in the time-point considered. Upon visual inspection of the extracted Ca^{2+} traces, the frames which contained movement artifacts were removed from any further analysis.

2.8.4 Sleep scoring

Long-time scale electrophysiological data were divided into 10-s epochs, which were manually classified in order to discriminate the different sleep stages (wakefulness, SWS, and REM sleep). The sleep stages classification was supported by custom routines using the software Spike2. The criteria adopted for the classification were the frequency bands of the frontal and parietal EEG electrodes and the EMG power (Ruigt et al. 1989; Trachsel et al. 1988; Neckelmann et al. 1994). Wakefulness was characterized by high and mixed frequencies in EEG and high amplitude in the EMG signal. SWS was identified by high amplitude and low-frequency oscillations (0.5-4 Hz), as well as sleep spindles (7-15 Hz) in the EEG signal, accompanied by a strong reduction of the muscular tone. REM sleep was defined by a reduced and faster frequency in EEG, resembling the features of the awake condition, high power in the theta band (6-10 Hz), especially visible in the parietal electrode, and complete suppression of the muscular tone (Figure 11 A). All epochs including signal saturated or movement artifacts in the EEG signals, were excluded from any further analyses. During the training and imaging sessions, sometimes we have also recorded the pupil size of the experimental animal, known to reflect its

behavioral state. Indeed, as reported in Yüzgeç et al. 2018, the pupil size tended to dramatically decrease during sleep, especially during REM sleep (Figure 11 B). Only animals that presented a naturally occurring sleep, consisting of alternations between SWS and REM sleep, were included in the analysis.

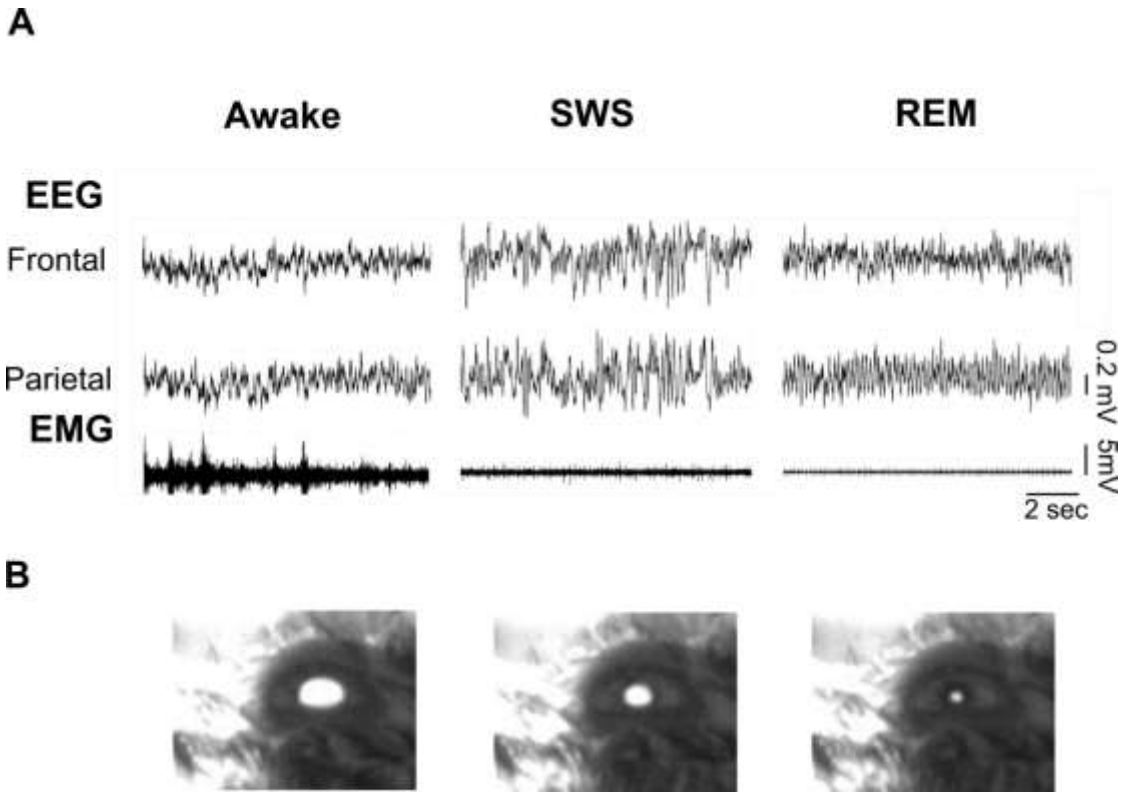

Figure 11. Alternation of brain states. (A) EEG (top) and EMG (bottom) recordings were recorded simultaneously to distinguish the brain states. (B) Images of the pupil across brain states during the imaging session with back infrared illumination.

2.8.5 Detection of sleep spindles and SOs

The algorithms for the detection of sleep spindles and SOs were adopted from previous studies (David *et al.*, 2013; Niethard, *et al.*, 2021). band-pass filtered between 7-15 Hz Sleep spindles were detected in EEG recordings, and rectified. Interpolation was used to yield the envelope for the frequency band of interest. A spindle event was identified whenever the envelope exceeded a threshold, based on the 1.5 SD of the filtered signals during SWS for a duration of 0.5-3 s. The

onset and the end of the spindle event were detected as the positive and negative envelope crossings, respectively. For the detection of SOs, the signals were band-pass filtered between 0.1-4-5 Hz. All positive-to-negative zero-crossings were marked. The event was marked as a SO if the duration between two succeeding positive-to-negative crossings was between 0.4 and 2 s and if the minimum-to-maximum amplitude was > 66.6% of the average of the respective amplitude values across the entire recording. Finally, when the onset of a spindle happened in the interval between the onset and the positive half-peak of a SO, it was identified as a SO+spindle event (Niethard et al. 2018).

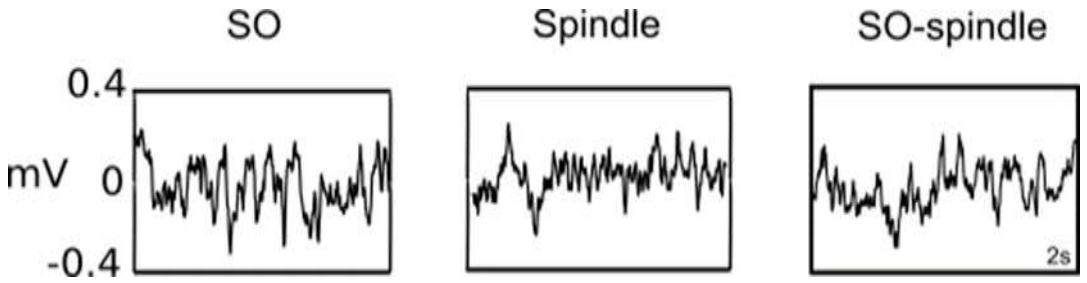

Figure 12. Representative traces of EEG during SWS, containing SOs, sleep spindles, or spindles nesting in the upstate of the SO, on an expanded time scale (2 seconds).

2.8.6 Alignment of the signals

After the scoring of the brain state activity and the detection of the peaks of Ca^{2+} transients from the pyramidal neurons in CA1, the data were loaded on Python and were aligned in time. During the acquisition of the images, the shutter of the microscope opened immediately prior to the beginning of the time series acquisition, and it closed at the end of it. The electrical signal coming from the opening of the shutter between the time series was acquired simultaneously to the EEG and EMG signals, and was used afterwards for the alignment of the signals (Figure 13).

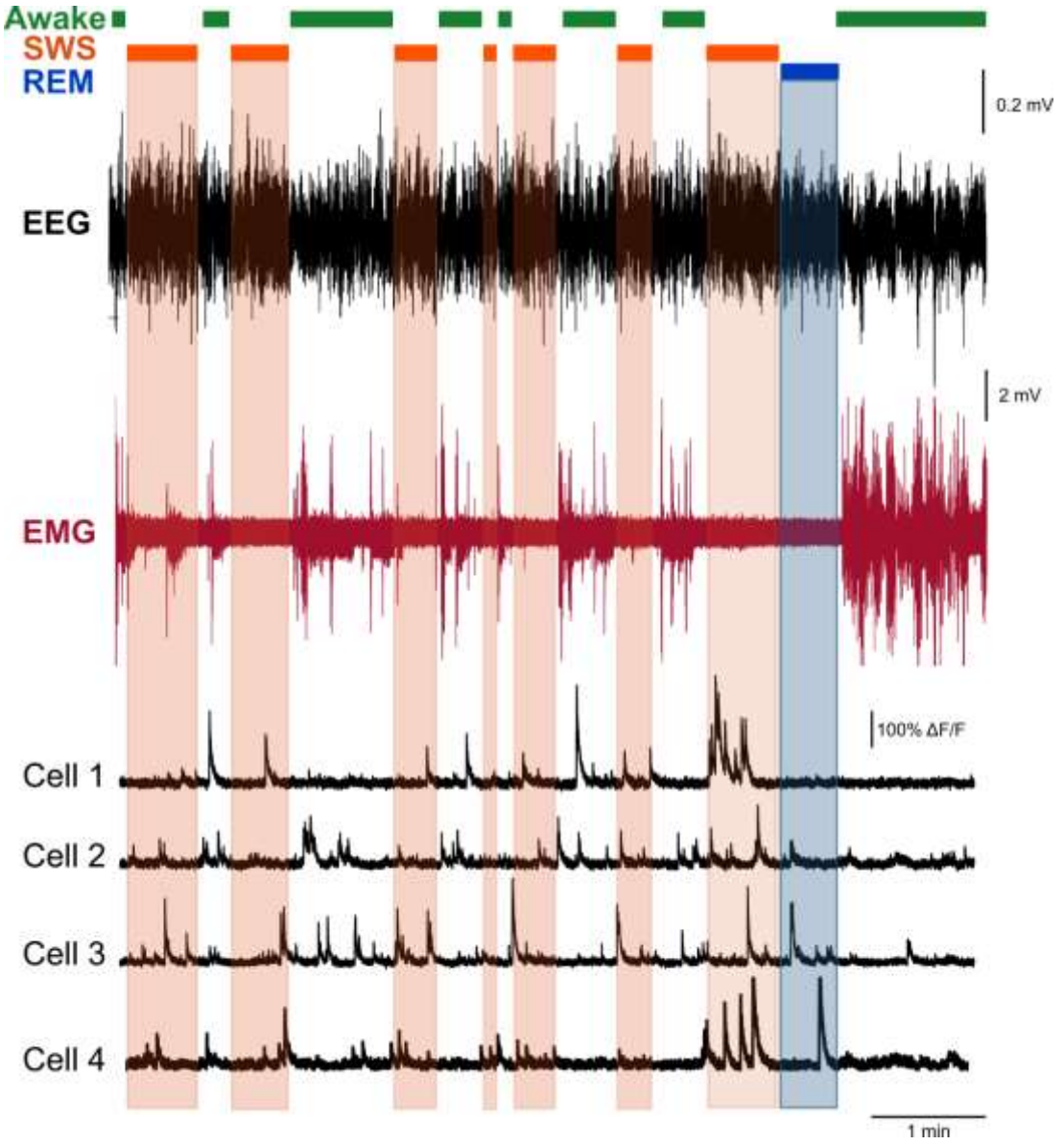

Figure 13. An example of an alignment of the neuronal Ca^{2+} signals with EEG and EMG recordings: Sample recording of wake (green), SWS sleep (orange) and REM sleep (blue) episodes, along with the respective EEG (black) and EMG (red) traces. Bottom traces (black) show the corresponding Ca^{2+} signals from 4 representative pyramidal cells

2.8.7 Detection of spindle-active/inactive and SO-active/inactive cells

For each cell and for each epoch, we calculated the difference between the mean frequency of the Ca^{2+} transients during a detected oscillatory event (i.e., SOs, spindles or SO+spindles) and the remaining period of the respective SWS

episode (Niethard et al. 2021). All cells with a positive difference were defined as SO-, spindle-, or SO+spindle-active cells, respectively, whereas the cells with a negative difference were considered as SO-, spindle-, or SO+spindle-inactive cells. Examples of such cells are shown in (Figure 14).

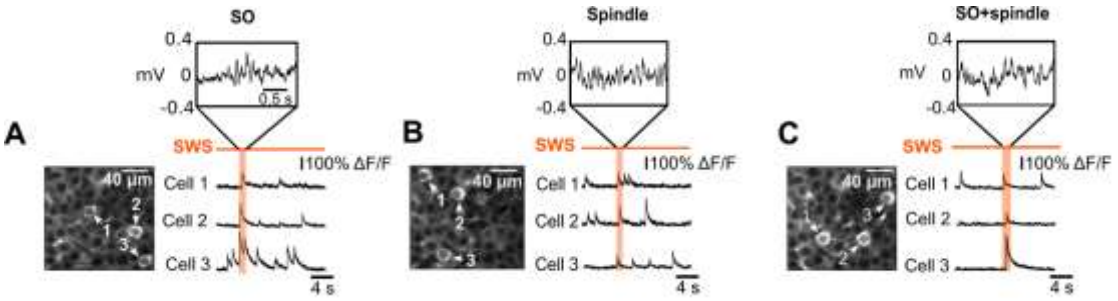

Figure 14. Identifying cells, active during SWS-related electrical activity patterns involved in sleep-dependent memory processing. (A-C) Mean images (average of 200 frames) showing the Ca^{2+} signals of the cells (labeled with the respective number in the left panel), active during slow oscillations (SOs) (A), sleep spindles (B) or SO+spindle (C). The vertical orange bands mark the time of occurrence of the respective electrical events, shown in inserts on an expanded time scale.

2.8.8 Activity across brain states

Analyses of cellular activity across brain states were performed by considering the frequency (Hz) and the amplitude (ΔF/F) of the detected Ca^{2+} transients. Comparative analyses across states were performed by measuring the average frequency and amplitude for each epoch.

Based on previous work (Grosmark et al. 2012), we aimed also to evaluate the slow changes in the activity within sleep. The epochs were divided into thirds, and the mean frequency and amplitude of Ca^{2+} transients were calculated for the 1^{st}, 2^{nd}, and 3^{rd} part of each epoch.

2.8.9 Transition analysis

To measure the number of active cells at the transition between brain states, we considered couples of brain states (e.g., awake-SWS). The states were divided into two windows with duration of 20 seconds (prior to transition) and 60 seconds (post-transition), respectively. Each window was subdivided into bins of 10 seconds (the time resolution used for the sleep scoring), and for each bin the cumulative number of active cells was counted.

2.8.10 Velocity of recruitment across brain states

The velocity of the recruitment of CA1 pyramidal cells across brain states for each normalized epoch was calculated as the empirical cumulative distribution function (ECDF) of cells activated for the first time at each time point. The length of each epoch was normalized to 1 second.

2.8.11 Data and statistical analysis

Box plots illustrate the median ± interquartile range (IQR) of the respective dataset. Statistics was performed with R (R Core Team 2016). Shapiro-Wilk test was adopted to check the normality of individual datasets. Kolmogorov-Smirnov test was performed to evaluate normality in the distributions of the standard deviations across SWS_n and SWS_{n+1}. In order to overcome the lack of normality and balanced groups, a permutation-based ANOVA (Wheeler and Torchiano 2016) was used for two or more paired comparisons, and in the latter case, it was followed by Tukey's *post-hoc* test.
For the correlation analyses of two variables, the Winsorized correlation (Mair and Wilcox 2020), a robust method to reduce the influence of extreme values was applied. Differences were considered significant if $p < 0.05$.

3. Results

First, we investigated how CA1 hippocampal pyramidal neurons modulate their activity across naturally occurring cycles of sleep and wakefulness using *in vivo* 2-photon-Ca^{2+} imaging (Figure 9). For this, we simultaneously recorded EEG and EMG in 7 mice that expressed a genetically encoded Ca^{2+} indicator (GCaMP7b). The fidelity for pyramidal neuron detection in CA1 was high, considering that the ratio of CA1 excitatory-inhibitory neurons is 120:1 (Jinno and Kosaka 2006). Based on EEG and EMG signals brain states were classified as wake, SWS or REM sleep (Figure 13; see methods). SWS was characterized by reduced muscular tone, high amplitude, and slow frequency waves (1-4 Hz) in the EEG, and by the presence of characteristic oscillations, like sleep spindles (10-15 Hz) and SOs (< 0.1 Hz). Theta frequency (5-10 Hz) EEG oscillations and complete muscular atonia were used as hallmarks of REM sleep. Mice spent 53% of the time awake, with a mean epoch duration of 84 ± 6 s seconds, and the remaining time sleeping (SWS 40%, mean epoch duration of 63 ± 1.99 s, REM sleep 7%, mean epoch duration 84 ± 6.1 s; Figure 15 A and B; $F = 5.7$, $p < 0.01$).

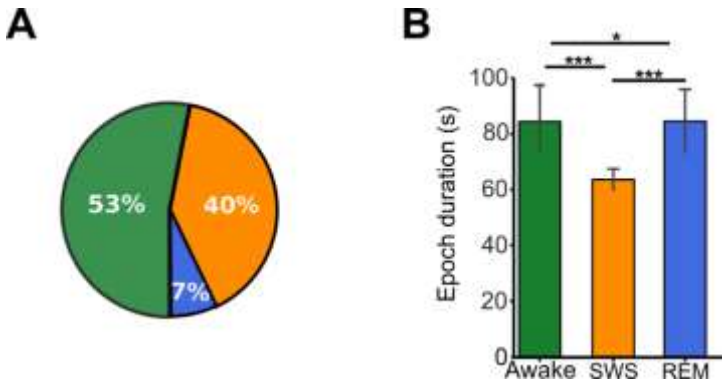

Figure 15. Sleep statistics. (A) Pie chart illustrating the percentage of recording time the animals spent in awake (green), SWS (orange) and REM (blue) state (35 h in total, 1 session per animal, n=7 mice). (B) Bar graph illustrating mean bout durations of the three brain states (n=7 mice, 856 awake, 854 SWS and 114 REM epochs). Data are shown as mean ± SEM. Significant changes are indicated by asterisks (*$p < 0.05$, **$p < 0.01$, ***$p < 0.001$; permutation-based ANOVA followed by Tukey's post-hoc test).

3.1 How does the Ca^{2+} signaling of CA1 pyramidal neurons evolve across brain states?

The imaging of neuronal Ca^{2+} transients with GECIs reflect action potential spiking of the individual cells (Yuste 2011). We evaluated the neuronal activity as changes in the GECI fluorescence, taking into consideration both frequency and amplitude of Ca^{2+} transients. Simultaneous Ca^{2+} imaging and sleep recordings of head-fixed naturally sleeping mice revealed brain-state specific activity of CA1 neuronal population. For example, the number of active cells differed across brain states. During wake the activity was sparse: only 28% of CA1 pyramidal cells were active. During sleep, the fraction of active cells progressively increased, leading to 42% active cells during SWS and 48% active cells during REM sleep (Figure 16 B; $\chi^2 = 8.82$, $p < 0.05$).

The cells showed the highest frequency of Ca^{2+} transients during SWS ($0.033 \pm 4 \times 10^{-4}$ Hz), intermediate during wake ($0.030 \pm 6 \times 10^{-4}$ Hz), and lowest during REM sleep ($0.025 \pm 9 \times 10^{-4}$ Hz) (Figure 17 A and C; $F = 11.91$, $p < 0.001$) (see Table 1). However, the median amplitude of the Ca^{2+} transients, had opposite dynamics, with the highest median amplitude during REM sleep ($120\% \pm 10^{-2}$ $\Delta F/F$) and no significant difference between SWS ($104\% \pm 4 \times 10^{-3}$ $\Delta F/F$) and wake ($105\% \pm 5 \times 10^{-3}$ $\Delta F/F$) (Figure 17 B and D) ($F = 99.27$, $p < 0.001$) (see Table 1).

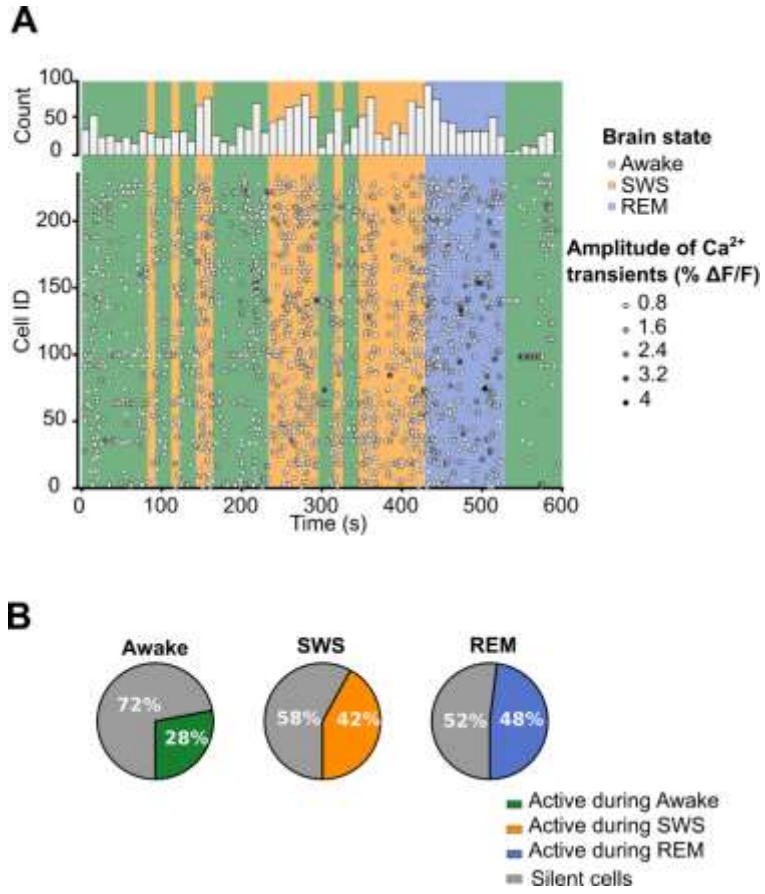

Figure 16. Temporal pattern of cellular activity across brain states. (A) Rasterplot showing the activity of 236 CA1 pyramidal cells during a 10-min-long recording period. The vertical lines indicate the brain state: awake (green), SWS (orange) and REM (light blue). Each dot represents a Ca^{2+} transient, whose amplitude is coded using a gray scale, as indicated. A histogram (top) gives the cumulative number of active cells in each 10-second-long bin. (B) Pie charts illustrating the fraction of active and silent pyramidal cells across brain states (n=1335 cells from 7 mice). The distributions are significantly different between the 3 brain states (Chi-square test, $\chi^2 = 8.82$, $p < 0.05$).

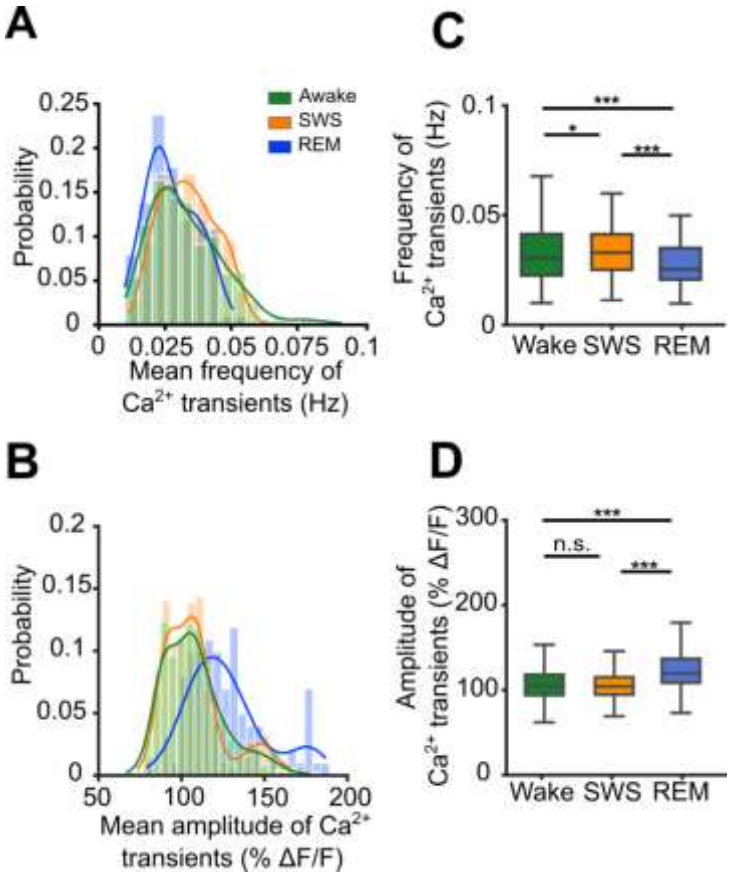

Figure 17. Distinct modulation of cellular activity across brain states. Normalized histograms of mean frequency (A) and amplitude (B) of Ca^{2+} transients across different brain states (here and in (C, D) n=7 mice, 517 awake epochs, 641 SWS epochs, 103 REM epochs). Box-and-whisker plots showing the median (per epoch) frequency (C) and amplitude (D) of Ca^{2+} transients across different brain states. *p < 0.05, ***p < 0.001; permutation-based ANOVA followed by Tukey's post-hoc test.

Table 1. Summary of frequencies and amplitudes of Ca^{2+} transients across brain states and *P* values for Figure 17.

Figure	Data (median ± IQR)	*P* value
Figure 17 A	Awake: 0.03 ± 6 x 10^{-4} Hz SWS: 0.033 ± 4 x 10^{-4} Hz REM: 0.025 ± 9 x 10^{-4} Hz	Awake vs SWS: p = 0.02 SWS vs REM: p = 2.8 x 10^{-7} Awake vs REM: p = 2.8 x 10^{-4}
Figure 17 B	Awake: 105% ± 8 x 10^{-3} ΔF/F SWS: 105% ± 7 x 10^{-3} ΔF/F REM: 122% ± 2 x 10^{-2} ΔF/F	Awake vs SWS: p = 0.8 SWS vs REM: p < 0.001 Awake vs REM: p < 0.001

3.2 Velocity of cell recruitments across brain states

Next, we investigated the dynamics of cell recruitment during wake, SWS, and REM sleep. In general, it seemed that during wake, the fraction of recruited cells was on average lower compared to SWS and REM sleep, confirming the pronounced sparseness in activity observed during wake. However, we observed that across all brain states, the fraction of activated neurons tended to increase with epoch duration but with different rates (Figure 18 A). For this reason, we normalized the length of the epochs and then quantified the velocity of recruitment by calculating, for each epoch, the fraction of neurons, which were activated at a given time (the empirical cumulative distribution function (ECDF)) of the neurons across in each brain state (Figure 18 B). We found that the recruitment was slowest during wake, intermediate during SWS, and fastest during REM sleep**,** resembling an exponential curve ($F = 391.8$, $p < 0.001$). The averaged vectors in Figure 18 C summarize the different velocities of recruitment across brain states.

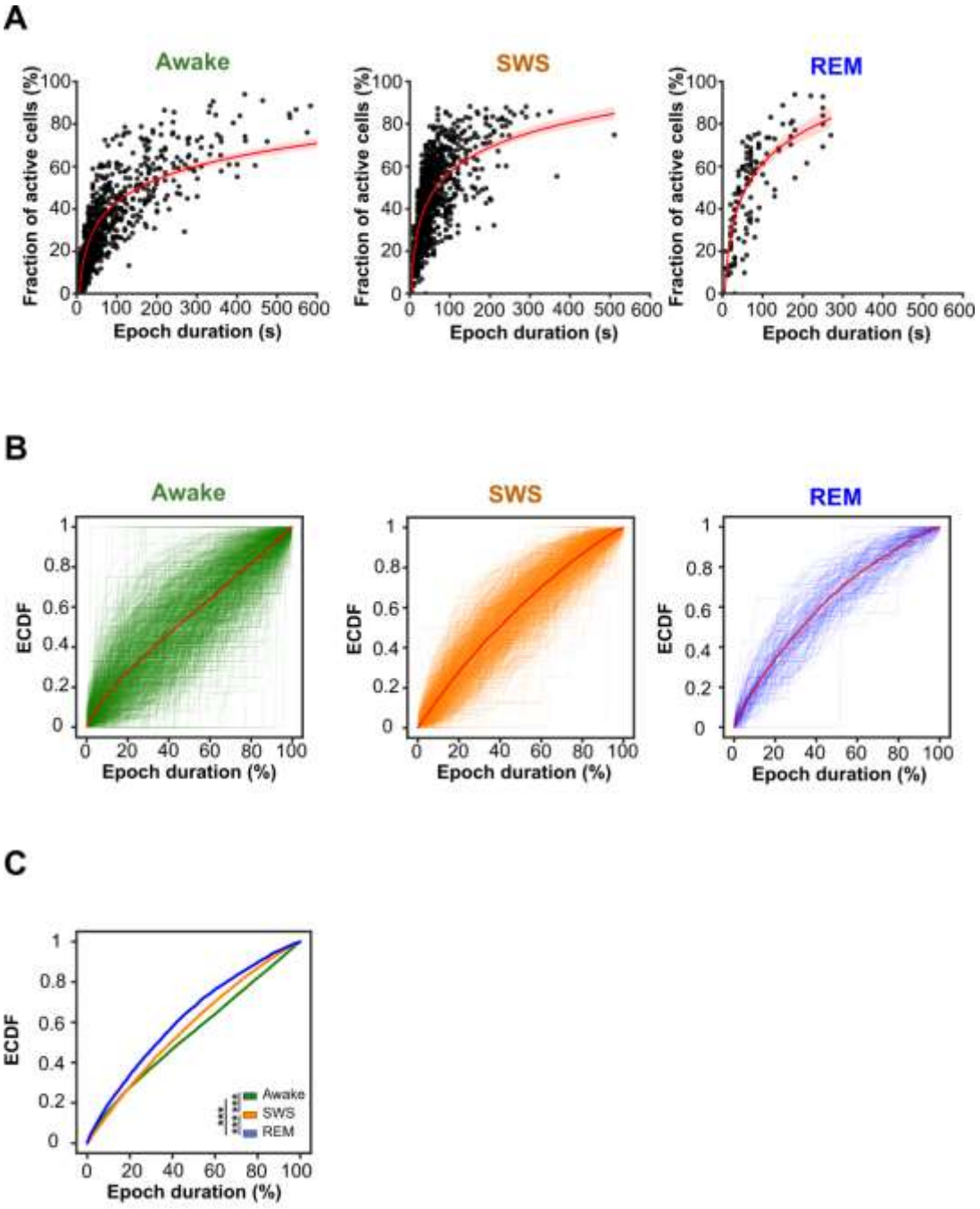

Figure 18. **Longer epochs recruit a higher fraction of cells in all brain states.** (A) Scatter plots showing the fraction of cells, active during a given epoch, as a function of epoch duration across wake, SWS and REM sleep. Red lines show the Kernel density estimations for the scatter plots. (B) Brain state-specific empirical cumulative distribution functions (ECDFs), illustrating for each epoch the temporal involvement of the cells in the network activity. (C) The averaged ECDF vectors for the three brain states (***$p < 0.001$). ***$p < 0.001$; permutation-based ANOVA followed by Tukey's post-hoc test.

.

3.3 Number of recruited cells at the brain state transitions

Next, we investigated how the cell recruitment changed during brain state transitions. The number of active cells increased during the transition from wake to SWS (Figure 19 A; F = 35.02, $p < 0.001$) and decreased at transitions from SWS to wake (Figure 19 B; F = 58.84, $p < 0.001$). Transitions from SWS to REM sleep were characterized by a decrease in cell recruitment (Figure 19 C; F = 5.6, $p < 0.05$), which became even more pronounced during REM to wake transitions (Figure 19 D; F = 40.57, $p < 0.001$).

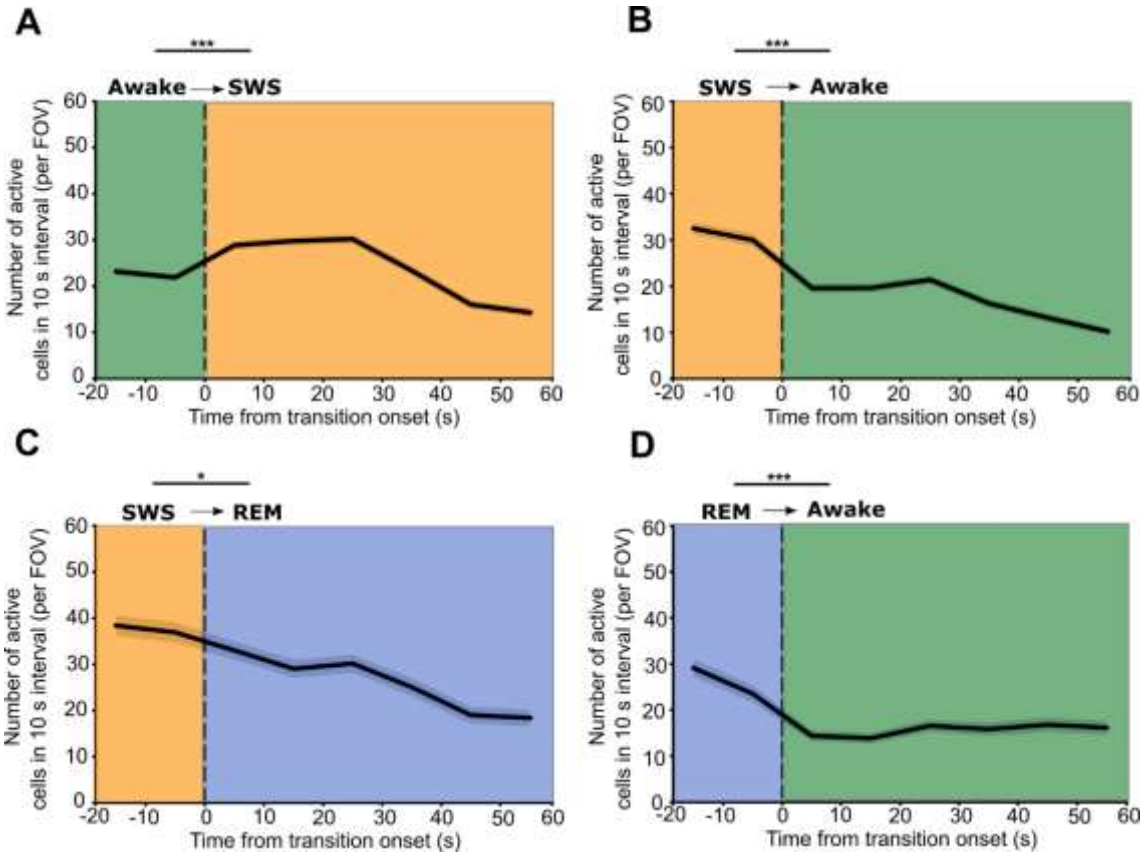

Figure 19. The number of active CA1 pyramidal cells is strongly affected by the brain state transition. Brain states are color-coded: awake (green), SWS (orange) and REM (blue). Time windows of 20 and 60 seconds were divided in 10-second bins. (A-D) Plots depicting mean (per state transition) numbers of active cells in 10-second-long bins (n = 355 awake to SWS (A), n = 253 SWS to awake (B), n = 93 SWS to REM (C) and n = 79 REM to awake (D) transitions. *$p < 0.05$, ***$p < 0.001$; permutation-based ANOVA.

3.4 Does REM sleep modulate the activity of pyramidal cells?

Following the idea that sleep renormalizes the excitability of the network (Vyazovskiy et al. 2008; Bellina et al. 2008; Olcese et al. 2010), we compared Ca^{2+} transient frequencies between the first and last third of each SWS and REM sleep epoch. In contrast to previously published work based on electrophysiological recordings (Grosmark et al. 2012), we did not find significant modulation of the Ca^{2+} transient frequency from the beginning to the end of SWS and REM sleep episodes (Figure 20 A-B; $p > 0.05$ for both brain states).

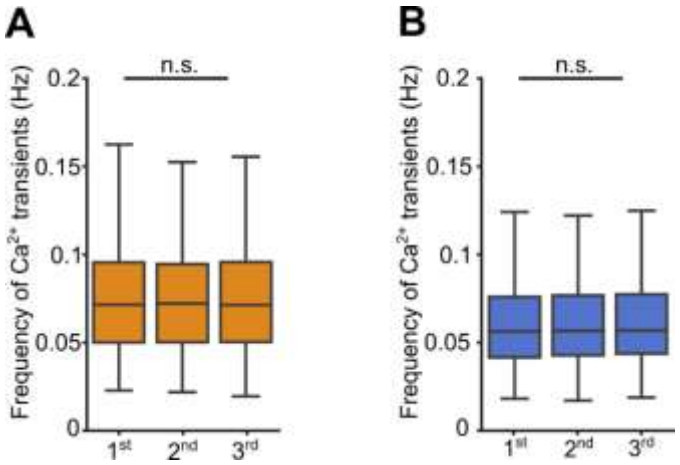

Figure 20. **The median frequencies of Ca^{2+} transients remain stable during SWS and REM sleep epochs.** Box-and-whisker plots showing the median frequencies of Ca^{2+} transients within the 1st, the 2nd and the 3rd thirds of epochs of (A) SWS and (B) REM sleep. $p > 0.05$, Permutation-based ANOVA.

Given that we have found reduced frequency of Ca^{2+} transients during REM sleep, we compared the activity between two consecutive SWS episodes (SWS_n and SWS_{n+1}) for all episodes that were interleaved by an episode of REM sleep (Figure 21 A) and, as a control, by an episode of wake (Figure 21 B). Again, contrary to previously published works based on electrophysiological recordings (Grosmark et al. 2012; Miyawaki and Diba 2016; Watson et al. 2016), we did not find any significant modulation of Ca^{2+} transient frequencies between SWS_n and SWS_{n+1} episodes interleaved either by REM sleep ($F = 5.3$, $p > 0.05$) or wake ($F = 2.5$, $p > 0.05$) (see Table 2).

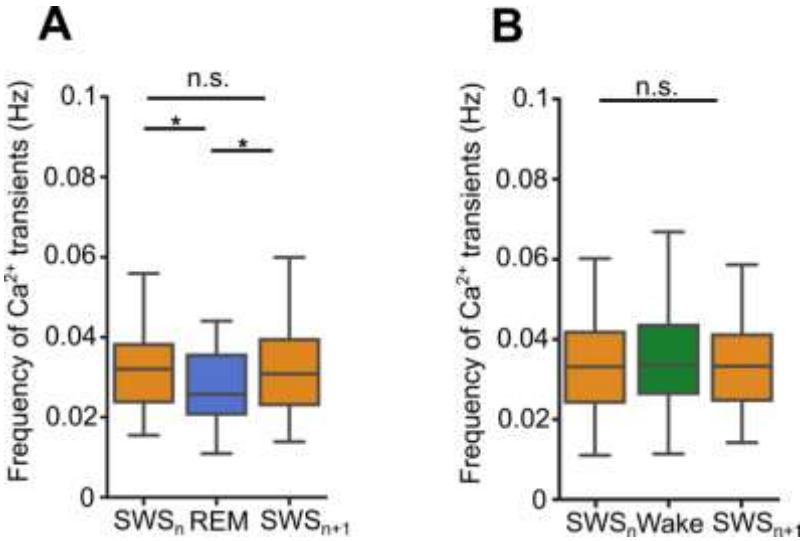

Figure 21. The SWS-specific activity of the entire CA1 cell population is not changed by the interleaved REM sleep or wake epochs. Box-and-whisker plots showing median (per epoch) frequencies of Ca^{2+} transients during two epochs of SWS interleaved by (A) REM (n = 78 triplets) or (B) wake (n = 192 triplets). *$p < 0.05$; permutation-based ANOVA followed by Tukey's post-hoc test. Note that the overall activity of pyramidal cells is not changed across epochs of SWS either when are interleaved by REM or wake.

Table 2. Summary of frequencies of Ca^{2+} transients across SWS epochs interleaved by REM sleep or awake and *P* values in Figure 21.

Figure	Data (median ± IQR)	*P* value
Figure 21 A	SWS_n: 0.032 ± 10^{-3} Hz REM: 0.025 ± 10^{-3} Hz SWS_{n+1}: 0.03 ± 10^{-3} Hz	SWS_n vs REM: $p = 0.014$ SWS_{n+1} vs REM: $p = 0.05$ SWS_n vs SWS_{n+1}: $p = 0.9$
Figure 21 B	SWS_n: 0.033 ± 7 x 10^{-4} Hz Awake: 0.033 ± 9 x 10^{-4} Hz SWS_{n+1}: 0.033 ± 7 x 10^{-4} Hz	SWS_n vs Awake: $p = 0.3$ SWS_{n+1} vs Awake: $p = 0.5$ SWS_n vs SWS_{n+1}: $p = 0.9$

Similar results were also observed when we considered the amplitude of the detected Ca^{2+} transients ($p > 0.05$). No modulation of activity was observed across SWS epochs, neither when interleaved by REM (Figure 22 A; F = 16.79, $p < 0.001$) nor wake (Figure 22 B; F = 0.169, $p > 0.8$). However, as also reported in Figure 16, we found that the amplitude of Ca^{2+} transients was higher during REM sleep (see Table 3).

Interestingly, when we compared the distribution of standard deviations for the frequency of Ca^{2+} transients between SWS_n and SWS_{n+1} we noticed a trend, that did not reach the statistical significance, but showed an increase of the variability across epochs of SWS interleaved by REM (Figure 31 A).

This led us to hypothesize that the entire cell population might be not uniformly regulated across sleep.

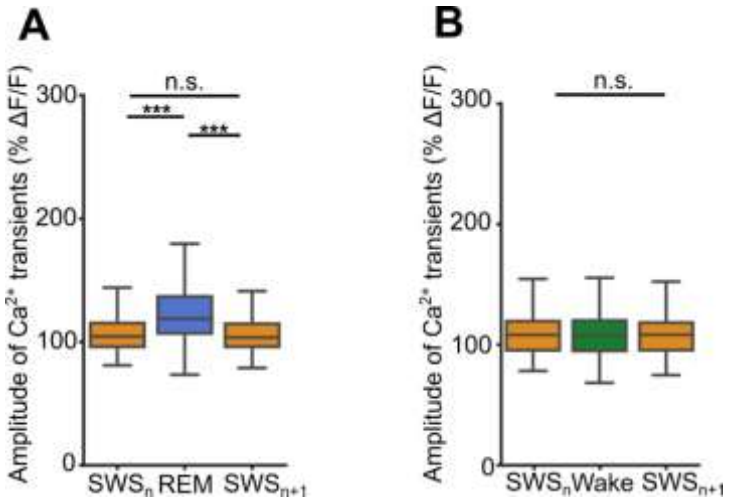

Figure 22. The SWS-specific amplitudes of Ca^{2+} transients of the entire CA1 cell population are not changed by the interleaved REM sleep or wake epochs. Box-and-whisker plot showing median (per epoch) amplitudes of Ca^{2+} transients during two epochs of SWS interleaved by REM (A, n = 78 triplets) or wake (B, n = 192 triplets). ***p < 0.001; permutation-based ANOVA followed by Tukey's post-hoc test.

Table 3. Summary of amplitudes of Ca2+ transients across SWS epochs interleaved by REM sleep or awake and *P* values in Figure 22.

Figure	Data (median ± IQR)	*P* value
Figure 22 A	SWS_n: 103% ± 2 x 10^{-2} ΔF/F REM: 120% ± 2 x 10^{-2} ΔF/F SWS_{n+1}: 100% ± 2 x 10^{-2} ΔF/F	SWS_n vs REM: p < 0.001 SWS_{n+1} vs REM: p < 0.001 SWS_n vs SWS_{n+1}: p = 0.8
Figure 22 B	SWS_n: 106% ± 10^{-2} ΔF/F Awake: 106% ± 10^{-2} ΔF/F SWS_{n+1}: 106% ± 10^{-2} ΔF/F	SWS_n vs Awake: p = 0.8 SWS_{n+1} vs Awake: p = 0.9 SWS_n vs SWS_{n+1}: p = 0.9

Altogether these results showed that in the *stratum pyramidale* of CA1, the number of active cells in the network tended to increase dramatically during both slow wave and REM sleep, showing higher velocity in cellular recruitment and the highest frequency of Ca^{2+} transients during SWS. This might suggest an increase in the excitability of the network specifically during sleep. For this, we decided to investigate deeper the role of sleep in the regulation of the network, with a focus on SWS and its characteristic oscillation patterns.

3.5 Detection of SO-active, spindle-active and SO+spindle-active cells

Considering the increased excitability of the network in CA1 occurring during sleep and the double role of sleep in preventing and promoting the downregulation of the activity (Tononi and Cirelli 2020), we decided to further investigate the cellular dynamics within SWS. Since SOs and sleep spindles play a central role for the consolidation of hippocampus-dependent memories during sleep, we dissected the neuronal population in subgroups of cells that were particularly active during solitary SOs and solitary spindles as well as during spindles that occurred during the SO upstate (SO-active, spindle-active and SO+spindle-active, respectively). For this, we calculated for each cell and for each epoch the difference between the mean frequency of the Ca^{2+} transients during a detected oscillatory event and the remaining period of the respective SWS episode (Figure 14) (Niethard et al. 2021). All cells with a positive difference were defined as SO-active, spindle-active, or SO+spindle-active cells, whereas the cells with a negative difference were considered SO-, spindle-, or SO+spindle-inactive cells.

In total, in 7 mice we identified 1556 solitary SO events, 2891 solitary spindles and 2251 spindles occurring during the upstate of SOs. The mean duration for SOs was 0.8 ± 6 x 10-3 s, spindles - 0.85 ± 6 x 10-3 s and SO+spindle - 0.82 ± 6 x 10-3 s. The density of all three event types strongly correlated with the frequency of Ca^{2+} transients during the respective SWS episode (SO: $r = 0.8$, $p < 0.001$; spindle: $r = 0.6$, $p < 0.001$; spindle-SO: $r = 0.72$, $p < 0.001$), underlying the impact of these oscillatory events on the cellular activity during SWS (Figure 23 A-C).

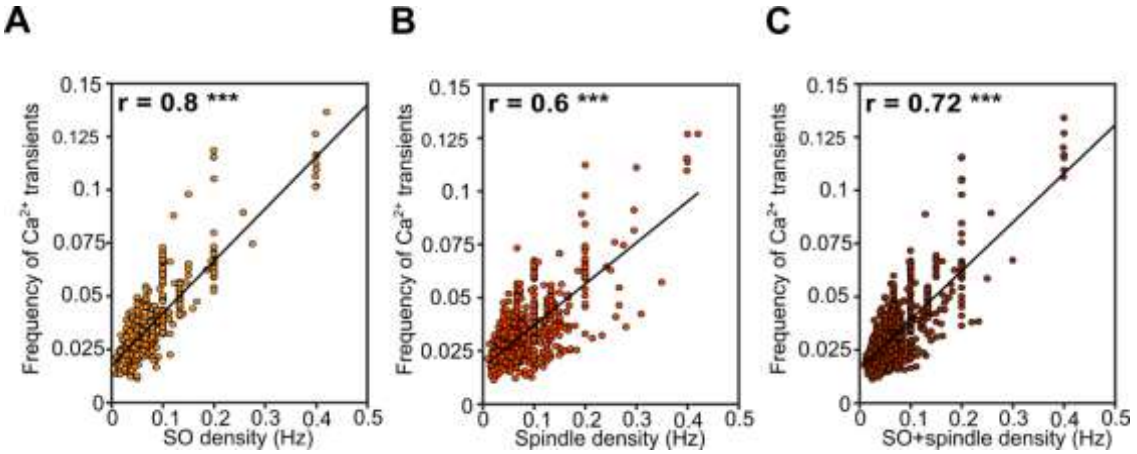

Figure 23. Activity of the entire CA1 cell population during SWS strongly correlates with the density of oscillatory events. Scatter plots showing the correlations between the mean frequency of Ca^{2+} transients during a given epoch of SWS and the density of SOs (A, n = 497), spindles (B, n = 581) and SO+spindles (C, n = 557). r values represent the coefficient of correlation. ***$p < 0.001$; Winsorized correlation.

In general, we found that sleep spindles occurred in a larger fraction of SWS (Figure 24 B; F = 7.07, $p < 0.001$) and had the highest density compared to the 2 other types of events (Figure 24 A; F = 42.48, $p < 0.001$) (see Table 4). Also, we found that the spindle power was higher when the spindles were nested in the upstate of the SO than in solitary spindles (Figure 24 D; F = 4.48, $p < 0.05$) (see Table 4).

On average, during an SWS episode SO-active, spindle-active as well as SO+spindle-active cells comprised 6%, 11% and 9% of active cells, respectively ($\chi^2 = 172.6$, $p < 0.05$). The rest of the neuronal population was mainly active outside of the detected oscillatory events. We found that SO-active cells and SO+spindle-active cells showed higher median activity during SWS compared to spindle-active cells (Figure 24 C; F = 11.59, $p < 0.001$) (see Table 4) and SO-, spindle- as well as SO+spindle-active cells showed significantly higher activity during SWS compared to the respective inactive cell group. The number of recruited cells between the identified oscillatory events did not differ ($p > 0.05$). No significant differences between the SO-, spindle- as well as SO+spindle-active cells cell clusters were observed when considering the amplitude of the detected Ca^{2+} transients.

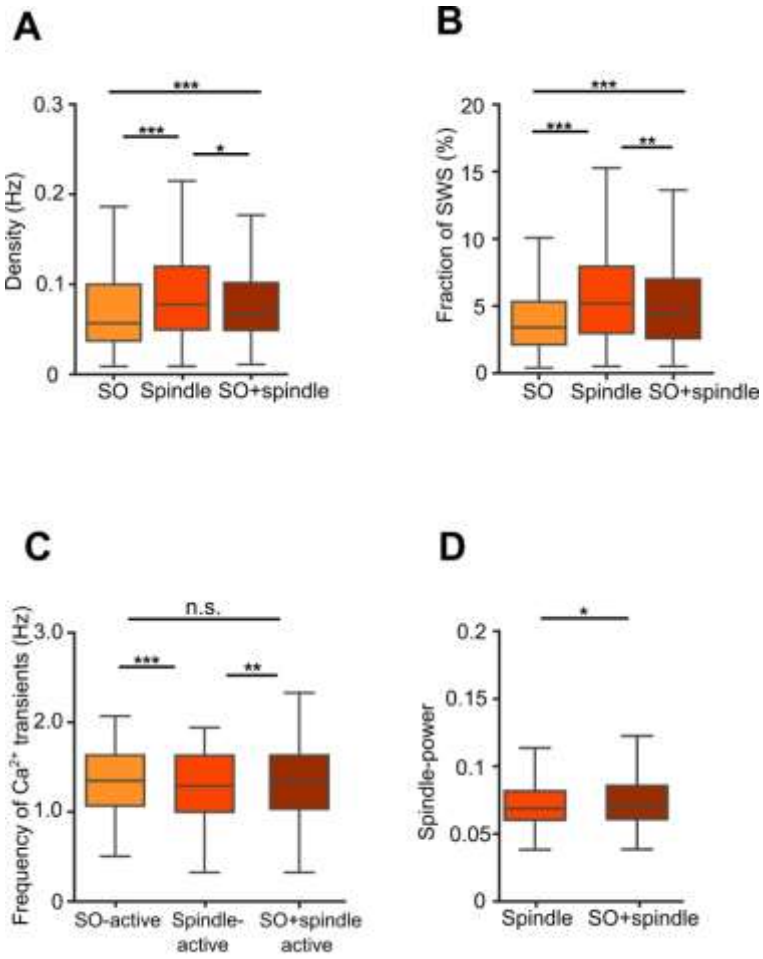

Figure 24. The neuronal population was dissected into three cell groups. (A) Box-and-whisker plot showing the median density of SOs (orange), spindles (red) and SO+spindles (maroon). (B) Box-and-whisker plot showing the median fraction (per epoch) of SWS spent in SOs, spindles and SO+spindles. (C) Box-and-whisker plot showing the median frequencies (per epoch) of Ca^{2+} transients in cells active during SO, spindles and SO+spindles. SOs, n = 497; spindles, n = 581; SO+spindles, n = 557). (D) Comparison of spindle power (spindles, n = 581; SO+spindles, n = 557). *p < 0.05, **p < 0.01, ***p < 0.001; permutation-based ANOVA followed by Tukey's post-hoc test.

Table 4. Summary of frequencies of Ca^{2+} transients for the SOs, sleep spindles and SO+spindle and respective identified subgroups of active cells and *P* values in Figure 24.

Figure	Data (median ± IQR)	*P* value
Figure 24 A	SO: 0.057 ± 3 x 10^{-3} Hz Spindle: 0.077 ± 2 x 10^{-3} Hz SO+Spindle: 0.066 ± 2 x 10^{-3} Hz	SO vs spindle: p < 0.001 SO vs SO+Spindle: p < 0.001 Spindle vs SO+Spindle: p = 0.04
Figure 24 B	SO: 3.42 ± 0.12 % Spindle: 5.2 ± 0.17 % SO+Spindle: 4.53 ± 0.16 %	SO vs spindle: p < 0.001 SO vs SO+Spindle: p < 0.001 Spindle vs SO+Spindle: p = 2.4 x 10^{-3}
Figure 24 C	SO: 1.34 ± 3 x 10^{-2} Hz Spindle: 1.29 ± 7 x 10^{-3} Hz SO+Spindle: 1.34 ± 8 x 10^{-3} Hz	SO vs spindle: p < 0.001 SO vs SO+Spindle: p = 0.5 Spindle vs SO+Spindle: p = 3 x 10^{-2}

3.6 Activity of the identified cell subgroups across brain states

Next, we evaluated how the activity of the detected subgroups of cells evolved across brain states (Figure 25). First, we tracked the cells belonging to one of the three subgroups, and evaluated their activity during SWS. Then, we considered how these cells were active during the previous wake and subsequent REM sleep episodes. As for the general population, we found that the frequency of Ca^{2+} transients was higher during SWS both for spindle-active cells (Figure 25 C-D; wake: 0.03 ± 2.7 x 10-3 Hz; SWS: 0.04 ± 4 x 10-3 Hz; REM: 0.027 ± 2.5 x 10^{-3} Hz) and SO+spindle-active cells (Figure 25 E-F; wake: 0.032 ± 3.3 x 10^{-3} Hz; SWS: 0.037 ± 5 x10-3 Hz; REM: 0.024 ± 2.7 x 10-3 Hz) (spindle-active: $F = 4.6$, $p < 0.05$; SO+spindle-active: $F = 3.5$, $p < 0.05$) (see Table 5). However, for both subgroups no significant differences were found between wake and REM sleep. Although SO-active cells showed a trend similar to the one described for the other two subgroups of cells, no significant difference was found (Figure 25 A-B; $p > 0.05$).

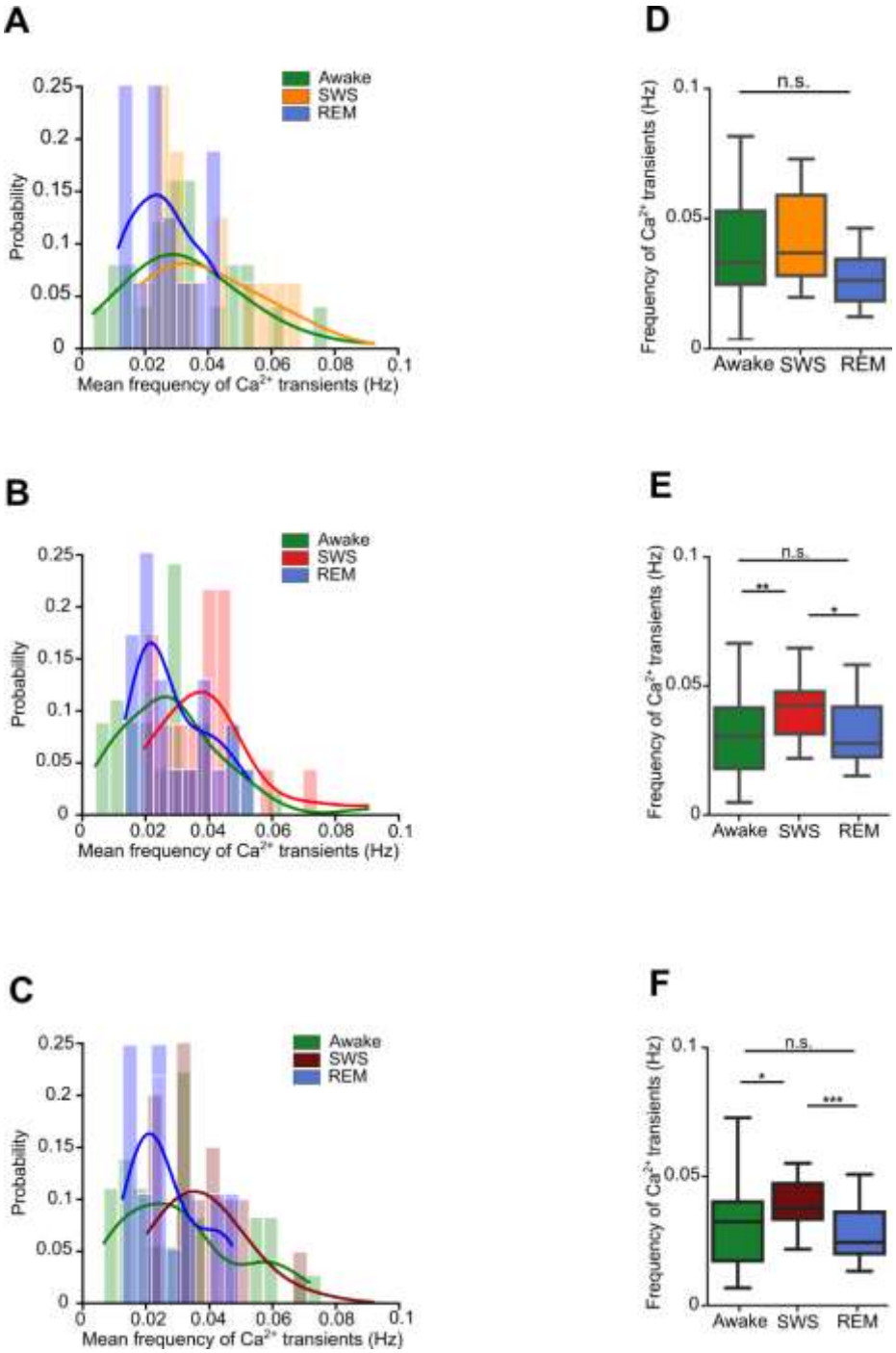

Figure 25. **Distinct modulation of frequencies of Ca^{2+} transients of SO-, spindle- and SO+spindle-active cells across brain states.** Normalized frequency histograms of SO-active cells (A, n = 64), spindle-active cells (B, n = 92) and SO+spindle-active cells (C, n= 80). Here and below n = 7 mice. Box-and-whisker plots showing the median (per epoch) frequencies of Ca^{2+} transients of SO-active cells (D, n = 64), spindle-active cells (E, n = 92) and SO+spindle-active cells (F, n= 80). For these analyses, cells, active during an oscillatory event during SWS, were tracked during the previous wake and subsequent REM sleep epoch. *$p < 0.05$, **$p < 0.01$, ***$p < 0.001$; permutation-based ANOVA followed by Tukey's post-hoc test.

Table 5. Summary of frequencies of Ca^{2+} transients across brain states for the SO, spindle- and SO+spindle-active cells and *P* values in Figure 25.

Figure	Data (median ± IQR)	*P* value
Figure 25 D	Awake: 0.033 ± 4 x 10^{-3} Hz SWS: 0.037 ± 7 x 10^{-3} Hz REM: 0.026 ± 2 x 10^{-3} Hz	Awake vs SWS: $p = 0.4$ SWS vs REM: $p = 0.2$ Awake vs REM: $p = 0.2$
Figure 25 E	Awake: 0.030 ± 2 x 10^{-3} Hz SWS: 0.04 ± 4 x 10^{-3} Hz REM: 0.027 ± 2 x 10^{-3} Hz	Awake vs SWS: $p = 0.01$ SWS vs REM: $p = 0.02$ Awake vs REM: $p = 0.9$
Figure 25 F	Awake: 0.032 ± 3 x 10^{-3} Hz SWS: 0.037 ± 5 x 10^{-3} Hz REM: 0.024 ± 2 x 10^{-3} Hz	Awake vs SWS: $p = 0.03$ SWS vs REM: $p < 0.001$ Awake vs REM: $p = 0.7$

Concerning the median amplitude of the detected Ca^{2+} transients, we found the highest values during REM, but no significant difference between wake and SWS both for spindle-active (Figure 26 C-D; $F = 6.8$, $p < 0.01$) (wake: 106% ± 3 x 10^{-2} ΔF/F; SWS: 113% ± 3 x 10^{-2} ΔF/F; REM 132% ± 4x10^{-2} ΔF/F) and SO+spindle-active cells (Figure 26 E-F; $F = 5.7$, $p < 0.01$) (wake: 101% ± 4 x 10^{-2} ΔF/F; SWS: 109% ± 4 x 10^{-2} ΔF/F; REM 121% ± 10^{-1} ΔF/F) (see Table 6). Although we observed a similar trend also for SO-active cells, the difference did not reach the level of statistical significance (Figure 26 A-B; $p > 0.05$).

When comparing the frequencies of Ca^{2+} transients between the first and last third of each SWS and REM sleep epoch we did not find any significant changes in Ca^{2+} signaling from the beginning to the end of SWS or REM sleep episodes for any of the three subgroups ($p > 0.05$ for all comparisons, permutation-based ANOVA).

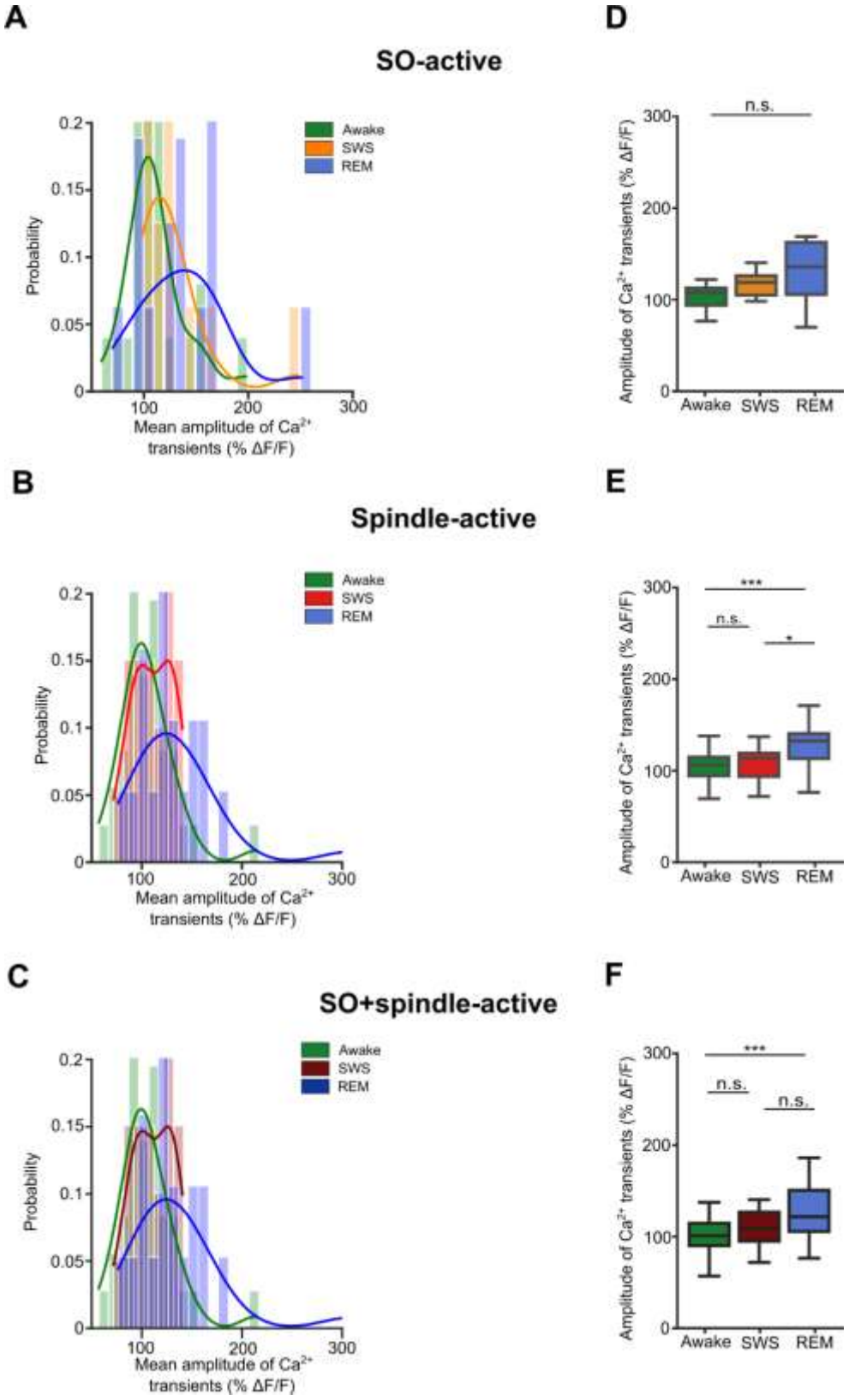

Figure 26. Distinct modulation of amplitudes of Ca^{2+} transients of SO-, spindle- and SO+spindle-active cells across brain states. Normalized amplitude histograms of SO-active cells (A, n = 64), spindle-active cells (B, n = 92) and SO+spindle-active cells (C, n= 80). Here and below n = 7 mice. Box-and-whisker plots showing the median (per epoch) amplitudes of Ca^{2+}

transients of SO-active cells (D, n = 64), spindle-active cells (E, n = 92) and SO+spindle-active cells (F, n= 80). For these analyses, cells, active during an oscillatory event during SWS, were tracked during the previous wake and subsequent REM sleep epoch. *$p < 0.05$, **$p < 0.01$, ***$p < 0.001$; permutation-based ANOVA followed by Tukey's post-hoc test.

Table 6. Summary of amplitudes of Ca^{2+} transients across brain states for the SO-, spindle- and SO+spindle-active cells and *P* values in Figure 27.

Figure	Data (median ± IQR)	*P* value
Figure 26 D	Awake: 107% ± 5 x 10^{-2} ΔF/F SWS: 119% ± 9 x 10^{-2} ΔF/F REM: 136% ± 10^{-1} ΔF/F	Awake vs SWS: $p = 0.1$ SWS vs REM: $p = 0.6$ Awake vs REM: $p = 0.06$
Figure 26 E	Awake: 106% ± 3 x 10^{-2} ΔF/F SWS: 113% ± 3 x 10^{-2} ΔF/F REM: 132% ± 4 x 10^{-2} ΔF/F	Awake vs SWS: $p = 0.7$ SWS vs REM: $p = 0.01$ Awake vs REM: $p < 0.001$
Figure 26 F	Awake: 101% ± 4 x 10-2 SWS: 109% ± 4 x 10-2 ΔF/F REM: 121% ± 10-1 ΔF/F	Awake vs SWS: $p = 0.45$ SWS vs REM: $p = 0.13$ Awake vs REM: $p < 0.001$

3.7 Does prior wake influence the activity during subsequent SWS?

Consistent with the idea that the activity during wake episodes might predict the activity of the cells during subsequent sleep, we analyzed the dynamics of ongoing Ca^{2+} signals of pyramidal cells across small sequences of brain states. For the entire population of CA1 pyramidal neurons, the frequency of ongoing Ca^{2+} signals did not change from wake to subsequent SWS ($p > 0.05$. Permutation-based ANOVA. Data not shown), and no correlation in activity as frequency of Ca^{2+} transient was observed. However, when we considered the three identified cell subgroups, we found that neurons active during SO+spindle events significantly increased their activity from wake to subsequent SWS (Figure 27 C; $F = 4.3$, $p < 0.05$). Similar effect was observed for the other two subgroups (SO- and spindle-active cells) but the difference did not reach the level of statistical significance (Figure 27 A-B; $p > 0.05$ for both groups).

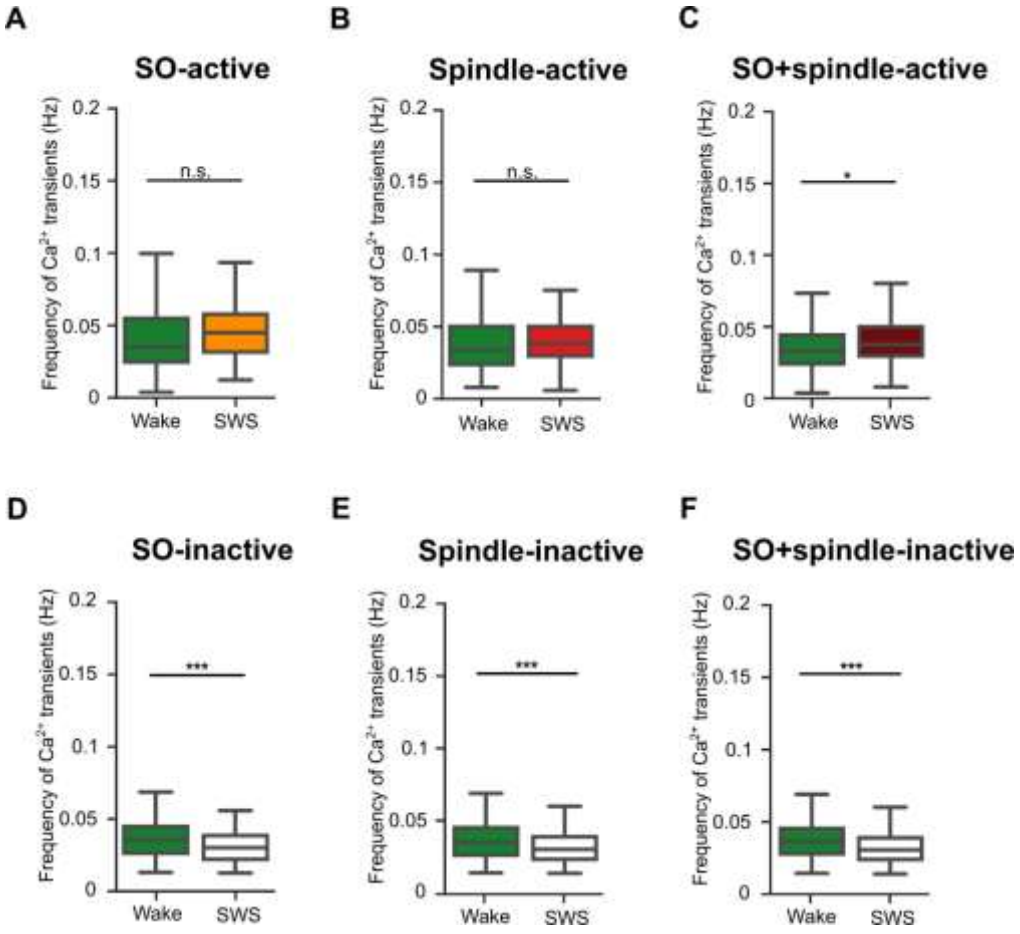

Figure 27. The activity of SO+spindle-active cells during SWS increases from the previous wake. Box-and-whisker plots showing the median (per epoch) frequencies of Ca^{2+} transients in sequences of wake and SWS for SO-active cells (A, n = 210), spindle-active cells (B, n = 248) and SO+spindle-active cells (C, n = 238). (D-F) Box-and-whisker plots showing the median (per epoch) frequencies of Ca^{2+} transients of cells, inactive during SO (D, n=210), spindles (E, n=248), SO+spindles (F, n=238). *p < 0.05, ***p < 0.001; permutation-based ANOVA. Note that SO+spindle-active cells significantly increase their activity during SWS, while the inactive cells show a significant decrease in activity.

Also, the activity of neurons active during SO+spindle was slightly correlated between epochs of wake and subsequent SWS (Figure 28 C; r = 0.2, p = < 0.01), suggesting that cells increasing their activity during a wake period might have been involved in the encoding of new and relevant information.

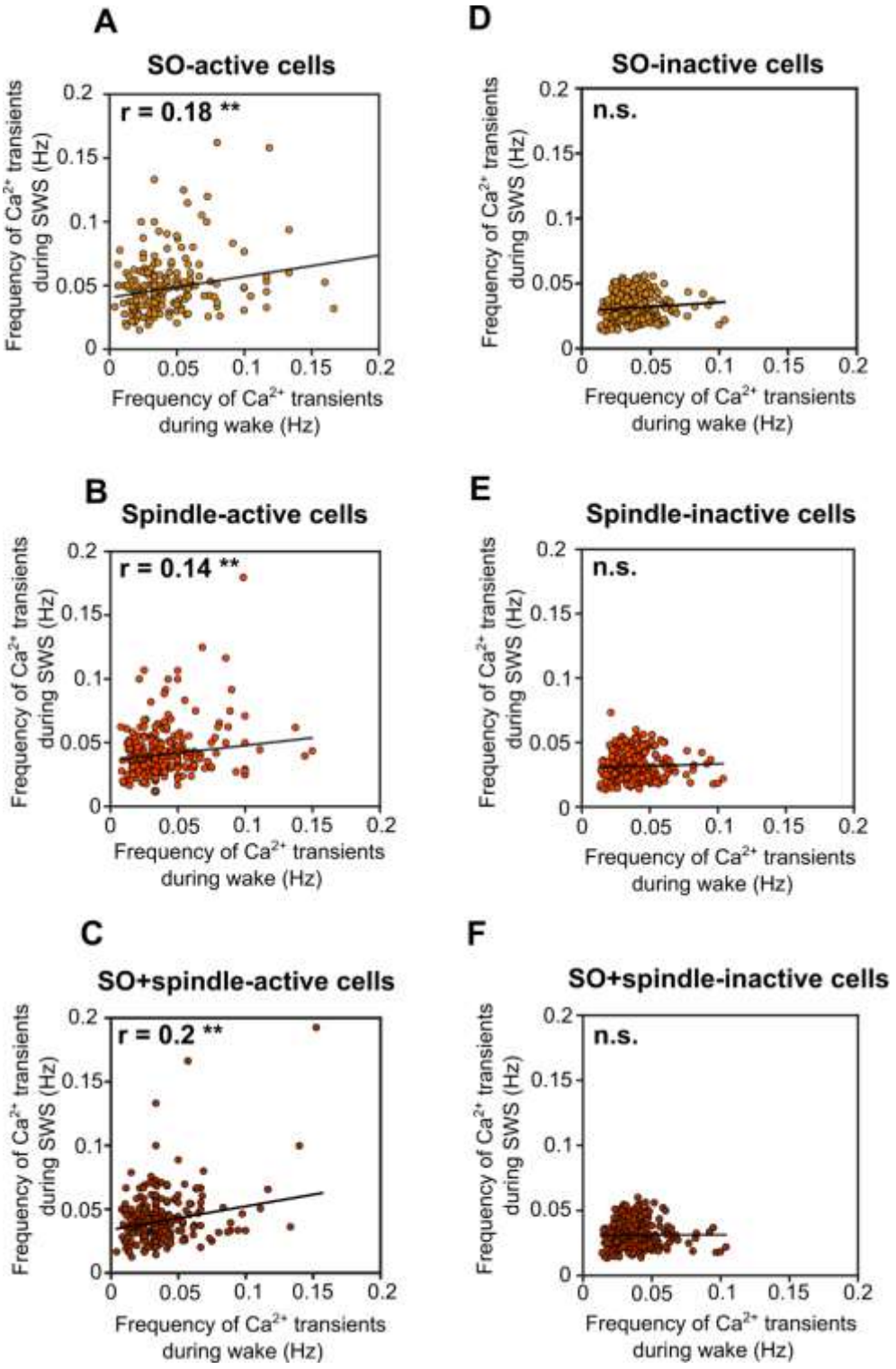

Figure 28. Activity during epochs of SWS are correlated with the activity of epochs during previous wake in the three identified cell clusters. Scatterplots for correlation between activity during awake and SWS. Each dot represents the mean frequency of Ca^{2+} transients during one epoch. (A) SO-active cells (n = 210), (B) spindle-active cells (n = 248) and (C) SO+spindle-active cells (n = 238). The inactive cell clusters are showed on the right (D-F). r values and significances are indicated by asterisks $^{**}p < 0.01$; Winsorized correlation. Note that SO+spindle-active cells showed a stronger correlation compared to the other subgroups, while the inactive cell clusters showed no correlation.

Nevertheless, we reported a weak correlation of activities between the two brain states (Figure 28 A-B; SO-active cells: $r = 0.18$, $p < 0.01$; spindle-active cells: $r = 0.14$, $p < 0.01$).

Interestingly, neurons inactive during SOs, spindles or SO+spindles displayed a significant decrease in activity during SWS (Figure 27 D-F; SO-inactive cells: $F = 28.78$, $p < 0.001$; spindle-inactive cells: $F = 28.67$, $p < 0.001$; SO+spindle-inactive cells: $F = 30.62$, $p < 0.001$) with no correlation between wake and subsequent SWS epochs (Figure 28 D-F; $p > 0.05$ for the three cell subgroups). These results are in line with the idea that the activity of cells not involved in the encoding of relevant information during wake is downregulated during subsequent sleep in order to prevent the overload of the network (Tononi and Cirelli 2020; Niethard et al. 2017). The same analyses as the ones described above were performed for the median amplitudes of the detected Ca^{2+} transients, but no differences were observed either in the entire population ($p > 0.05$. Data not shown) of neurons or in the identified subgroups of cells (SO-active cells: $F = 1.36$, $p > 0.05$; spindle-active cells: $F = 0.1$, $p > 0.05$; spindle-SO-active cells: $F = 0.258$, $p > 0.05$. Data not shown).

3.8 REM exerts different effects on the activity of the identified cell subgroups

Next, we evaluated whether REM sleep exerts different effects on the activity of the identified cell subgroups. For this, we measured how the frequency of ongoing Ca^{2+} transients of the three identified subgroups evolved across epochs of SWS, interleaved by REM sleep (Figure 29 A-D). We found a significant decrease in the median frequency of ongoing Ca^{2+} transients of SO+spindle-active cells ($F = 7.2$, $p < 0.001$) but neither SO-active cells ($p = 0.3$) nor spindle-active cells ($F = 14.72$, $p = 0.06$) between the two consecutive SWS episodes (SWS_n and SWS_{n+1}) interleaved by REM sleep. This decrease was not present when the two SWS episodes were interleaved by wakefulness (Figure 29 E-H; $p > 0.05$ for the three cell clusters) (see Table 7).

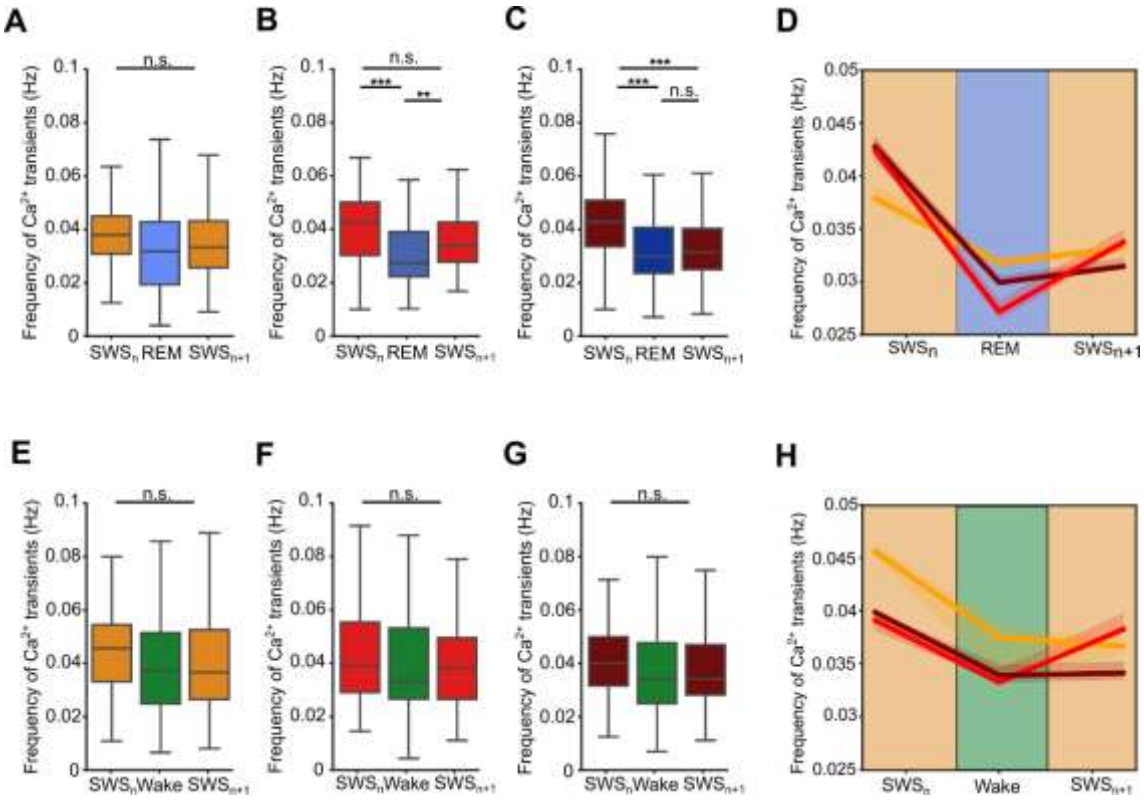

Figure 29. The activity of spindle-active and SO+spindle-active cells is downregulated during REM sleep. (*upper row*) Box-and-whisker plots showing the median (per epoch) frequencies of Ca^{2+} transients during two epochs of SWS interleaved by REM sleep in SO-active cells (A, n = 61), spindle-active cells (B, n= 70) and SO+spindle-active cells (C, n= 65). (*lower row*) Box-and-whisker plots showing the median (per epoch) frequencies of Ca^{2+} transients during two epochs of SWS interleaved by a wake in SO-active cells (D, n = 113), spindle-active cells (E, n= 134) and SO+spindle-active cells (F, n= 120). (D and H) Line-plots summarizing the activity changes across SWS epochs (orange) when interleaved by REM (blue) and wake (green). *p < 0.05, ** p < 0.01, ***p < 0.001; permutation-based ANOVA, followed by Tukey's *post hoc* test. Note that REM sleep occurring between SWS episodes induced a persisting downscaling of activity of SO+spindle-active cells, continuing in the next SWS episode (SWS_{n+1}).

Table 7. Summary of frequencies of Ca^{2+} transients across brain states and *P* values in Figure 29.

Figure	Data (median ± IQR)	*P* value
Figure 29 A	SWS_n: 0.037 ± 2 x 10^{-3} Hz REM: 0.031 ± 2 x 10^{-3} Hz SWS_{n+1}: 0.033 ± 2 x 10^{-3} Hz	SWS_n vs REM: p = 0.1 SWS_{n+1} vs REM: p = 0.6 SWS_n vs SWS_{n+1}: p = 0.3
Figure 29 B	SWS_n: 0.042 ± 10^{-3} Hz REM: 0.027 ± 10^{-3} Hz SWS_{n+1}: 0.033 ± 10^{-3} Hz	SWS_n vs REM: p < 0.001 SWS_{n+1} vs REM: p = 3.4 x 10^{-3} SWS_n vs SWS_{n+1}: p = 0.06
Figure 29 C	SWS_n: 0.042 ± 2 x 10^{-3} Hz REM: 0.029 ± 2 x 10^{-3} Hz SWS_{n+1}: 0.031 ± 2 x 10^{-2} Hz	SWS_n vs REM: p < 0.001 SWS_{n+1} vs REM: p = 0.87 SWS_n vs SWS_{n+1}: p < 0.001
Figure 29 E	SWS_n: 0.037 ± 2 x 10^{-3} Hz Awake: 0.031 ± 2 x 10^{-3} Hz SWS_{n+1}: 0.033 ± 2 x 10^{-3} Hz	SWS_n vs Awake: p = 0.17 SWS_{n+1} vs Awake: p = 0.9 SWS_n vs SWS_{n+1}: p = 0.09

Figure 29 F	SWS_n: 0.039 ± 2 x 10^{-3} Hz Awake: 0.033 ± 2 x 10^{-3} Hz SWS_{n+1}: 0.038 ± 2 x 10^{-3} Hz	SWS_n vs Awake: p = 0.7 SWS_{n+1} vs Awake: p = 0.9 SWS_n vs SWS_{n+1}: p = 0.6
Figure 29 G	SWS_n: 0.039 ± 10^{-3} Hz Awake: 0.025 ± 10^{-3} Hz SWS_{n+1}: 0.034 ± 10^{-3} Hz	SWS_n vs Awake: p = 0.08 SWS_{n+1} vs Awake: p = 0.9 SWS_n vs SWS_{n+1}: p = 0.1

No downregulation across consecutive SWS epochs, interleaved by REM sleep was observed in SO-inactive, spindle-inactive and SO+spindle-inactive cells (Figure 30 A-C; $p > 0.05$ for all cell subgroups) (see Table 8). Interestingly, these cells showed an increase of activity across SWS epochs when interleaved by wake epochs (Figure 30 D-F; SO-inactive: F = 16.89 $p < 0.001$; spindle-inactive: F = 18.10, $p < 0.001$; SO+spindle: F = 17.59, $p < 0.001$).

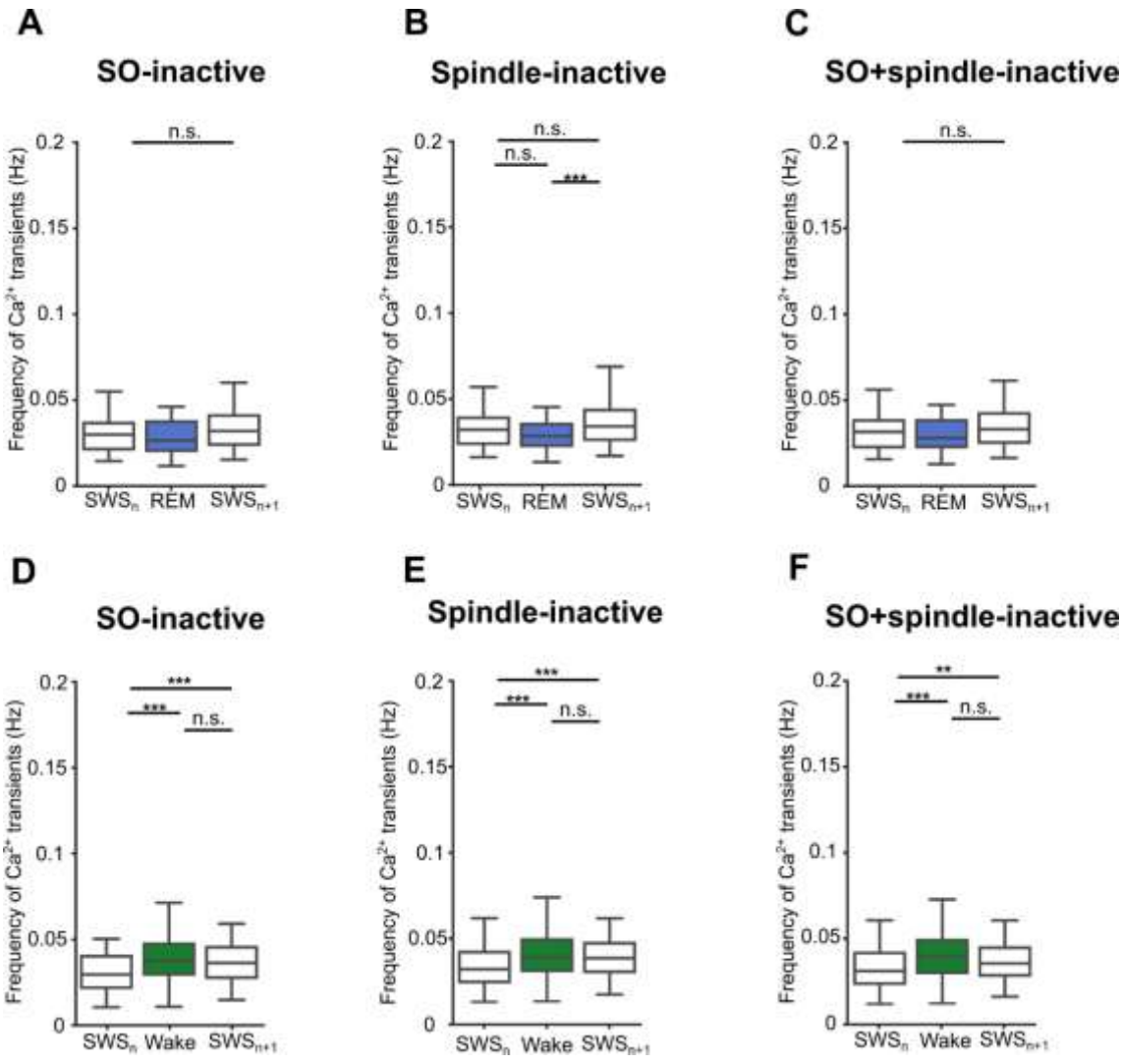

Figure 30. REM sleep does not downregulate the activity of SO-inactive, spindle-inactive and SO+spindle-inactive cells. (*upper row*) Box-and-whisker plots showing the median (per epoch) frequencies of Ca^{2+} transients during two epochs of SWS interleaved by REM sleep in SO-inactive cells (A, n = 61), spindle-inactive cells (B, n= 70) and SO+spindle-inactive cells (C, n= 65). (*lower row*) Box-and-whisker plots showing the median (per epoch) frequencies of Ca^{2+} transients during two epochs of SWS interleaved by wake in SO-inactive cells (D, n = 113), spindle-inactive cells (E, n= 134) and SO+spindle-inactive cells (F, n= 120). *$p < 0.05$, ** $p < 0.01$, ***$p < 0.001$; permutation-based ANOVA, followed by Tukey's *post hoc* test.

Table 8. Summary of frequencies of Ca^{2+} transients across brain states for the SO, spindle- and SO+spindle-inactive cells and *P* values in Figure 30.

Figure	Data (median ± IQR)	*P* value
Figure 30 A	SWS_n: 0.037 ± 2 x 10^{-3} Hz REM: 0.031 ± 2 x 10^{-3} Hz SWS_{n+1}: 0.033 ± 2 x 10^{-3} Hz	SWS_n vs REM: $p = 0.7$ SWS_{n+1} vs REM: $p = 0.07$ SWS_n vs SWS_{n+1}: $p = 0.3$
Figure 30 B	SWS_n: 0.042 ± 10^{-3} Hz REM: 0.027 ± 10^{-3} Hz SWS_{n+1}: 0.033 ± 10^{-3} Hz	SWS_n vs REM: $p = 0.2$ SWS_{n+1} vs REM: $p < 0.001$ SWS_n vs SWS_{n+1}: $p = 0.3$
Figure 30 C	SWS_n: 0.042 ± 2 x 10^{-3} Hz REM: 0.029 ± 2 x 10^{-3} Hz SWS_{n+1}: 0.031 ± 2 x 10^{-2} Hz	SWS_n vs REM: $p = 0.5$ SWS_{n+1} vs REM: $p = 0.07$ SWS_n vs SWS_{n+1}: $p = 0.5$
Figure 30 D	SWS_n: 0.030 ± 9 x 10^{-4} Hz Awake: 0.038 ± 10^{-3} Hz SWS_{n+1}: 0.037 ± 10^{-3} Hz	SWS_n vs Awake: $p < 0.001$ SWS_{n+1} vs Awake: $p = 0.6$ SWS_n vs SWS_{n+1}: $p < 0.001$
Figure 30 E	SWS_n: 0.030 ± 8 x 10^{-3} Hz Awake: Awake: 0.037 ± 10^{-3} Hz SWS_{n+1}: 0.036 ± 9 x 10^{-4} Hz	SWSn vs Awake: p < 0.001 SWSn+1 vs Awake: p = 0.5 SWSn vs SWSn+1: p < 0.001
Figure 30 F	SWS_n: 0.030 ± 9 x 10^{-4} Hz Awake: 0.038 ± 10^{-3} Hz SWS_{n+1}: 0.034 ± 9 x 10^{-4} Hz	SWS_n vs Awake: $p < 0.001$ SWS_{n+1} vs Awake: $p = 0.9$ SWS_n vs SWS_{n+1}: $p < 0.01$

The same analyses as the ones described above were performed considering the amplitude of the detected Ca^{2+} transients as ΔF/F. Here, no modulation across SWS epochs was observed in all identified subgroups of cells ($p > 0.05$ for all cell subgroups. Permutation-based ANOVA. Data not shown).

Additionally, REM sleep reduced the variability of the frequency of Ca^{2+} transients across SWS epochs of SO+spindle-active cells (F = 6.58, $p = 0.01$) (Figure 31 C), but neither for SO-active cells ($p = 0.07$) (Figure 31 A) nor for spindle active cells ($p = 0.051$) (Figure 31 B). Interestingly, when we considered the variability of the frequency of Ca^{2+} transients of the respective inactive cell subgroups, we observed opposing dynamics. Indeed, the variability tended to increase for SO-inactive (F = 5.32, $p = 0.02$) (Figure 31 D) and spindle-inactive (F = 6.08, $p = 0.014$) (Figure 31 E), but not for SO+spindle-inactive cells ($p = 0.06$) (Figure 31 F).

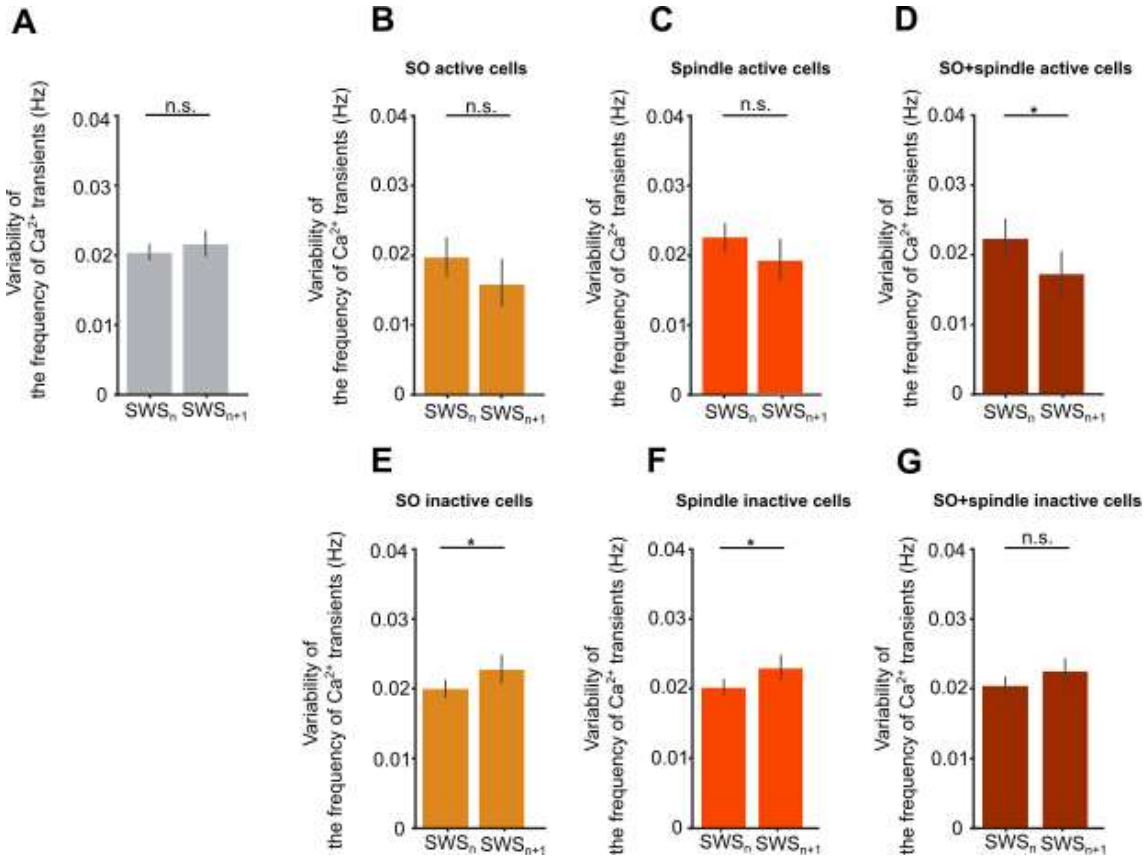

Figure 31. REM sleep renormalizes the variability of spindle-active and SO+spindle-active cells. Bar plots showing mean ± SEM of standard deviations of the frequencies (per epoch) of the detected Ca^{2+} transients during epochs of SWS_n and SWS_{n+1}, interleaved by REM sleep in (A) the entire neuronal population (grey; n = 78), (B) SO-active cells (left, orange; n = 61), spindle-active (middle, red; n = 70) and SO+spindle-active cells (right, maroon; n = 65). (C) Similar analyses were performed for the respective inactive cellular subgroups. *$p < 0.05$; permutation-based ANOVA. Note, the variability across SWS epochs decreases for SO+spindle-active cells. On the other hand, the inactive cell clusters showed an increase in variability across SWS epochs.

For all three subgroups no correlation was found between the change in activity across SWS epochs and the duration of the interleaved REM epochs, ($p > 0.05$ for all cell subgroups. Winsorized correlation. Data not shown).

Hypothesizing that during longer epochs of SWS_n the load of encoded information is higher (Lüthi 2014), we correlated the duration of SWS_n with the difference in frequency of Ca^{2+} transients across epochs of SWS interleaved by REM sleep (Figure 32). The frequency of Ca^{2+} transients during shorter epochs of SWS_n was more prone to be downscaled, for SO-active cells (r = 0.45, $p < 0.001$), spindle-

active cells (r = 0.5, $p < 0.001$) as well as SO+spindle-active cells (r = 0.55, $p < 0.001$).

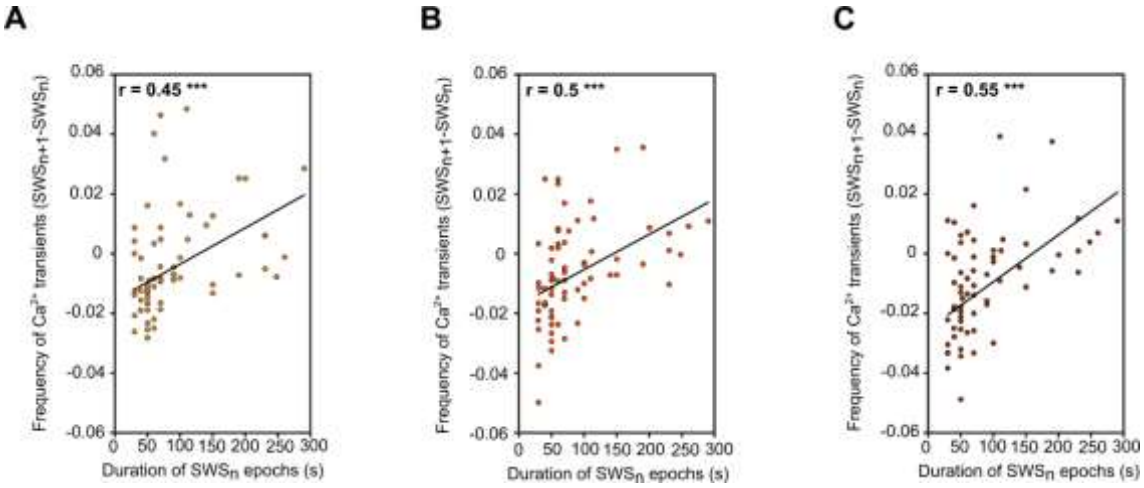

Figure 32. Correlation analysis between the difference in activity across SWS epochs and the duration of SWS_n epochs. Scatterplots for (A) SO-active cells (orange; n = 61), (B) spindle-active cells (red; n = 70) and (C) SO+spindle-active cells (maroon; n = 65), showing the correlation between the difference in frequencies across SWS epochs and duration of SWS_n epochs. r values and significances are indicated by asterisks (**$p < 0.01$; Winsorized correlation). Note that the modulation of the activity of the three subgroups of cells across REM sleep is not dramatic in long epochs of SWSn.

Altogether, these data suggest that REM sleep exerts strong downregulating effects on the networks, involved in the encoding of new information, in particular on neurons active during SO+spindles.

4. Discussion

The present work examined the Ca^{2+} dynamics of the hippocampal network in the CA1 area to explore how sleep influences neuronal activity. Natural sleep was recorded from head-fixed mice and the recorded sleep architecture was in line with that described in other studies with the same experimental condition (Cox et al. 2016; Lecci et al. 2017; Niethard et al. 2016; Seibt et al. 2017; Yüzgeç et al. 2018; Bojarskaite et al. 2020).

Contrary to previous electrophysiological studies, we were able to clearly define cell identities and follow the same individual cells across long-lasting experiments with high spatial resolution, considering also inactive neurons.

The present study described a significant increase in cellular activity during SWS and REM sleep, both in terms of cell recruitment and the frequency of Ca^{2+} transients in individual cells. In contrast to previous work (Zhou et al. 2019), we found that the activity of cells was lowest during wake and highest during sleep. The discrepancy with our study might be explained by the different adopted experimental approach. In our study we did not discriminate the wake state in “quite” or “active”, but our sleep scoring was more reliable, since it was based on the analysis of the EMG trace and not only on the signal from the EEG electrode or on the posture of the animal.

Furthermore, surprisingly, we found that REM sleep did not exert long-lasting effects on the overall activity of the entire population of CA1 pyramidal neurons across SWS (Figure 21 A). However, we observed a trend towards an increase of the variability of the frequencies of Ca^{2+} transients across epochs of SWS interleaved by REM sleep, suggesting that the neuronal population in CA1 did not respond to the REM sleep in a uniform manner. For this reason, the neuronal population was subdivided in cell subgroups active during SWS specific-oscillatory events: SOs, solitary sleep spindles, and spindles nested in the upstate of a SO event. Until now, the regulatory effects of these oscillatory events on the activity of pyramidal cells in the hippocampus has been unknown.

4.1 Sparse activity

The efficient coding hypothesis (Barlow 1961) suggests that only small subsets of neurons should be active to encode novel information to reduce the cost of computation (Lennie 2003). The present study represents the first evidence with *in vivo* Ca^{2+} imaging of the sparseness of activity in the CA1 region of the hippocampus. Sparse activity is one of the main hallmark for cortical and hippocampal circuits (Diamantaki et al. 2016; Karlsson and Frank 2008), and it has been considered as the most efficient way for the hippocampal neurons to acquire new memories (Wixted et al. 2014; Kumar et al. 2020), improve the velocity of learning (Spanne and Jörntell 2015) and enhance readout accuracy (Froudarakis et al. 2014). Also, the distribution of firing rates in the hippocampus is highly skewed, suggesting the existence of subpopulations of cells which are responsible for specific information encoding (Buzsáki and Mizuseki 2014). As previously reported (Karlsson and Frank 2008), we found that in CA1 the majority of the neurons were silent during wakefulness. However, during sleep we observed a global increase in the fraction of recruited cells and their activity. Indeed, the activity in terms of frequency and amplitude of Ca^{2+} transients was the highest during SWS and REM, respectively. Also, we observed that the fraction of active cells tended to increase at the transition from wake to SWS or REM sleep and to decrease from sleep to wake. Considering that the hippocampus plays a central role in the active consolidation theory and represents the region where memories are stored for short periods before being transferred to the more stable neocortical storages, the sparseness in activity might represent a vital feature of the network's activity. In order not to reach a state of hyper-excitability and low-selectivity, during wake the observed sparseness in activity represents a conservative mechanism to maximize the storage capacity of the network and to increase the signal to noise ratio (Olshausen and Field 1996). On the other hand, the surprising transition to a denser and stronger type of activity during subsequent sleep, satisfies the need to distribute the information to a higher number of cells, or so-called "channels of information". In this way, the transmission of the information to neocortical structures is boosted through multiple reactivations across multiple cellular hubs.

Another explanation for the pattern of sparse activation observed during wake is that the animals before the experiment underwent to an extensive training and the sparseness in activity could also be interpreted as an adaptation to the statistical features of the experimental environment (Spanne and Jörntell 2015). Interestingly, Ca^{2+} imaging in the DG revealed that adult-born granule cells (abGCs) showed sparse activity not only during wakefulness (Danielson et al. 2016), but even more in SWS and REM sleep (Kumar et al. 2020), showing that the sparse activity of these cells during REM is necessary for memory consolidation. The sparse activation of abGCs during REM sleep after learning might coordinate the maturation of a memory trace in the downstream structures, perhaps through theta-related mechanisms (Kumar et al. 2020). Indeed, we found that during SWS and especially during REM sleep, neurons were more prone to be recruited than during wake, suggesting that during sleep the network in CA1 is characterized by higher excitability, contrary to what it has been reported in cortex (Niethard et al. 2016) and in the DG (Diamantaki et al. 2016; Kumar et al. 2020).

4.2 Role of REM sleep

Electrophysiological studies in the hippocampus and the cortex reported that REM sleep plays a main role in exerting a global reduction in the activity of pyramidal neurons across SWS epochs. In our study we did not observe this effect on the general population. However, we found that the variability of frequency of Ca^{2+} transients across epochs of SWS, interleaved by REM sleep, tended to increase. This supported the view that sleep does not modulate the activity of the network in a uniform way. Moreover, REM sleep since its discovery has been described as an active state (Aserinsky and Kleitman 1953). Theta waves are the dominating oscillations during REM sleep and are especially visible in the parietal areas above the hippocampus. Optogenetic inhibition of the GABAergic neurons in the medial septum, driving the hippocampal theta activity, during REM sleep resulted in impairment in contextual memory (Boyce et al. 2016). Also, hippocampal place cells encoding a novel environment are reactivated during REM sleep at the theta peak, while the place cells encoding

familiar environment are rather activated at the trough of the theta phase, suggesting that novel spatial information is strengthened and the older one is weakened (Poe et al. 2000). Our study is the first to link changes in Ca^{2+} signaling exerted during REM sleep on the neurons active during SOs and sleep spindles, which are EEG oscillations well-known to be involved in memory formation. Indeed, we found that REM sleep played a more selective and differential role targeting exclusively the cells which were active during spindles nesting in the up-state of a SO event, by reducing their activity across SWS epochs (Figure 29 C). This result is in line with previous findings, that reported the role of REM sleep in downscaling or protecting specific circuits (Li et al. 2017). The discrepancy, observed for the general population, with electrophysiological findings (Grosmark et al. 2012) might reside in the used technique. Although electrical studies are able to record single action potentials, high-speed Ca^{2+} imaging allows to image large FOV with more than 200 neurons, including the ones characterized by low spiking activity, while electrophysiological studies run the risk of focusing only on the most active cells (Kerr et al. 2005). Also, we did not extract the Ca^{2+} spikes, but we based our analyses on the fluorescence signal, in line with many studies investigating the brain state-dependent changes of Ca^{2+} signaling (Cox et al. 2016; Kumar et al. 2020; Niethard et al. 2021).

SOs represent the pattern emerging from the cortical network and propagating caudally to reach subcortical structures (Massimini et al. 2004). As mentioned above, SOs are involved in memory consolidation and improve memory performance after sleep. Also, in a recent study, optogenetic inhibition of the firing activity during the upstate of SOs caused a dramatic impairment of the performance of a brain-machine interface (BMI) task after sleep. This finding suggests that the SO-associated firing is required for the preservation of memory (Kim et al. 2019). Interestingly, in the present work we found that REM sleep did not exert any modulating effect on the activity of SO-active cells across epochs of SWS.

The active consolidation theory (Diekelmann and Born 2010; Klinzing et al. 2019) suggests that sleep spindles open fine-tuned windows for synchronization and plasticity (Helfrich et al. 2019; Sejnowski and Destexhe 2000; Seibt et al. 2017;

Niethard et al. 2018), as demonstrated by an increase in functional connectivity across cortical (Laventure et al. 2018) and subcortical regions (Andrade et al. 2011). Also, the coupling of sleep spindles in the upstate of a SO event has been suggested to strongly promote memory consolidation. The increase in the density of SO-coupled spindles has a beneficial role on memory performance (Kim et al. 2019) and on synaptic plasticity (Latchoumane et al. 2017), by driving the reactivation of newly encoded information in neuronal ensembles. Interestingly, our data showed that the spindle power was significantly higher in spindle events co-occurring in the upstate of a SO, suggesting higher computational load (Figure 24 D).

In this context, our findings showed that REM sleep plays an active role in targeting the cells which are active during SO+spindle complexes, by promoting the downscaling of their activity across SWS. It has also been suggested that SWS might drive homeostatic changes in theta activity during subsequent REM sleep (Bjorness et al. 2018). In addition, the density of sleep spindles during SWS is predictive of the theta power and also triggers the onset of subsequent REM sleep (Bandarabadi et al. 2020). This suggests that the modulatory effects observed during REM sleep are in some way initialized during previous SWS epochs. Indeed, we are tempted to speculate that the activity during long and stable epochs of SWS is necessary for the processing of relevant information that needs to be further consolidated.

In this way, in order to maintain the capacity of the network to process new plastic events at optimal levels, REM sleep might play a double role, by preventing the downscaling of specific information during SOs or solitary spindles, while promoting the downregulation of cells active during spindle-complexes, encoding for other information that has been already consolidated and transferred from the hippocampus to the cortex.

4.3 Future directions

Despite the new insights provided by the present study on the regulation of the hippocampal circuit across brain states, especially during SOs and sleep spindles, three main limitations need to be considered. First, since we do not manipulate the neuronal activity during specific timeframes, we cannot directly explain the mechanism involved in the selective targeting during REM sleep. A critical point is the heterogeneity of CA1 pyramidal cells (Soltesz and Losonczy 2018) and further studies need to be done to describe if different layers in CA1 might be modulated differently across sleep. Second, in the present study hippocampal LFP electrode(s) were not implanted and therefore SWRs were not detected. Considering the role of these oscillations either during wakefulness or sleep in memory consolidation (O'Neill et al. 2010; Girardeau et al. 2009; Girardeau et al. 2014; Ego-Stengel and Wilson 2010), future studies might evaluate how the activity of the pyramidal neurons in CA1 are affected during SWRs. In a recent set of Ca^{2+} imaging studies (Malvache et al. 2016; Grosmark et al. 2021; Rolotti et al. 2022), it was reported that the somatic activity in CA1 increased during quite wakefulness-related SWRs, but it was not measured during SWRs occurring during SWS. Also, the interplay between SOs, sleep spindles and SWRs seems to be critical for memory consolidation (Klinzing et al. 2019). As a matter of fact, it has been observed that sleep spindles group SWRs (Siapas and Wilson 1998; Sirota et al. 2003), suggesting that spindles might organize the transfer of information from the hippocampus to cortical sites (Rosanova and Ulrich 2005; Sejnowski and Destexhe 2000). Third, the present study analyzes excitatory CA1 pyramidal neurons. Considering the high heterogeneity of the GABAergic population (Klausberger and Somogyi 2008), an interesting question that needs to be addressed in the future is how the activity of the inhibitory components is regulated across brain states. In a recent study, 3D Ca^{2+} imaging and post-hoc immunolabeling were used to study the population of molecularly defined subtypes of interneurons in CA1 across different behavioral conditions (Geiller et al. 2020), but not during sleep. Considering the pattern of activity of somatostatin-positive (SOM^+) and parvalbumin-positive (PV^+) interneurons during sleep in the

cortex (Niethard et al. 2018; Niethard 2021), it would be interesting to observe how these subtypes of interneurons are modulated across sleep in CA1 and if there are any complementary mechanisms to those observed in the cortex. This might provide additional information on the crosstalk between hippocampus and cortex. It is also interesting to mention cholecystokinin (CCK^+) interneurons, which seem to be involved in the regulation of the CA1 pyramidal neurons in the process of input-output transformation (Klausberger et al. 2005; Milstein et al. 2015). Interestingly, CCK^+ interneurons seem to be involved in supporting the sparse coding in CA1 (Klausberger and Somogyi 2008). High-firing cells in CA1 are capable of removing the inhibition by cannabinoid receptors, while weakly or inactive cells are still inhibited (Tukker et al. 2007; Wilson and Nicoll 2001; Katona et al. 1999).

Summary

In sum, the present study revealed that during sleep in CA1 region of the hippocampus, the activity of pyramidal cells tends to increase dramatically and the network becomes more excitable. However, we found that in the pyramidal population, REM sleep exerts different regulatory effects, by targeting the cells active during solitary spindles and SO+spindles events and downregulating their activity across sleep. This is the first two-photon study describing the sparseness of activity in CA1 and the regulatory effects of SWS-associated brain oscillations on the activity of pyramidal cells in CA1.

References

Abraham, Wickliffe C., and Anthony Robins. 2005. “Memory Retention - The Synaptic Stability versus Plasticity Dilemma.” *Trends in Neurosciences* 28 (2): 73–78. https://doi.org/10.1016/j.tins.2004.12.003.

Achermann, Peter, Derk-Jan Dijk, Daniel P Brunner, and Alexander A Borbély. 1993. “A Model of Human Sleep Homeostasis Based on EEG Slow-Wave Activity: Quantitative Comparison of Data and Simulations.” *Brain Research Bulletin* 31 (1): 97–113. https://doi.org/https://doi.org/10.1016/0361-9230(93)90016-5.

Adamantidis, Antoine R., Carolina Gutierrez Herrera, and Thomas C. Gent. 2019. “Oscillating Circuitries in the Sleeping Brain.” *Nature Reviews Neuroscience* 20 (12): 746–62. https://doi.org/10.1038/s41583-019-0223-4.

Aharoni, Daniel, Baljit S. Khakh, Alcino J. Silva, and Peyman Golshani. 2018. “All the Light That We Can See: A New Era in Miniaturized Microscopy.” *Nature Methods 2018 16:1* 16 (1): 11–13. https://doi.org/10.1038/s41592-018-0266-x.

Ahmed, Omar J., and Mayank R. Mehta. 2009. “The Hippocampal Rate Code: Anatomy, Physiology and Theory.” *Trends in Neurosciences* 32 (6): 329–38. https://doi.org/10.1016/j.tins.2009.01.009.

Amaral, D G, and M P Witter. 1989. “The Three-Dimensional Organization of the Hippocampal Formation: A Review of Anatomical Data.” *Neuroscience* 31 (3): 571–91. https://doi.org/https://doi.org/10.1016/0306-4522(89)90424-7.

Anafi, Ron C, Matthew S Kayser, and David M Raizen. 2019. “Exploring Phylogeny to Find the Function of Sleep.” https://doi.org/10.1038/s41583-018-0098-9.

Andersen, Richard Morris, David Amaral, Tim Bliss, and John O’Keefe. 2006. *The Hippocampus Book*. *Oxford Neuroscience Series*. New York: Oxford University Press. https://doi.org/10.1093/acprof:oso/9780195100273.001.0001.

Andrade, Kátia C., Victor I. Spoormaker, Martin Dresler, Renate Wehrle, Florian Holsboer, Philipp G. Sämann, and Michael Czisch. 2011. “Sleep Spindles

and Hippocampal Functional Connectivity in Human NREM Sleep." *The Journal of Neuroscience* 31 (28): 10331. https://doi.org/10.1523/JNEUROSCI.5660-10.2011.

Aronov, Dmitriy, Rhino Nevers, and David W. Tank. 2017. "Mapping of a Non-Spatial Dimension by the Hippocampal-Entorhinal Circuit." *Nature* 543 (7647): 719–22. https://doi.org/10.1038/nature21692.

Asavapanumas, Nithi, Bianca Brawek, Peter Martus, and Olga Garaschuk. 2019. "Role of Intracellular Ca2+ Stores for an Impairment of Visual Processing in a Mouse Model of Alzheimer's Disease." *Neurobiology of Disease* 121: 315–26. https://doi.org/10.1016/j.nbd.2018.10.015.

Aserinsky, E, and N Kleitman. 1953. "Regularly Occurring Periods of Eye Motility, and Concomitant Phenomena, during Sleep." *Science (New York, N.Y.)* 118 (3062): 273–74. https://doi.org/10.1126/science.118.3062.273.

Baker, Mary Ann, and James N. Hayward. 1967. "Carotid Rete and Brain Temperature of Cat." Nature 1967 216:5111 216 (5111): 139–41. https://doi.org/10.1038/216139a0.

Balduzzi, David, and Giulio Tononi. 2013. "What Can Neurons Do for Their Brain? Communicate Selectivity with Bursts." *Theory in Biosciences = Theorie in Den Biowissenschaften* 132 (1): 27–39. https://doi.org/10.1007/s12064-012-0165-0.

Bandarabadi, Mojtaba, Carolina Gutierrez Herrera, Thomas C. Gent, Claudio Bassetti, Kaspar Schindler, and Antoine R. Adamantidis. 2020a. "A Role for Spindles in the Onset of Rapid Eye Movement Sleep." *Nature Communications* 11 (1): 5247. https://doi.org/10.1038/s41467-020-19076-2.

Barlow, H. B. 1961. "Possible Principles Underlying the Transformations of Sensory Messages." *Sensory Communication*, 216–34. https://doi.org/10.7551/mitpress/9780262518420.003.0013.

Basu, Jayeeta, and Steven A Siegelbaum. 2015. "The Corticohippocampal Circuit, Synaptic Plasticity, and Memory Jayeeta," 1–26.

Bellina, V, R Huber, M Rosanova, M Mariotti, G Tononi, and M Massimini. 2008. "Cortical Excitability and Sleep Homeostasis in Humans: A TMS/Hd-EEG Study." In *Journal of Sleep Research*, 17:39.

Bergmann, Til O, Matthias Mölle, Jens Diedrichs, Jan Born, and Hartwig R Siebner. 2012. “Sleep Spindle-Related Reactivation of Category-Specific Cortical Regions after Learning Face-Scene Associations.” *NeuroImage* 59 (3): 2733–42. https://doi.org/10.1016/j.neuroimage.2011.10.036.

Binder, Sonja, Julia Rawohl, Jan Born, Lisa Marshall, and Clive R Bramham. 2014. “Transcranial Slow Oscillation Stimulation during NREM Sleep Enhances Acquisition of the Radial Maze Task and Modulates Cortical Network Activity in Rats.” https://doi.org/10.3389/fnbeh.2013.00220.

Bjorness, T. E., V. Booth, and Gina R. Poe. 2018. “Hippocampal Theta Power Pressure Builds over Non-REM Sleep and Dissipates within REM Sleep Episodes.” *Archives Italiennes de Biologie* 156 (3): 112–26. https://doi.org/10.12871/00039829201833.

Bojarskaite, Laura, Daniel M Bjørnstad, Klas H Pettersen, Céline Cunen, Gudmund Horn Hermansen, Knut Sindre Åbjørsbråten, Anna R Chambers, et al. n.d. “Astrocytic Ca 2+ Signaling Is Reduced during Sleep and Is Involved in the Regulation of Slow Wave Sleep.” https://doi.org/10.1038/s41467-020-17062-2.

Borbély, A A. 1982. “A Two Process Model of Sleep Regulation.” *Human Neurobiology* 1 (3): 195–204.

Borbély, A A, and P Achermann. 1999. “Sleep Homeostasis and Models of Sleep Regulation.” *Journal of Biological Rhythms* 14 (6): 557–68. https://doi.org/10.1177/074873099129000894.

Boyce, Richard, Stephen D. Glasgow, Sylvain Williams, and Antoine Adamantidis. 2016. “Sleep Research: Causal Evidence for the Role of REM Sleep Theta Rhythm in Contextual Memory Consolidation.” *Science* 352 (6287): 812–16. https://doi.org/10.1126/SCIENCE.AAD5252/SUPPL_FILE/BOYCE-SM.PDF.

Burgess, Christian, Diane Lai, Jerome Siegel, and John Peever. 2008. “An Endogenous Glutamatergic Drive onto Somatic Motoneurons Contributes to the Stereotypical Pattern of Muscle Tone across the Sleep-Wake Cycle.” *The Journal of Neuroscience : The Official Journal of the Society for Neuroscience* 28 (18): 4649–60. https://doi.org/10.1523/JNEUROSCI.0334-08.2008.

Buzsáki, yörgy 1989. “Two-Stage Model of Memory Trace Formation: A Role for ‘Noisy’ Brain States.” *Neuroscience* 31 (3): 551–70. https://doi.org/10.1016/0306-4522(89)90423-5.

Buzsáki, György 1996. “The Hippocampo-Neocortical Dialogue.” *Cerebral Cortex*: 81–92. https://doi.org/10.1093/cercor/6.2.81.

Buzsáki, György 1998. “Memory Consolidation during Sleep: A Neurophysiological Perspective.” *Journal of Sleep Research* 7 Suppl 1: 17–23. https://doi.org/10.1046/j.1365-2869.7.s1.3.x.

Buzsáki, György. 2004. “Large-Scale Recording of Neuronal Ensembles.” *Nature Neuroscience 2004 7:5* 7 (5): 446–51. https://doi.org/10.1038/nn1233.

Buzsáki, György, and Kenji Mizuseki. 2014. “The Log-Dynamic Brain: How Skewed Distributions Affect Network Operations.” https://doi.org/10.1038/nrn3687.

Buzsáki, György, and Edvard I. Moser. 2013. “Memory, Navigation and Theta Rhythm in the Hippocampal-Entorhinal System.” *Nature Neuroscience* 16 (2): 130–38. https://doi.org/10.1038/nn.3304.

Cantero, Jose L, Mercedes Atienza, Robert Stickgold, Michael J Kahana, Joseph R Madsen, and Bernat Kocsis. 2003. “Sleep-Dependent Theta Oscillations in the Human Hippocampus and Neocortex.” *The Journal of Neuroscience : The Official Journal of the Society for Neuroscience* 23 (34): 10897–903. https://doi.org/10.1523/JNEUROSCI.23-34-10897.2003.

Carr, Margaret F, Shantanu P Jadhav, and Loren M Frank. 2011. “Hippocampal Replay in the Awake State: A Potential Substrate for Memory Consolidation and Retrieval.” *Nature Neuroscience* 14 (2): 147–53. https://doi.org/10.1038/nn.2732.

Chauvette, Sylvain, Josée Seigneur, and Igor Timofeev. 2012. “Sleep Oscillations in the Thalamocortical System Induce Long-Term Neuronal Plasticity.” *Neuron* 75 (6): 1105–13. https://doi.org/10.1016/j.neuron.2012.08.034.

Chauvette, Sylvain, Maxim Volgushev, and Igor Timofeev. 2010. “Origin of Active States in Local Neocortical Networks during Slow Sleep Oscillation.” *Cerebral Cortex* 20 (11): 2660–74. https://doi.org/10.1093/cercor/bhq009.

Chen, Tsai-Wen, Trevor J Wardill, Yi Sun, Stefan R Pulver, Sabine L Renninger, Amy Baohan, Eric R Schreiter, et al. 2013. “Ultrasensitive Fluorescent Proteins for Imaging Neuronal Activity.” https://doi.org/10.1038/nature12354.

Cirelli, Chiara, and Giulio Tononi. 2008. “Is Sleep Essential?” *PLOS Biology* 6 (8): 1–7. https://doi.org/10.1371/journal.pbio.0060216.

Clawson, Brittany C, Jaclyn Durkin, and Sara J Aton. 2016. “Form and Function of Sleep Spindles across the Lifespan.” *Neural Plasticity* 2016: 6936381. https://doi.org/10.1155/2016/6936381.

Corkin, Suzanne. 1984. “Lasting Consequences of Bilateral Medial Temporal Lobectomy: Clinical Course and Experimental Findings in H.M.” *Seminars in Neurology* 4: 249–59.

Cox, Julia, Lucas Pinto, and Yang Dan. 2016. “Calcium Imaging of Sleep–Wake Related Neuronal Activity in the Dorsal Pons.” *Nature Communications 2016 7:1* 7 (1): 1–7. https://doi.org/10.1038/ncomms10763.

Dana, Hod, Yi Sun, Boaz Mohar, Brad K. Hulse, Aaron M. Kerlin, Jeremy P. Hasseman, Getahun Tsegaye, et al. 2019a. “High-Performance Calcium Sensors for Imaging Activity in Neuronal Populations and Microcompartments.” *Nature Methods 2019 16:7* 16 (7): 649–57. https://doi.org/10.1038/s41592-019-0435-6.

Danielson, Nathan B., Jeffrey D. Zaremba, Patrick Kaifosh, John Bowler, Max Ladow, and Attila Losonczy. 2016. “Sublayer-Specific Coding Dynamics during Spatial Navigation and Learning in Hippocampal Area CA1.” *Neuron* 91 (3): 652–65. https://doi.org/10.1016/j.neuron.2016.06.020.

David, François, Joscha T. Schmiedt, Hannah L. Taylor, Gergely Orban, Giuseppe Di Giovanni, Victor N. Uebele, John J. Renger, Régis C. Lambert, Nathalie Leresche, and Vincenzo Crunelli. 2013. “Essential Thalamic Contribution to Slow Waves of Natural Sleep.” *Journal of Neuroscience* 33 (50): 19599–610. https://doi.org/10.1523/JNEUROSCI.3169-13.2013.

Destexhe, A, D Contreras, and M Steriade. 1998. “Mechanisms Underlying the Synchronizing Action of Corticothalamic Feedback through Inhibition of Thalamic Relay Cells.” *Journal of Neurophysiology* 79 (2): 999–1016. https://doi.org/10.1152/jn.1998.79.2.999.

Diamantaki, Maria, Markus Frey, Philipp Berens, Patricia Preston-Ferrer, and Andrea Burgalossi. 2016. “Sparse Activity of Identified Dentate Granule Cells during Spatial Exploration.” *ELife* 5: 1–17. https://doi.org/10.7554/elife.20252.

Diekelmann, Susanne, and Jan Born. 2010. “The Memory Function of Sleep.” *Nature Reviews Neuroscience*. https://doi.org/10.1038/nrn2762.

Dombeck, Daniel A., Christopher D. Harvey, Lin Tian, Loren L. Looger, and David W. Tank. 2010. “Functional Imaging of Hippocampal Place Cells at Cellular Resolution during Virtual Navigation.” *Nature Neuroscience*. https://doi.org/10.1038/nn.2648.

Dragoi, George, and Susumu Tonegawa. 2011. “Preplay of Future Place Cell Sequences by Hippocampal Cellular Assemblies.” *Nature* 469 (7330): 397–401. https://doi.org/10.1038/nature09633.

Dupret, David, Joseph O’Neill, Barty Pleydell-Bouverie, and Jozsef Csicsvari. 2010. “The Reorganization and Reactivation of Hippocampal Maps Predict Spatial Memory Performance.” *Nature Neuroscience* 13 (8): 995–1002. https://doi.org/10.1038/nn.2599.

Ego-Stengel, Valérie, and Matthew A. Wilson. 2010. “Disruption of Ripple-Associated Hippocampal Activity during Rest Impairs Spatial Learning in the Rat.” *Hippocampus* 20 (1): 1–10. https://doi.org/10.1002/HIPO.20707.

Eichenbaum, H., M. Kuperstein, A. Fagan, and J. Nagode. 1987. “Cue-Sampling and Goal-Approach Correlates of Hippocampal Unit Activity in Rats Performing an Odor-Discrimination Task.” *Journal of Neuroscience* 7 (3): 716–32. https://doi.org/10.1523/jneurosci.07-03-00716.1987.

Eichenbaum, Howard. 2000. “A Cortical–Hippocampal System for Declarative Memory.” *Nature Reviews Neuroscience*. https://doi.org/10.1038/35036213.

Eichenbaum, Howard. 2004. “Hippocampus: Cognitive Processes and Neural Representations That Underlie Declarative Memory.” *Neuron* 44 (1): 109–20. https://doi.org/10.1016/j.neuron.2004.08.028.

Einstein, Michael C., Pierre Olivier Polack, Duy T. Tran, and Peyman Golshani. 2017. “Visually Evoked 3-5 Hz Membrane Potential Oscillations Reduce the Responsiveness of Visual Cortex Neurons in Awake Behaving Mice.”

Journal of Neuroscience 37 (20): 5084–98. https://doi.org/10.1523/JNEUROSCI.3868-16.2017.

Euston, David R, Masami Tatsuno, and Bruce L McNaughton. 2007. “Fast-Forward Playback of Recent Memory Sequences in Prefrontal Cortex during Sleep.” *Science (New York, N.Y.)* 318 (5853): 1147–50. https://doi.org/10.1126/science.1148979.

Fogel, Stuart M, and Carlyle T Smith. 2006. “Learning-Dependent Changes in Sleep Spindles and Stage 2 Sleep.” *Journal of Sleep Research* 15 (3): 250–55. https://doi.org/10.1111/j.1365-2869.2006.00522.x.

Frankland, Paul W, and Bruno Bontempi. 2005. “The Organization of Recent and Remote Memories.” *Nature Reviews Neuroscience* 6 (2): 119–30. https://doi.org/10.1038/nrn1607.

Freund, Tamás F, and István Katona. 2007. “Perisomatic Inhibition.” *Neuron* 56 (1): 33–42. https://doi.org/https://doi.org/10.1016/j.neuron.2007.09.012.

Fried, Itzhak, Katherine MacDonald, and Charles Wilson. 1997. “Single Neuron Activity in Human Hippocampus and Amygdala during Recognition of Faces and Objects.” *Neuron*.

Froudarakis, Emmanouil, Philipp Berens, Alexander S. Ecker, R. James Cotton, Fabian H. Sinz, Dimitri Yatsenko, Peter Saggau, Matthias Bethge, and Andreas S. Tolias. 2014. “Population Code in Mouse V1 Facilitates Readout of Natural Scenes through Increased Sparseness.” *Nature Neuroscience* 17 (6): 851–57. https://doi.org/10.1038/nn.3707.

Funk, Chadd M., Kayla Peelman, Michele Bellesi, William Marshall, Chiara Cirelli, and Giulio Tononi. 2017. “Role of Somatostatin-Positive Cortical Interneurons in the Generation of Sleep Slow Waves.” *Journal of Neuroscience* 37 (38): 9132–48. https://doi.org/10.1523/JNEUROSCI.1303-17.2017.

Gais, Steffen, Matthias Mölle, Kay Helms, and Jan Born. 2002. “Learning-Dependent Increases in Sleep Spindle Density.” *The Journal of Neuroscience : The Official Journal of the Society for Neuroscience* 22 (15): 6830–34. https://doi.org/10.1523/JNEUROSCI.22-15-06830.2002.

Geiller, Tristan, Bert Vancura, Satoshi Terada, Eirini Troullinou, Spyridon Chavlis,

Grigorios Tsagkatakis, Panagiotis Tsakalides, et al. 2020. “Large-Scale 3D Two-Photon Imaging of Molecularly Identified CA1 Interneuron Dynamics in Behaving Mice.” *Neuron* 108 (5): 968-983.e9. https://doi.org/10.1016/j.neuron.2020.09.013.

Gelbard-Sagiv, Hagar, Roy Mukamel, Michal Harel, Rafael Malach, and Itzhak Fried. 2008. “Internally Generated Reactivation of Single Neurons in Human Hippocampus during Free Recall.” *Science (New York, N.Y.)* 322 (5898): 96–101. https://doi.org/10.1126/science.1164685.

Gennaro, L. De, M. Ferrara, and M. Bertini. 2013. “Muscle Twitch Activity during REM Sleep: Effect of Sleep Deprivation and Relation with Rapid Eye Movement Activity.” *Psychobiology 2000 28:3* 28 (3): 432–36. https://doi.org/10.3758/BF03332001.

Gentet, Luc J, Yves Kremer, Hiroki Taniguchi, Z Josh Huang, Jochen F Staiger, and Carl C H Petersen. 2012. “Unique Functional Properties of Somatostatin-Expressing GABAergic Neurons in Mouse Barrel Cortex.” *Nature Neuroscience* 15 (4): 607–12. https://doi.org/10.1038/nn.3051.

Girardeau, Gabrielle, Karim Benchenane, Sidney I. Wiener, György Buzsáki, and Michaël B. Zugaro. 2009a. “Selective Suppression of Hippocampal Ripples Impairs Spatial Memory.” *Nature Neuroscience* 12 (10): 1222–23. https://doi.org/10.1038/nn.2384.

Girardeau, Gabrielle, Anne Cei, and Michaël Zugaro. 2014. “Learning-Induced Plasticity Regulates Hippocampal Sharp Wave-Ripple Drive.” *The Journal of Neuroscience* 34 (15): 5176. https://doi.org/10.1523/JNEUROSCI.4288-13.2014.

Giuditta, A, M V Ambrosini, P Montagnese, P Mandile, M Cotugno, G Grassi Zucconi, and S Vescia. 1995. “The Sequential Hypothesis of the Function of Sleep.” *Behavioural Brain Research* 69 (1–2): 157–66. https://doi.org/10.1016/0166-4328(95)00012-i.

Grinvald, Amiram, and Rina Hildesheim. 2004. “VSDI: A New Era in Functional Imaging of Cortical Dynamics.” *Nature Reviews. Neuroscience* 5 (11): 874–85. https://doi.org/10.1038/NRN1536.

Groen, Thomas van, and J. Michael Wyss. 1990. “The Connections of

Presubiculum and Parasubiculum in the Rat." *Brain Research* 518 (1–2): 227–43. https://doi.org/10.1016/0006-8993(90)90976-I.

Grosmark, Andres D., Kenji Mizuseki, Eva Pastalkova, Kamran Diba, and György Buzsáki. 2012a. "REM Sleep Reorganizes Hippocampal Excitability." *Neuron*. https://doi.org/10.1016/j.neuron.2012.08.015.

Grosmark, Andres D, and György Buzsáki. 2016. "Diversity in Neural Firing Dynamics Supports Both Rigid and Learned Hippocampal Sequences." *Science (New York, N.Y.)* 351 (6280): 1440–43. https://doi.org/10.1126/science.aad1935.

Grosmark, Andres D, Fraser T Sparks, Matt J Davis, and Attila Losonczy. 2021. "Reactivation Predicts the Consolidation of Unbiased Long-Term Cognitive Maps." *Nature Neuroscience* 24: 1574–1585. https://doi.org/10.1038/s41593-021-00920-7.

Hainmueller, Thomas, and Marlene Bartos. 2018. "Letter." *Nature* 558 (7709): 292–96. http://dx.doi.org/10.1038/s41586-018-0191-2.

Hartzell, Andrea L., Sara N. Burke, Lan T. Hoang, James P. Lister, Crystal N. Rodriguez, and Carol A. Barnes. 2013. "Transcription of the Immediate-Early Gene Arc in CA1 of the Hippocampus Reveals Activity Differences along the Proximodistal Axis That Are Attenuated by Advanced Age." *Journal of Neuroscience* 33 (8): 3424–33. https://doi.org/10.1523/JNEUROSCI.4727-12.2013.

Hashmi, Atif, Andrew Nere, and Giulio Tononi. 2013. "Sleep-Dependent Synaptic Down-Selection (II): Single-Neuron Level Benefits for Matching, Selectivity, and Specificity." *Frontiers in Neurology* 4. https://doi.org/10.3389/fneur.2013.00148.

Helfrich, Randolph F, Janna D Lendner, Bryce A Mander, Heriberto Guillen, Michelle Paff, Lilit Mnatsakanyan, Sumeet Vadera, Matthew P Walker, Jack J Lin, and Robert T Knight. 2019. "Bidirectional Prefrontal-Hippocampal Dynamics Organize Information Transfer during Sleep in Humans." *Nature Communications* 10 (1): 3572. https://doi.org/10.1038/s41467-019-11444-x.

Hendricks, J C, S M Finn, K A Panckeri, J Chavkin, J A Williams, A Sehgal, and A I Pack. 2000. "Rest in Drosophila Is a Sleep-like State." *Neuron* 25 (1):

129–38. https://doi.org/10.1016/s0896-6273(00)80877-6.

Hengen, Keith B, Alejandro Torrado Pacheco, James N McGregor, Stephen D Van Hooser, and Gina G Turrigiano. 2016. “Neuronal Firing Rate Homeostasis Is Inhibited by Sleep and Promoted by Wake.” *Cell* 165 (1): 180–91. https://doi.org/https://doi.org/10.1016/j.cell.2016.01.046.

Hoffman, K L, and B L McNaughton. 2002. “Coordinated Reactivation of Distributed Memory Traces in Primate Neocortex.” *Science (New York, N.Y.)* 297 (5589): 2070–73. https://doi.org/10.1126/science.1073538.

Ito, Hiroshi T., and Erin M. Schuman. 2012. “Functional Division of Hippocampal Area CA1 via Modulatory Gating of Entorhinal Cortical Inputs.” *Hippocampus* 22 (2): 372–87. https://doi.org/10.1002/hipo.20909.

James J. Knierim, Joshua P. Neunuebel and Sachin S. Deshmukh, and Solomon. 2014. “Functional Correlates of the Lateral and Medial Entorhinal Cortex: Objects, Path Integration and Local–Global Reference Frames.” *Philosophical Transactions of the Royal Society B*.

Jarsky, Mady, Kennedy, Spruston. 2008. “Distribution of Bursting Neurons in the CA1 Region and the Subiculum of the Rat Hippocampus.” *Journal of Comparative Neurology* 346 (October 2007): 339–46. https://doi.org/10.1002/cne.

Ji, Daoyun, and Matthew A Wilson. 2007. “Coordinated Memory Replay in the Visual Cortex and Hippocampus during Sleep.” *Nature Neuroscience* 10 (1): 100–107. https://doi.org/10.1038/nn1825.

Jinno, Shozo, and Toshio Kosaka. 2006. “Cellular Architecture of the Mouse Hippocampus: A Quantitative Aspect of Chemically Defined GABAergic Neurons with Stereology.” *Neuroscience Research* 56 (3): 229–45. https://doi.org/10.1016/J.NEURES.2006.07.007.

Johnson, Lise A, Tim Blakely, Dora Hermes, Shahin Hakimian, Nick F Ramsey, and Jeffrey G Ojemann. 2012. “Sleep Spindles Are Locally Modulated by Training on a Brain-Computer Interface.” *Proceedings of the National Academy of Sciences of the United States of America* 109 (45): 18583–88. https://doi.org/10.1073/pnas.1207532109.

Jones, B E. 2004. “Paradoxical REM Sleep Promoting and Permitting Neuronal

Networks.” *Archives Italiennes de Biologie* 142 (4): 379–96.

Jouvet, M. 1965. “Paradoxical Sleep — A Study of Its Nature and Mechanisms**This Work Was Carried out with the Help of the United States Air Force under Grant 62/67, (European Office of Aerospace Research), the Fonds de DéAveloppement de La Recherche Scientifique and the D.” In *Sleep Mechanisms*, edited by K Akert, C Bally, and J P Schadé, 18:20–62. Progress in Brain Research. Elsevier. https://doi.org/https://doi.org/10.1016/S0079-6123(08)63582-7.

Kaifosh, Patrick, Matthew Lovett-Barron, Gergely F. Turi, Thomas R. Reardon, and Attila Losonczy. 2013. “Septo-Hippocampal GABAergic Signaling across Multiple Modalities in Awake Mice.” *Nature Neuroscience* 16 (9): 1182–84. https://doi.org/10.1038/nn.3482.

Kales, A, A Rechtschaffen, Los Angeles. Brain Information Service of California, and NINDB Neurological Information Network (U.S.). 1968. *A Manual of Standardized Terminology, Techniques and Scoring System for Sleep Stages of Human Subjects: Allan Rechtschaffen and Anthony Kales, Editors*. NIH Publication. U. S. National Institute of Neurological Diseases and Blindness, Neurological Information Network. https://books.google.de/books?id=Z41IvQEACAAJ.

Kammer, H von der, M Mayhaus, C Albrecht, J Enderich, M Wegner, and R M Nitsch. 1998. “Muscarinic Acetylcholine Receptors Activate Expression of the EGR Gene Family of Transcription Factors.” *The Journal of Biological Chemistry* 273 (23): 14538–44. https://doi.org/10.1074/jbc.273.23.14538.

Kanaya, Hiroyuki J, Sungeon Park, Ji-hyung Kim, Junko Kusumi, Sofian Krenenou, Etsuko Sawatari, Aya Sato, et al. 2020. “A Sleep-like State in *Hydra* Unravels Conserved Sleep Mechanisms during the Evolutionary Development of the Central Nervous System.” *Science Advances* 6 (41): eabb9415. https://doi.org/10.1126/sciadv.abb9415.

Karalis, Nikolaos, and Anton Sirota. 2022. “Breathing Coordinates Cortico-Hippocampal Dynamics in Mice during Offline States.” *Nature Communications* 13 (1): 467. https://doi.org/10.1038/s41467-022-28090-5.

Karlsson, Mattias P., and Loren M. Frank. 2008. “Network Dynamics Underlying

the Formation of Sparse, Informative Representations in the Hippocampus." *Journal of Neuroscience* 28 (52): 14271–81. https://doi.org/10.1523/JNEUROSCI.4261-08.2008.

Katona, István, Beáta Sperlágh, Attila Sík, Attila Käfalvi, E. Sylvester Vizi, Ken Mackie, and Tamás F. Freund. 1999. "Presynaptically Located CB1 Cannabinoid Receptors Regulate GABA Release from Axon Terminals of Specific Hippocampal Interneurons." *The Journal of Neuroscience* 19 (11): 4544. https://doi.org/10.1523/JNEUROSCI.19-11-04544.1999.

Kerr, Jason N.D., David Greenberg, and Fritjof Helmchen. 2005. "Imaging Input and Output of Neocortical Networks in Vivo." *Proceedings of the National Academy of Sciences of the United States of America* 102 (39): 14063–68. https://doi.org/10.1073/pnas.0506029102.

Kim, Jaekyung, Tanuj Gulati, and Karunesh Ganguly. 2019. "Competing Roles of Slow Oscillations and Delta Waves in Memory Consolidation versus Forgetting." *Cell* 179 (2): 514-526.e13. https://doi.org/10.1016/J.CELL.2019.08.040.

Kim, Yujin, and Nelson Spruston. 2012. "Target-Specific Output Patterns Are Predicted by the Distribution of Regular-Spiking and Bursting Pyramidal Neurons in the Subiculum." *Hippocampus* 22 (4): 693–706. https://doi.org/10.1002/hipo.20931.

Klausberger, Thomas, Laszlo F. Marton, Joseph O'Neill, Jojanneke H.J. Huck, Yannis Dalezios, Pablo Fuentealba, Wai Yee Suen, et al. 2005. "Complementary Roles of Cholecystokinin- and Parvalbumin-Expressing GABAergic Neurons in Hippocampal Network Oscillations." *Journal of Neuroscience* 25 (42): 9782–93. https://doi.org/10.1523/JNEUROSCI.3269-05.2005.

Klausberger, Thomas, and Peter Somogyi. 2008. "Neuronal Diversity and Temporal Dynamics: The Unity of Hippocampal Circuit Operations." *Science* 321 (5885): 53–57. https://doi.org/10.1126/science.1149381.

Klinzing, Jens G., Niels Niethard, and Jan Born. 2019. "Mechanisms of Systems Memory Consolidation during Sleep." *Nature Neuroscience* 22 (October): 1598–1610. https://doi.org/10.1038/s41593-019-0467-3.

Klinzing, Jens G, Matthias Mölle, Frederik Weber, Gernot Supp, Jörg F Hipp, Andreas K Engel, and Jan Born. 2016. “Spindle Activity Phase-Locked to Sleep Slow Oscillations.” *NeuroImage* 134: 607–16. https://doi.org/https://doi.org/10.1016/j.neuroimage.2016.04.031.

Kovalchuk, Yury, Ryota Homma, Yajie Liang, Anatoliy Maslyukov, Marina Hermes, Thomas Thestrup, Oliver Griesbeck, Jovica Ninkovic, Lawrence B. Cohen, and Olga Garaschuk. 2015. “In Vivo Odourant Response Properties of Migrating Adult-Born Neurons in the Mouse Olfactory Bulb.” *Nature Communications* 6. https://doi.org/10.1038/ncomms7349.

Kumar, Deependra, Iyo Koyanagi, Alvaro Carrier-Ruiz, Pablo Vergara, Sakthivel Srinivasan, Yuki Sugaya, Masatoshi Kasuya, et al. 2020. “Sparse Activity of Hippocampal Adult-Born Neurons during REM Sleep Is Necessary for Memory Consolidation.” *Neuron* 107 (3): 552-565.e10. https://doi.org/10.1016/j.neuron.2020.05.008.

Latchoumane, Charles Francois V., Hong Viet V. Ngo, Jan Born, and Hee Sup Shin. 2017. “Thalamic Spindles Promote Memory Formation during Sleep through Triple Phase-Locking of Cortical, Thalamic, and Hippocampal Rhythms.” *Neuron* 95 (2): 424-435.e6. https://doi.org/10.1016/j.neuron.2017.06.025.

Laventure, Samuel, Basile Pinsard, Ovidiu Lungu, Julie Carrier, Stuart Fogel, Habib Benali, Jean Marc Lina, Arnaud Boutin, and Julien Doyon. 2018. “Beyond Spindles: Interactions between Sleep Spindles and Boundary Frequencies during Cued Reactivation of Motor Memory Representations.” *Sleep* 41 (9). https://doi.org/10.1093/SLEEP/ZSY142.

Lecci, Sandro, Laura M.J. Fernandez, Frederik D. Weber, Romain Cardis, Jean Yves Chatton, Jan Born, and Anita Lüthi. 2017. “Coordinated Infraslow Neural and Cardiac Oscillations Mark Fragility and Offline Periods in Mammalian Sleep.” *Science Advances* 3 (2). https://doi.org/10.1126/SCIADV.1602026/SUPPL_FILE/1602026_SM.PDF.

Lee, Heekyung, Douglas GoodSmith, and James J. Knierim. 2020. “Parallel Processing Streams in the Hippocampus.” *Current Opinion in Neurobiology* 64: 127–34. https://doi.org/10.1016/j.conb.2020.03.004.

Lennie, Peter. 2003. “The Cost of Cortical Computation.” *Current Biology* 13 (6): 493–97. https://doi.org/10.1016/S0960-9822(03)00135-0.

Li, Wei, Lei Ma, Guang Yang, and Wen Biao Gan. 2017. “REM Sleep Selectively Prunes and Maintains New Synapses in Development and Learning.” *Nature Neuroscience* 20 (3): 427–37. https://doi.org/10.1038/nn.4479.

Liang, Yajie, Kaizhen Li, Kristoffer Riecken, Anatoliy Maslyukov, Diego Gomez-Nicola, Yury Kovalchuk, Boris Fehse, and Olga Garaschuk. 2016. “Long-Term in Vivo Single-Cell Tracking Reveals the Switch of Migration Patterns in Adult-Born Juxtaglomerular Cells of the Mouse Olfactory Bulb.” *Cell Research* 26 (7): 805–21. https://doi.org/10.1038/cr.2016.55.

Lisman, John E., and Anthony A. Grace. 2005. “The Hippocampal-VTA Loop: Controlling the Entry of Information into Long-Term Memory.” *Neuron* 46 (5): 703–13. https://doi.org/10.1016/j.neuron.2005.05.002.

Lisman, John, and Richard Morris. 2001. “Why Is the Cortex a Slow Learner?” *Nature* 411 (6835): 248–49. https://doi.org/10.1038/35077185.

Lorente De Nó, R. 1934. “Studies on the Structure of the Cerebral Cortex. II. Continuation of the Study of the Ammonic System.” *Journal Für Psychologie Und Neurologie* 46: 113–77.

Louie, K, and M A Wilson. 2001. “Temporally Structured Replay of Awake Hippocampal Ensemble Activity during Rapid Eye Movement Sleep.” *Neuron* 29 (1): 145–56. https://doi.org/10.1016/s0896-6273(01)00186-6.

Lovett-Barron, Matthew, Patrick Kaifosh, Mazen A. Kheirbek, Nathan Danielson, Jeffrey D. Zaremba, Thomas R. Reardon, Gergely F. Turi, René Hen, Boris V. Zemelman, and Attila Losonczy. 2014. “Dendritic Inhibition in the Hippocampus Supports Fear Learning.” *Science (New York, N.Y.)* 343 (6173): 857–63. https://doi.org/10.1126/SCIENCE.1247485.

Lustenberger, Caroline, Michael R Boyle, Sankaraleengam Alagapan, Juliann M Mellin, Bradley V Vaughn, and Flavio Fröhlich. 2016. “Feedback-Controlled Transcranial Alternating Current Stimulation Reveals a Functional Role of Sleep Spindles in Motor Memory Consolidation.” *Current Biology : CB* 26 (16): 2127–36. https://doi.org/10.1016/j.cub.2016.06.044.

Lüthi, Anita. 2014. “Sleep Spindles: Where They Come from, What They Do.”

Neuroscientist. https://doi.org/10.1177/1073858413500854.

Maingret, Nicolas, Gabrielle Girardeau, Ralitsa Todorova, Marie Goutierre, and Michaël Zugaro. 2016. “Hippocampo-Cortical Coupling Mediates Memory Consolidation during Sleep.” *Nature Neuroscience* 19 (7): 959–64. https://doi.org/10.1038/NN.4304.

Mair, Patrick, and Rand Wilcox. 2020. “Robust Statistical Methods in R Using the WRS2 Package.” *Behavior Research Methods* 52: 464–88.

Malvache, Arnaud, Susanne Reichinnek, Vincent Villette, Caroline Haimerl, and Rosa Cossart. 2016. “Awake Hippocampal Reactivations Project onto Orthogonal Neuronal Assemblies.” *Science* 353 (6305): 1280–83. https://doi.org/10.1126/SCIENCE.AAF3319.

Maria V. Sanchez-Vives, David A. McCormick. n.d. “Cellular and Network Mechanismsof Rhythmic Recurrent Activity Inneocortex.”

Marr, D. 1971. “Simple Memory: A Theory for Archicortex.” *Philosophical Transactions of the Royal Society of London. Series B, Biological Sciences* 262 (841): 23–81. https://doi.org/10.1098/rstb.1971.0078.

Marshall, Lisa, Halla Helgadóttir, Matthias Mölle, and Jan Born. 2006. “Boosting Slow Oscillations during Sleep Potentiates Memory.” https://doi.org/10.1038/nature05278.

Marshall, Lisa, Matthias Mölle, Manfred Hallschmid, and Jan Born. 2004. “Transcranial Direct Current Stimulation during Sleep Improves Declarative Memory.” *Journal of Neuroscience* 24 (44): 9985–92. https://doi.org/10.1523/JNEUROSCI.2725-04.2004.

Massimini, Marcello, Reto Huber, Fabio Ferrarelli, Sean Hill, and Giulio Tononi. 2004. “The Sleep Slow Oscillation as a Traveling Wave.” *The Journal of Neuroscience* 24 (31): 6862 LP – 6870. https://doi.org/10.1523/JNEUROSCI.1318-04.2004.

McClelland, James L., Bruce L. McNaughton, and Randall C. O’Reilly. 1995. “Why There Are Complementary Learning Systems in the Hippocampus and Neocortex: Insights from the Successes and Failures of Connectionist Models of Learning and Memory.” *Psychological Review*. https://doi.org/10.1037/0033-295X.102.3.419.

Milstein, Aaron D., Erik B. Bloss, Pierre F. Apostolides, Sachin P. Vaidya, Geoffrey A. Dilly, Boris V. Zemelman, and Jeffrey C. Magee. 2015. “Inhibitory Gating of Input Comparison in the CA1 Microcircuit.” *Neuron* 87 (6): 1274–89. https://doi.org/10.1016/J.NEURON.2015.08.025.

Miyawaki, Hiroyuki, and Kamran Diba. 2016a. “Regulation of Hippocampal Firing by Network Oscillations during Sleep.” *Current Biology* 26 (7): 893–902. https://doi.org/https://doi.org/10.1016/j.cub.2016.02.024.

Mizrahi, Adi, Justin C. Crowley, Eran Shtoyerman, and Lawrence C. Katz. 2004. “High-Resolution in Vivo Imaging of Hippocampal Dendrites and Spines.” *Journal of Neuroscience* 24 (13): 3147–51. https://doi.org/10.1523/JNEUROSCI.5218-03.2004.

Mizuseki, Kenji, Kamran Diba, Eva Pastalkova, and György Buzsáki. 2011. “Hippocampal CA1 Pyramidal Cells Form Functionally Distinct Sublayers.” *Nature Neuroscience* 14 (9): 1174–83. https://doi.org/10.1038/nn.2894.

Mohajerani, Majid H, David A McVea, Matthew Fingas, and Timothy H Murphy. 2010. “Mirrored Bilateral Slow-Wave Cortical Activity within Local Circuits Revealed by Fast Bihemispheric Voltage-Sensitive Dye Imaging in Anesthetized and Awake Mice.” *The Journal of Neuroscience* 30 (10): 3745 LP – 3751. https://doi.org/10.1523/JNEUROSCI.6437-09.2010.

Mölle, Matthias, Til O Bergmann, Lisa Marshall, and Jan Born. 2011. “Fast and Slow Spindles during the Sleep Slow Oscillation: Disparate Coalescence and Engagement in Memory Processing.” *Sleep* 34 (10): 1411–21. https://doi.org/10.5665/SLEEP.1290.

Mölle, Matthias, Oxana Eschenko, Steffen Gais, Susan J. Sara, and Jan Born. 2009. “The Influence of Learning on Sleep Slow Oscillations and Associated Spindles and Ripples in Humans and Rats.” *European Journal of Neuroscience* 29 (5): 1071–81. https://doi.org/10.1111/j.1460-9568.2009.06654.x.

Mölle, Matthias, Oxana Yeshenko, Lisa Marshall, Susan J. Sara, and Jan Born. 2006. “Hippocampal Sharp Wave-Ripples Linked to Slow Oscillations in Rat Slow-Wave Sleep.” *Journal of Neurophysiology* 96 (1): 62–70. https://doi.org/10.1152/JN.00014.2006.

Moscovitch, Morris, Roberto Cabeza, Gordon Winocur, and Lynn Nadel. 2016. “Episodic Memory and Beyond: The Hippocampus and Neocortex in Transformation.” *Annual Review of Psychology*. https://doi.org/10.1146/annurev-psych-113011-143733.

Moser, E, M B Moser, and P Andersen. 1993. “Synaptic Potentiation in the Rat Dentate Gyrus during Exploratory Learning.” *Neuroreport* 5 (3): 317–20. https://doi.org/10.1097/00001756-199312000-00035.

Mukhametov, L M. 1987. “Unihemispheric Slow-Wave Sleep in the Amazonian Dolphin, Inia Geoffrensis.” *Neuroscience Letters* 79 (1–2): 128–32. https://doi.org/10.1016/0304-3940(87)90684-7.

Naber, Pieterke A., Fernando H. Lopes Da Silva, and Menno P. Witter. 2001. “Reciprocal Connections between the Entorhinal Cortex and Hippocampal Fields CA1 and the Subiculum Are in Register with the Projections from CA1 to the Subiculum.” *Hippocampus* 11 (2): 99–104. https://doi.org/10.1002/hipo.1028.

Nakamura, Nozomu H., Vera Flasbeck, Nicolas Maingret, Takashi Kitsukawa, and Magdalena M. Sauvage. 2013. “Proximodistal Segregation of Nonspatial Information in CA3: Preferential Recruitment of a Proximal CA3-Distal CA1 Network in Nonspatial Recognition Memory.” *Journal of Neuroscience* 33 (28): 11506–14. https://doi.org/10.1523/JNEUROSCI.4480-12.2013.

Neckelmann, D., O. E. Olsen, S. Fagerland, and R. Ursin. 1994. “The Reliability and Functional Validity of Visual and Semiautomatic Sleep/Wake Scoring in the Moll-Wistar Rat.” *Sleep* 17 (2): 120–31. https://doi.org/10.1093/sleep/17.2.120.

Neunuebel, Joshua P., D. Yoganarasimha, Geeta Rao, and James J. Knierim. 2013. “Conflicts between Local and Global Spatial Frameworks Dissociate Neural Representations of the Lateral and Medial Entorhinal Cortex.” *Journal of Neuroscience* 33 (22): 9246–58. https://doi.org/10.1523/JNEUROSCI.0946-13.2013.

Ngo, Hong-Viet V, Jens C Claussen, Jan Born, and Matthias Mölle. 2013. “Induction of Slow Oscillations by Rhythmic Acoustic Stimulation.” *Journal of Sleep Research* 22 (1): 22–31. https://doi.org/https://doi.org/10.1111/j.1365-

2869.2012.01039.x.

Ngo, Hong Viet, Juergen Fell, and Bernhard Staresina. 2020. “Sleep Spindles Mediate Hippocampal-Neocortical Coupling during Long-Duration Ripples.” *ELife* 9 (July): 1–18. https://doi.org/10.7554/ELIFE.57011.

Niethard, Niels, Svenja Brodt, and Jan Born. 2021. “Cell-Type-Specific Dynamics of Calcium Activity in Cortical Circuits over the Course of Slow-Wave Sleep and Rapid Eye Movement Sleep.” *Journal of Neuroscience* 41 (19): 4212–22. https://doi.org/10.1523/JNEUROSCI.1957-20.2021.

Niethard, Niels, Andrea Burgalossi, and Jan Born. 2017. “Plasticity during Sleep Is Linked to Specific Regulation of Cortical Circuit Activity.” *Frontiers in Neural Circuits* 11 (September): 1–9. https://doi.org/10.3389/fncir.2017.00065.

Niethard, Niels, Masashi Hasegawa, Takahide Itokazu, Carlos N. Oyanedel, Jan Born, and Takashi R. Sato. 2016a. “Sleep-Stage-Specific Regulation of Cortical Excitation and Inhibition.” *Current Biology*. https://doi.org/10.1016/j.cub.2016.08.035.

Niethard, Niels, Hong-Viet V. Ngo, Ingrid Ehrlich, and Jan Born. 2018. “Cortical Circuit Activity Underlying Sleep Slow Oscillations and Spindles.” *Proceedings of the National Academy of Sciences* 115 (39): E9220–29. https://doi.org/10.1073/pnas.1805517115.

Nir, Yuval, Richard J. Staba, Thomas Andrillon, Vladyslav V. Vyazovskiy, Chiara Cirelli, Itzhak Fried, and Giulio Tononi. 2011. “Regional Slow Waves and Spindles in Human Sleep.” *Neuron* 70 (1): 153–69. https://doi.org/10.1016/j.neuron.2011.02.043.

O’Keefe and Dostrovsky, J. (1971). 1971. “Short Communications The Hippocampus as a Spatial Map . Preliminary Evidence from Unit Activity in the Freely-Moving Rat.” *Brain Research* 34 (1): 171–75. http://www.ncbi.nlm.nih.gov/pubmed/5124915.

O’Keefe, John, and Lynn Nadel. 1978. *The Hippocampus as a Cognitive Map*. Oxford: Clarendon Press. http://hdl.handle.net/10150/620894.

O’Neill, Joseph, Barty Pleydell-Bouverie, David Dupret, and Jozsef Csicsvari. 2010. “Play It Again: Reactivation of Waking Experience and Memory.”

Trends in Neurosciences 33 (5): 220–29. https://doi.org/https://doi.org/10.1016/j.tins.2010.01.006.

O'Reilly, R C, and J W Rudy. 2000. "Computational Principles of Learning in the Neocortex and Hippocampus." *Hippocampus* 10 (4): 389–97. https://doi.org/10.1002/1098-1063(2000)10:4<389::AID-HIPO5>3.0.CO;2-P.

Ohki, Kenichi, Sooyoung Chung, Yeang H. Ch'ng, Prakash Kara, and R. Clay Reid. 2005. "Functional Imaging with Cellular Resolution Reveals Precise Micro-Architecture in Visual Cortex." *Nature* 433 (7026): 597–603. https://doi.org/10.1038/NATURE03274.

Oishi, Yo, Yohko Takata, Yujiro Taguchi, Sayaka Kohtoh, Yoshihiro Urade, and Michael Lazarus. 2016. "Polygraphic Recording Procedure for Measuring Sleep in Mice." *Journal of Visualized Experiments* 2016 (107): 1–7. https://doi.org/10.3791/53678.

Olcese, Umberto, Steve K Esser, and Giulio Tononi. 2010. "Sleep and Synaptic Renormalization: A Computational Study." *Journal of Neurophysiology* 104 (6): 3476–93. https://doi.org/10.1152/jn.00593.2010.

Olshausen, Bruno A, and David J Field. 1996. "Code for Natural Images." *Nature* 381 (June): 607–9.

Ong, Ju Lynn, June C Lo, Nicholas I Y N Chee, Giovanni Santostasi, Ken A Paller, Phyllis C Zee, and Michael W L Chee. 2016. "Effects of Phase-Locked Acoustic Stimulation during a Nap on EEG Spectra and Declarative Memory Consolidation." *Sleep Medicine* 20: 88–97. https://doi.org/https://doi.org/10.1016/j.sleep.2015.10.016.

Pachitariu, Marius, Carsen Stringer, Mario Dipoppa, Sylvia Schröder, L. Federico Rossi, Henry Dalgleish, Matteo Carandini, and Kenneth Harris. 2016. "Suite2p: Beyond 10,000 Neurons with Standard Two-Photon Microscopy." *BioRxiv*, 061507. https://doi.org/10.1101/061507.

Pavlides, C, and J Winson. 1989. "Influences of Hippocampal Place Cell Firing in the Awake State on the Activity of These Cells during Subsequent Sleep Episodes." *Journal of Neuroscience* 9 (8): 2907–18. https://doi.org/10.1523/JNEUROSCI.09-08-02907.1989.

Penfield, Wilder, and Brenda Milner. 1958. "Memory Deficit Produced by Bilateral

Lesions in the Hippocampal Zone." *A.M.A. Archives of Neurology & Psychiatry* 79 (5): 475–97. https://doi.org/10.1001/archneurpsyc.1958.02340050003001.

Penicaud, Luc, Alexandre Benani, Frédérique Datiche, Xavier Fioramonti, Corinne Leloup, and Fabienne Lienard. 2013. "Chapter 24 - Animal Models and Methods to Study the Relationships Between Brain and Tissues in Metabolic Regulation." In *Animal Models for the Study of Human Disease*, edited by P Michael Conn, 569–93. Boston: Academic Press. https://doi.org/https://doi.org/10.1016/B978-0-12-415894-8.00024-5.

Pennartz, C M A, E Lee, J Verheul, P Lipa, C A Barnes, and B L McNaughton. 2004. "The Ventral Striatum in Off-Line Processing: Ensemble Reactivation during Sleep and Modulation by Hippocampal Ripples." *Journal of Neuroscience* 24 (29): 6446–56. https://doi.org/10.1523/JNEUROSCI.0575-04.2004.

Peyrache, Adrien, Mehdi Khamassi, Karim Benchenane, Sidney I Wiener, and Francesco P Battaglia. 2009. "Replay of Rule-Learning Related Neural Patterns in the Prefrontal Cortex during Sleep." *Nature Neuroscience* 12 (7): 919–26. https://doi.org/10.1038/nn.2337.

Pilz, Gregor Alexander, Stefano Carta, Andreas Stäuble, Asll Ayaz, Sebastian Jessberger, and Fritjof Helmchen. 2016. "Functional Imaging of Dentate Granule Cells in the Adult Mouse Hippocampus." *Journal of Neuroscience* 36 (28): 7407–14. https://doi.org/10.1523/JNEUROSCI.3065-15.2016.

Poe, Gina R., Douglas A. Nitz, Bruce L. McNaughton, and Carol A. Barnes. 2000. "Experience-Dependent Phase-Reversal of Hippocampal Neuron Firing during REM Sleep." *Brain Research* 855 (1): 176–80. https://doi.org/10.1016/S0006-8993(99)02310-0.

Puentes-Mestril, Carlos, and Sara J Aton. 2017. "Linking Network Activity to Synaptic Plasticity during Sleep: Hypotheses and Recent Data." *Frontiers in Neural Circuits* 11. https://doi.org/10.3389/fncir.2017.00061.

R Core Team. 2016. "R: A Language and Environment for Statistical Computing." Vienna, Austria. https://www.r-project.org/.

Raizen, David M, John E Zimmerman, Matthew H Maycock, Uyen D Ta, Young-

Jai You, Meera V Sundaram, and Allan I Pack. n.d. “Lethargus Is a Caenorhabditis Elegans Sleep-like State.” https://doi.org/10.1038/nature06535.

Ramadan, Wiâm, Oxana Eschenko, and Susan J Sara. 2009. “Hippocampal Sharp Wave/Ripples during Sleep for Consolidation of Associative Memory.” *PloS One* 4 (8): e6697. https://doi.org/10.1371/journal.pone.0006697.

Rasch, B, and J Born. 2013. “About Sleep’s Role in Memory.” *Physiol Rev* 93: 681–766. https://doi.org/10.1152/physrev.00032.2012.-Over.

Rasch, Björn, Christian Büchel, Steffen Gais, and Jan Born. 2007. “Odor Cues during Slow-Wave Sleep Prompt Declarative Memory Consolidation.” *Science (New York, N.Y.)* 315 (5817): 1426–29. https://doi.org/10.1126/science.1138581.

Rasch, Björn, Julian Pommer, Susanne Diekelmann, and Jan Born. 2009. “Pharmacological REM Sleep Suppression Paradoxically Improves Rather than Impairs Skill Memory.” *Nature Neuroscience* 12 (4): 396–97. https://doi.org/10.1038/nn.2206.

Rattenborg, Niels C, Bruce H Mandt, William H Obermeyer, Peter J Winsauer, Reto Huber, Martin Wikelski, and Ruth M Benca. 2000. “Migratory Sleeplessness in the White-Crowned Sparrow (Zonotrichia Leucophrys Gambelii).” https://doi.org/10.1371/journal.pbio.0020212.

Rochefort, Nathalie L., Olga Garaschuk, Ruxandra Iulia Milos, Madoka Narushima, Nima Marandi, Bruno Pichler, Yury Kovalchuk, and Arthur Konnerth. 2009. “Sparsification of Neuronal Activity in the Visual Cortex at Eye-Opening.” *Proceedings of the National Academy of Sciences of the United States of America* 106 (35): 15049–54. https://doi.org/10.1073/PNAS.0907660106/SUPPL_FILE/0907660106SI.PDF.

Rolotti, Sebi V., Heike Blockus, Fraser T. Sparks, James B. Priestley, and Attila Losonczy. 2022. “Reorganization of CA1 Dendritic Dynamics by Hippocampal Sharp-Wave Ripples during Learning.” *Neuron* 110 (6): 977-991.e4. https://doi.org/10.1016/j.neuron.2021.12.017.

Roman, F, U Staubli, and G Lynch. 1987. “Evidence for Synaptic Potentiation in

a Cortical Network during Learning." *Brain Research* 418 (2): 221–26. https://doi.org/https://doi.org/10.1016/0006-8993(87)90089-8.

Rosanova, Mario, and Daniel Ulrich. 2005. "Pattern-Specific Associative Long-Term Potentiation Induced by a Sleep Spindle-Related Spike Train." *Journal of Neuroscience* 25 (41): 9398–9405. https://doi.org/10.1523/JNEUROSCI.2149-05.2005.

Rossum, Guido Van, and Fred L Drake. 2009. *Python 3 Reference Manual*. Scotts Valley, CA: CreateSpace.

Rubin, Alon, Liron Sheintuch, Noa Brande-Eilat, Or Pinchasof, Yoav Rechavi, Nitzan Geva, and Yaniv Ziv. 2019. "Revealing Neural Correlates of Behavior without Behavioral Measurements." *Nature Communications 2019 10:1* 10 (1): 1–14. https://doi.org/10.1038/s41467-019-12724-2.

Ruigt, G. S.F., J. N. Van Proosdij, and A. M.L. Van Delft. 1989. "A Large Scale, High Resolution, Automated System for Rat Sleep Staging. I. Methodology and Technical Aspects." *Electroencephalography and Clinical Neurophysiology* 73 (1): 52–63. https://doi.org/10.1016/0013-4694(89)90019-9.

Sakurai, Y. 2002. "Coding of Auditory Temporal and Pitch Information by Hippocampal Individual Cells and Cell Assemblies in the Rat." *Neuroscience* 115 (4): 1153–63. https://doi.org/10.1016/S0306-4522(02)00509-2.

Salim, Samina. 2017. "Oxidative Stress and the Central Nervous System." *The Journal of Pharmacology and Experimental Therapeutics* 360 (1): 201–5. https://doi.org/10.1124/jpet.116.237503.

Sargolini, Francesca, Marianne Fyhn, Torkel Hafting, Bruce L. McNaughton, Menno P. Witter, May Britt Moser, and Edvard I. Moser. 2006. "Conjunctive Representation of Position, Direction, and Velocity in Entorhinal Cortex." *Science* 312 (5774): 758–62. https://doi.org/10.1126/science.1125572.

Sawangjit, Anuck, Carlos N. Oyanedel, Niels Niethard, Carolina Salazar, Jan Born, and Marion Inostroza. 2018. "The Hippocampus Is Crucial for Forming Non-Hippocampal Long-Term Memory during Sleep." *Nature*. https://doi.org/10.1038/s41586-018-0716-8.

Schabus, Manuel, Georg Gruber, Silvia Parapatics, Cornelia Sauter, Gerhard

Klösch, Peter Anderer, Wolfgang Klimesch, Bernd Saletu, and Josef Zeitlhofer. 2004. “Sleep Spindles and Their Significance for Declarative Memory Consolidation.” *Sleep* 27 (8): 1479–85. https://doi.org/10.1093/sleep/27.7.1479.

Seibt, Julie, Clément J. Richard, Johanna Sigl-Glöckner, Naoya Takahashi, David I. Kaplan, Guy Doron, Denis De Limoges, Christina Bocklisch, and Matthew E. Larkum. 2017. “Cortical Dendritic Activity Correlates with Spindle-Rich Oscillations during Sleep in Rodents.” *Nature Communications* 8 (1): 684. https://doi.org/10.1038/s41467-017-00735-w.

Sejnowski, Terrence J., and Alain Destexhe. 2000. “Why Do We Sleep?” *Brain Research* 886 (1–2): 208–23. https://doi.org/10.1016/S0006-8993(00)03007-9.

Shaw J. Paul, Cirelli Chiara, Greenspan J. Ralph, and Tononi Giulio. 2000. “Correlates of Sleep and WakinginDrosophila Melanogaster.” http://science.sciencemag.org/.

Sheffield, Mark E.J., and Daniel A. Dombeck. 2015. “Calcium Transient Prevalence across the Dendritic Arbour Predicts Place Field Properties.” *Nature* 517 (7533): 200–204. https://doi.org/10.1038/nature13871.

Siapas, A G, and M A Wilson. 1998. “Coordinated Interactions between Hippocampal Ripples and Cortical Spindles during Slow-Wave Sleep.” *Neuron* 21 (5): 1123–28. https://doi.org/10.1016/s0896-6273(00)80629-7.

Sirota, Anton, and György Buzsáki. 2005. “Interaction between Neocortical and Hippocampal Networks via Slow Oscillations.” *Thalamus and Related Systems* 3 (4): 245–59. https://doi.org/10.1017/S1472928807000258.

Sirota, Anton, Jozsef Csicsvari, Derek Buhl, and György Buzsáki. 2003. “Communication between Neocortex and Hippocampus during Sleep in Rodents.” *Proceedings of the National Academy of Sciences of the United States of America* 100 (4): 2065–69. https://doi.org/10.1073/pnas.0437938100.

Solstad, T., N. Boccara, E. Kropff, May Britt Moser, and Edward I. Moser. 2014. “Representation of Geometric Borders in the Developing Rat.” *Neuron* 82 (1): 71–78. https://doi.org/10.1016/j.neuron.2014.02.014.

Soltani, Sara, Sylvain Chauvette, Olga Bukhtiyarova, Jean Marc Lina, Jonathan Dubé, Josée Seigneur, Julie Carrier, and Igor Timofeev. 2019. “Sleep–Wake Cycle in Young and Older Mice.” *Frontiers in Systems Neuroscience* 13 (September): 1–14. https://doi.org/10.3389/fnsys.2019.00051.

Soltesz, Ivan, and Attila Losonczy. 2018. “CA1 Pyramidal Cell Diversity Enabling Parallel Information Processing in the Hippocampus.” *Nature Neuroscience* 21 (4): 484–93. https://doi.org/10.1038/s41593-018-0118-0.

Spanne, Anton, and Henrik Jörntell. 2015. “Questioning the Role of Sparse Coding in the Brain.” *Trends in Neurosciences* 38 (7): 417–27. https://doi.org/10.1016/j.tins.2015.05.005.

Squire, Larry R. 1992. “Memory and the Hippocampuss: A Synthesis From Findings With Rats, Monkeys, and Humans.” *Psychological Review* 99 (2): 195–231. https://doi.org/10.1037/0033-295X.99.2.195.

Staresina, Bernhard P, Til Ole Bergmann, Mathilde Bonnefond, Roemer van der Meij, Ole Jensen, Lorena Deuker, Christian E Elger, Nikolai Axmacher, and Juergen Fell. 2015. “Hierarchical Nesting of Slow Oscillations, Spindles and Ripples in the Human Hippocampus during Sleep.” *Nature Neuroscience* 18 (11): 1679–86. https://doi.org/10.1038/nn.4119.

Steriade, M. 2006. “Grouping of Brain Rhythms in Corticothalamic Systems.” *Neuroscience* 137 (4): 1087–1106. https://doi.org/10.1016/j.neuroscience.2005.10.029.

Steriade, M, D Contreras, R Curró Dossi, and A Nuñez. 1993. “The Slow (< 1 Hz) Oscillation in Reticular Thalamic and Thalamocortical Neurons: Scenario of Sleep Rhythm Generation in Interacting Thalamic and Neocortical Networks.” *The Journal of Neuroscience : The Official Journal of the Society for Neuroscience* 13 (8): 3284–99. https://doi.org/10.1523/JNEUROSCI.13-08-03284.1993.

Steriade, Mircea, and Igor Timofeev. 2003. “Neuronal Plasticity in Thalamocortical Networks during Sleep and Waking Oscillations.” *Neuron* 37 (4): 563–76. https://doi.org/10.1016/s0896-6273(03)00065-5.

Stosiek, Christoph, Olga Garaschuk, Knut Holthoff, and Arthur Konnerth. 2003. “In Vivo Two-Photon Calcium Imaging of Neuronal Networks.” *Proceedings*

of the National Academy of Sciences of the United States of America. https://doi.org/10.1073/pnas.1232232100.

Strien, N. M. Van, N. L.M. Cappaert, and M. P. Witter. 2009. “The Anatomy of Memory: An Interactive Overview of the Parahippocampal- Hippocampal Network.” *Nature Reviews Neuroscience* 10 (4): 272–82. https://doi.org/10.1038/nrn2614.

Stroh, Albrecht, Helmuth Adelsberger, Alexander Groh, Charlotta Rühlmann, Sebastian Fischer, Anja Schierloh, Karl Deisseroth, and Arthur Konnerth. 2013. “Making Waves: Initiation and Propagation of Corticothalamic Ca2+ Waves in Vivo.” *Neuron* 77 (6): 1136–50. https://doi.org/10.1016/j.neuron.2013.01.031.

Tamaki, Masako, Tatsuya Matsuoka, Hiroshi Nittono, and Tadao Hori. 2008. “Fast Sleep Spindle (13-15 Hz) Activity Correlates with Sleep-Dependent Improvement in Visuomotor Performance.” *Sleep* 31 (2): 204–11. https://doi.org/10.1093/sleep/31.2.204.

Teplan. 2002. “FUNDAMENTALS OF EEG MEASUREMENT M.” *MEASUREMENT SCIENCE REVIEW* 2.

Teyler, T J, and P DiScenna. 1986. “The Hippocampal Memory Indexing Theory.” *Behavioral Neuroscience* 100 (2): 147–54. https://doi.org/10.1037//0735-7044.100.2.147.

Tonegawa, Susumu, Xu Liu, Steve Ramirez, and Roger Redondo. 2015. “Memory Engram Cells Have Come of Age.” *Neuron* 87 (5): 918–31. https://doi.org/10.1016/j.neuron.2015.08.002.

Tononi, Giulio, and Chiara Cirelli. 2003. “Sleep and Synaptic Homeostasis: A Hypothesis.” *Brain Research Bulletin* 62 (2): 143–50. https://doi.org/10.1016/j.brainresbull.2003.09.004.

Tononi, Giulio, and Chiara Cirelli. 2006. “Sleep Function and Synaptic Homeostasis.” *Sleep Medicine Reviews* 10 (1): 49–62. https://doi.org/10.1016/j.smrv.2005.05.002.

Tononi, Giulio, and Chiara Cirelli. 2014. “Sleep and the Price of Plasticity: From Synaptic and Cellular Homeostasis to Memory Consolidation and Integration.” *Neuron*. https://doi.org/10.1016/j.neuron.2013.12.025.

Tononi, Giulio, and Chiara Cirelli. 2020. “Sleep and Synaptic Down-Selection.” *European Journal of Neuroscience* 51 (1): 413–21. https://doi.org/10.1111/ejn.14335.

Tononi, Giulio, Brady Alexander Riedner, Brad K Hulse, Fabio Ferrarelli, and Simone Sarasso. 2010. “Enhancing Sleep Slow Waves with Natural Stimuli The Importance of Sleep.” In .

Trachsel, L., I. Tobler, and A. A. Borbely. 1988. “Electroencephalogram Analysis of Non-Rapid Eye Movement Sleep in Rats.” *American Journal of Physiology - Regulatory Integrative and Comparative Physiology* 255 (1). https://doi.org/10.1152/ajpregu.1988.255.1.r27.

Tukker, John J, Pablo Fuentealba, Katja Hartwich, Peter Somogyi, and Thomas Klausberger. 2007. “Cell Type-Specific Tuning of Hippocampal Interneuron Firing during Gamma Oscillations In Vivo.” • *The Journal of NeuroscienceThe Journal of Neuroscience*. https://doi.org/10.1523/JNEUROSCI.1685-07.2007.

Tulving, Endel. 2002. “Episodic : From Mind to Brain.” *Annual Review of Psychology* 53 (1): 1–25. www.annualreviews.org.

Varela, C, • S Kumar, • J Y Yang, and M A Wilson. 2013. “Anatomical Substrates for Direct Interactions between Hippocampus, Medial Prefrontal Cortex, and the Thalamic Nucleus Reuniens.” https://doi.org/10.1007/s00429-013-0543-5.

Vivo, Luisa de, Michele Bellesi, William Marshall, Eric A Bushong, Mark H Ellisman, Giulio Tononi, and Chiara Cirelli. 2017. “Ultrastructural Evidence for Synaptic Scaling across the Wake/Sleep Cycle.” *Science (New York, N.Y.)* 355 (6324): 507–10. https://doi.org/10.1126/science.aah5982.

Vogler, Emily C., Daniel T. Flynn, Federico Busciglio, Ryan C. Bohannan, Alison Tran, Matthew Mahavongtrakul, and Jorge A. Busciglio. 2017. “Low Cost Electrode Assembly for EEG Recordings in Mice.” *Frontiers in Neuroscience* 11 (NOV): 1–8. https://doi.org/10.3389/fnins.2017.00629.

Vorster, Albrecht P., and Jan Born. 2015. “Sleep and Memory in Mammals, Birds and Invertebrates.” *Neuroscience and Biobehavioral Reviews* 50: 103–19. https://doi.org/10.1016/j.neubiorev.2014.09.020.

Vyazovskiy, Vladyslav V, Chiara Cirelli, Martha Pfister-Genskow, Ugo Faraguna, and Giulio Tononi. 2008. “Molecular and Electrophysiological Evidence for Net Synaptic Potentiation in Wake and Depression in Sleep.” *Nature Neuroscience* 11 (2): 200–208. https://doi.org/10.1038/nn2035.

Vyazovskiy, Vladyslav V, Ugo Faraguna, Chiara Cirelli, and Giulio Tononi. 2009. “Triggering Slow Waves During NREM Sleep in the Rat by Intracortical Electrical Stimulation: Effects of Sleep/Wake History and Background Activity.” *Journal of Neurophysiology* 101 (4): 1921–31. https://doi.org/10.1152/jn.91157.2008.

Vyazovskiy, Vladyslav V, Umberto Olcese, Erin C Hanlon, Yuval Nir, Chiara Cirelli, and Giulio Tononi. 2011. “Local Sleep in Awake Rats.” *Nature* 472 (7344): 443–47. https://doi.org/10.1038/nature10009.

Wasilczuk, Andrzej Z., Alexander Proekt, Max B. Kelz, and Andrew R. McKinstry-Wu. 2016. “High-Density Electroencephalographic Acquisition in a Rodent Model Using Low-Cost and Open-Source Resources.” *Journal of Visualized Experiments* 2016 (117): 1–10. https://doi.org/10.3791/54908.

Watson, Brendon O., Daniel Levenstein, J. Palmer Greene, Jennifer N. Gelinas, and György Buzsáki. 2016. “Network Homeostasis and State Dynamics of Neocortical Sleep.” *Neuron* 90 (4): 839–52. https://doi.org/10.1016/j.neuron.2016.03.036.

Wei, Ziqiang, Bei-Jung Lin, Tsai-Wen Chen, Kayvon Daie, Karel Svoboda, and Shaul Druckmann. 2020. “A Comparison of Neuronal Population Dynamics Measured with Calcium Imaging and Electrophysiology.” https://doi.org/10.1371/journal.pcbi.1008198.

Wheeler, Bob, and Marco Torchiano. 2016. “LmPerm: Permutation Tests for Linear Models.” https://cran.r-project.org/package=lmPerm.

Wilson, M A, and B L McNaughton. 1994. “Reactivation of Hippocampal Ensemble Memories during Sleep.” *Science (New York, N.Y.)* 265 (5172): 676–79. https://doi.org/10.1126/science.8036517.

Wilson, R. I., and R. A. Nicoll. 2001. “Endogenous Cannabinoids Mediate Retrograde Signalling at Hippocampal Synapses.” *Nature* 410 (6828): 588–92. https://doi.org/10.1038/35069076.

Witter, Menno P. 2010. “Hippocampal Microcircuits.” *Hippocampal Microcircuits*, no. V: 5–6. https://doi.org/10.1007/978-1-4419-0996-1.

Wixted, John T., Larry R. Squire, Yoonhee Jang, Megan H. Papesh, Stephen D. Goldinger, Joel R. Kuhn, Kris A. Smith, David M. Treiman, and Peter N. Steinmetz. 2014. “Sparse and Distributed Coding of Episodic Memory in Neurons of the Human Hippocampus.” *Proceedings of the National Academy of Sciences of the United States of America* 111 (26): 9621–26. https://doi.org/10.1073/pnas.1408365111.

Wolansky, Trish, Elizabeth A Clement, Steven R Peters, Michael A Palczak, and Clayton T Dickson. 2006. “Hippocampal Slow Oscillation: A Novel EEG State and Its Coordination with Ongoing Neocortical Activity.” *Journal of Neuroscience* 26 (23): 6213–29. https://doi.org/10.1523/JNEUROSCI.5594-05.2006.

Xi, M C, F R Morales, and M H Chase. 2001. “The Motor Inhibitory System Operating during Active Sleep Is Tonically Suppressed by GABAergic Mechanisms during Other States.” *Journal of Neurophysiology* 86 (4): 1908–15. https://doi.org/10.1152/jn.2001.86.4.1908.

Yang, Guang, Cora Sau Wan Lai, Joseph Cichon, Lei Ma, Wei Li, and Wen Biao Gan. 2014. “Sleep Promotes Branch-Specific Formation of Dendritic Spines after Learning.” *Science*. https://doi.org/10.1126/science.1249098.

Yetton, Benjamin D, Elizabeth A Mcdevitt, Nicola Cellini, Christian Shelton, and Sara C Mednick. 2018. “Quantifying Sleep Architecture Dynamics and Individual Differences Using Big Data and Bayesian Networks.” https://doi.org/10.1371/journal.pone.0194604.

Yuste, Rafael. 2011. “Dendritic Spines and Distributed Circuits.” *Neuron* 71 (5): 772–81. https://doi.org/10.1016/J.NEURON.2011.07.024.

Yüzgeç, Özge, Mario Prsa, Robert Zimmermann, and Daniel Huber. 2018a. “Pupil Size Coupling to Cortical States Protects the Stability of Deep Sleep via Parasympathetic Modulation.” *Current Biology*. https://doi.org/10.1016/j.cub.2017.12.049.

Zhou, Heng, Kevin R. Neville, Nitsan Goldstein, Shushi Kabu, Naila Kausar, Rong Ye, Thuan Tinh Nguyen, Noah Gelwan, Bradley T. Hyman, and Stephen N.

Gomperts. 2019. “Cholinergic Modulation of Hippocampal Calcium Activity across the Sleep-Wake Cycle.” *ELife* 8: 1–19. https://doi.org/10.7554/eLife.39777.

Zhou, Yanmei, Cora Sau Wan Lai, Yang Bai, Wei Li, Ruohe Zhao, Guang Yang, Marcos G. Frank, and Wen Biao Gan. 2020. “REM Sleep Promotes Experience-Dependent Dendritic Spine Elimination in the Mouse Cortex.” *Nature Communications* 11 (1): 1–12. https://doi.org/10.1038/s41467-020-18592-5.

Zong, Weijian, Horst A. Obenhaus, Emilie R. Skytøen, Hanna Eneqvist, Nienke L. de Jong, Ruben Vale, Marina R. Jorge, May Britt Moser, and Edvard I. Moser. 2022. “Large-Scale Two-Photon Calcium Imaging in Freely Moving Mice.” *Cell* 185 (7): 1240-1256.e30. https://doi.org/10.1016/j.cell.2022.02.017.

Declaration of contribution

The dissertation work was carried out in the Institute of Physiology, Department of Neurophysiology at the Eberhard Karls Universität Tübingen under the supervision of Professor Dr. Olga Garaschuk. The study was conceived by Professor Dr. Olga Garaschuk. I established, in collaboration with Dr. Yury Kovalchuk, the experimental procedure, including surgeries and data acquisition. I performed all the experiments in this study. Dr. Nima Mojtahedi was responsible for the design of the toolbox for the analyses. Dr. Niels Niethard contributed in the analysis for the detection of SOs and sleep spindles. I accomplished anything else (~90%) in this study.
I wrote the thesis under the supervision of Prof. Dr. Olga Garaschuk.